POLYMER GRAFTED TEMPO AS A MEDIATOR FOR CELLULOSE OXIDATION

POLYMER GRAFTED TEMPO AS A MEDIATOR FOR CELLULOSE OXIDATION

By

QIANG FU, B. Eng., M. Eng.

A Thesis

Submitted to the School of Graduate Studies

in Partial Fulfillment of the Requirements

for the Degree

Doctor of Philosophy

McMaster University

DOCTOR OF PHILOSOPHY (2016) McMaster University

(Chemical Engineering) Hamilton, Ontario

TITLE: Polymer grafted TEMPO as a mediator for cellulose oxidation

AUTHOR: Qiang Fu

B.Eng. (Shandong Normal University)

M.Eng. (Zhejiang University)

SUPERVISOR: Professor Robert H. Pelton

NUMBER OF PAGES: viii, 124

Abstract

TEMPO-mediated oxidation is a widely used approach to introduce aldehyde and carboxyl groups on cellulose. In the conventional TEMPO-mediated oxidation, the mediator TEMPO is a small molecule. Previous research in our group advanced TEMPO-mediated oxidation by grafting TEMPO onto high molecular weight poly(acrylic acid) and polyvinylamine. The polymer grafted TEMPO-mediated oxidation required less TEMPO and had a lower environmental impact.

This thesis describes new insights into the role of polymer grafted TEMPO as mediator for cellulose oxidation. The redox-activity of grafted TEMPO was analyzed by electrochemical techniques and the resulting aldehyde densities on cellulose surfaces, produced by polymer grafted TEMPO, were determined with a fluorescence-labeling method.

The properties of polymer grafted TEMPO solutions are essential to understanding the role of grafted TEMPO as the oxidation mediator. TEMPO substitution compacted both the conformation of poly(acrylic acid) and polyvinylamine due to the lower hydrophilicity of the TEMPO substituents. Poly(acrylic acid-g-TEMPO) (PAA-T) solutions phase separated over the pH range 2-4, whereas at lower and higher pH the polymer was water-soluble. The phase separation at low pH was proposed to be the combined result of the hydrophobic contributions of the TEMPO moieties and electrostatic interactions between the acid-induced cationic TEMPO species and the anionic ionized carboxyl groups. Polyvinylamine-g-TEMPO (PVAm-T) was water-soluble over a larger pH range (pH 1-9) due to the ionization of the amine groups. Both the PAA-T and PVAm-T were slightly surface active.

Multilayer films composed of PVAm-T and poly(styrene sulfonate) were stable and redox-active. Charge transport in the redox multilayer films was realized through TEMPO-to-TEMPO electron hopping between neighboring TEMPO moieties. Only 20-30% of TEMPO moieties were redox-active, reflecting the requirement that TEMPO moieties must be closer than ~ 0.6 nm for electron hopping to occur. The redox multilayer films displayed significant interpenetration of layers. The ability of PVAm-T to spontaneously adsorb onto negatively charged surfaces in aqueous solutions provides an easy route to TEMPO-rich surfaces for other applications.

Specific attention was focused on the role of PVAm-T as mediator for cellulose oxidation in the presence of laccase. Positively charged PVAm-T formed colloidal complexes with negatively charged laccase. The behaviors of PVAm-T/laccase mixtures displayed the classic features of polyelectrolyte complexes formed between oppositely charged polyelectrolytes. For the first time, electrochemical quartz crystal microbalance with dissipation (EQCM-D) measurements were used to characterize the redox properties of the adsorbed PVAm-T/laccase complexes. The role of PVAm-T as mediator for cellulose oxidation depended upon TEMPO-to-TEMPO electron transfer within PVAm-T/laccase colloidal complexes. The aldehyde density on oxidized cellulose surfaces scaled with the square root of surface molar density of redox-active TEMPOs which, in turn, was a linear function of TEMPO degree of substitution in PVAm-T. As a result, the aldehyde density on cellulose surfaces, generated by PVAm-T/laccase oxidation, can be controlled by varying the TEMPO degree of substitution in PVAm-T.

Acknowledgements

First, I would like to express my deep appreciation to my supervisor, Professor Robert Pelton, for his kind guidance and constant support through the years. He is not only supervising my research, but also the way how to be an excellent scientist. He encouraged me every single step of my research, patiently supervised me, taught me skills of writing papers and went through several drafts. I appreciate all the opportunities Professor Pelton provided to attend academic conferences.

I would like to thank my supervisory committee, Professor Emily Cranston, and Professor Leyla Soleymani, for their instruction and suggestions. They provided me tremendous help on experimental designs and data analysis. Their encouragement motivated me through the ups and downs of my research.

I would like to thank Professor Art van der Est, from Brock university, Canada, for his help with electron paramagnetic resonance spectroscopy; Professor Shuxian Shi, from Beijing University of chemical technology, China, for her help with cellulose oxidation.

I would like to acknowledge my colleagues in McMaster Interfacial Technologies Group for their support and friendship. Specifically, I would like to thank Dr. Emil Gustafsson, Mr. Dong Yang, Mr. Jieyi Liu, Dr. Xudong Deng, Dr. Zuohe Wang, Dr. Monsur Ali, Dr. Zhuyuan Zhang, Dr. Zhen Hu, Ms. Xiaofei Dong, Dr. Jingyun Wang, Dr. Roozbeh Mafi, Ms. Yuanhua li, and Ms. Fengyan Wang. I would also like to thank summer students Zachary Gray, Igor Zoudanov, and Alexander Sutherland for their hard work.

I would like to thank Dr. Danielle Covelli for her help with Ellipsometer, Dynamic light scattering, and viscometer, Dr. Marta Princz for her help with Gel Electrophoresis Imaging- Chemidoc MP, Ms. Marnie Timleck for her help with confocal microscopy.

I would like to thank our laboratory manager Mr. Doug Keller and administrative sectary Ms. Sally Watson Ms. Kathy Goodram, Ms. Cathie Roberts, Ms. Kristina Trollip, Ms. Michelle Whalen, and Ms. Linda Ellis for their administrative assistance, Mr. Paul Gatt, Ms. Justyna Derkach, and Mr. Dan Wright For their technical assistance.

I would like to acknowledge Natural Sciences and Engineering Research Council of Canada and BASF Canada for their financial support.

Finally, I would like to thank my parents, my brother and sister, and Ms. Liu for their everlasting love and support.

Table of Contents

Abbreviations

CMC	carboxymethyl cellulose
CV	cyclic voltammetry
DH	degree of hydrolysis
DLS	dynamic light scattering
DS	degree of substitution
EDC	1-ethyl-3-(3-(dimethylamino)propyl)carbodiimide
EPR	electron paramagnetic resonance spectroscopy
EQCM-D	electrochemical quartz crystal microbalance with dissipation monitoring
Fc	ferrocene
FTIR	Fourier transform infrared spectroscopy
i_p	peak current of cyclic voltammogram
kDa	kilodalton
LbL	layer-by-layer
LCST	lower critical solution temperature
MPS	sodium 3-mercapto-1-propanesulfonate
Mw	molecular weight
MWCO	molecular weight cut-off

PAA	poly(acrylic acid)
PAA-T	poly(acrylic acid-g-TEMPO)
PEG	polyethylene glycol
PEI	poly(ethyleneimine)
PSS	sodium poly(styrene sulfonate)
PVAm	polyvinylamine
PVAm-T	polyvinylamine-g-TEMPO
Sulfo-NHS	N-hydroxysulfosuccinimide sodium salt
TEMPO	2,2,6,6-Tetramethyl-1-piperidinyloxy
TEMPO+	TEMPO oxoammonium ion
TEMPOH	hydroxylamine
UCST	upper critical solution temperature
ν	scan rate during cyclic voltammetry

Chapter 1 Introduction

Can you imagine what will happen if towel paper and tissue break immediately after contacting water? Paper is a bonded network of cellulose fibers. When exposed to water, cellulose fibers absorb water and swell quickly due to the inherent hydrophilicity of cellulose fibers[1]. The fiber-fiber joints that hold the paper together are weakened, due to the loss of hydrogen bonding and other interactions, such as polymer interdiffusion[2]. As a result, paper loses most of its strength and breaks. To help maintain some of the strength in the wet state, polymeric wet strength additives are usually added[3]. The basic function of most wet strength additives is that they form a cross-linked network with themselves, the cellulose fibers or a combination thereof[4-5].

Today, the wet strength additives used in the paper industry can be classified into two main categories: formaldehyde based resins and polyamidoamine-epichlorohydrin resins[1, 6]. Both the two categories have some issues. For example, formaldehyde based resins release formaldehyde, which is allergenic, and might lead to the development of contact dermatitis[6-7]. Polyamidoamine-epichlorohydrin resins contain low molecular weight organic chlorine by-products, which are suspected to have some mutagenic activity[8]. Therefore, more environmental friendly wet strength additives are required.

It has previously been shown that the cationic, water soluble polymer polyvinylamine (PVAm) is a good adhesive to wet cellulose when the cellulose is slightly oxidized to give aldehyde groups[3, 9]. The primary amines of PVAm form imines and aminal covalent bonds with the aldehyde groups on oxidized cellulose under mild conditions. Initially, small molecular 2, 2, 6, 6-tetramethyl-1-piperidinoxy (TEMPO) was employed for cellulose oxidation in the presence of sodium bromideand sodium hypochlorite[3, 10-11]. However, the application of TEMPO/NaClO/NaBr oxidation in the papermaking industry is limited by the requirement of a reaction pH of 10-11 and by the cost and environmental challenge of recovering and treating the waste.[10] Ren[12], a previous group member, grafted TEMPO onto PVAm, forming PVAm-g-TEMPO (PVAm-T). This way, TEMPO could be concentrated at cellulose surfaces as a result of electrostatic interaction between cationic PVAm-T and anionic cellulose surfaces. The increased surface concentration of TEMPO greatly lowered the total TEMPO requirement since the reaction with free TEMPO is dependent on the diffusion of TEMPO to the cellulose surface. Liu *et al.*[13] explored cellulose oxidation by PVAm-T in the presence of the enzyme laccase. The oxidation pH for this reaction is 5, which is more compatible to modern papermaking

technologies. Shi *et al.*[10] grafted TEMPO onto anionic poly(acrylic acid), forming PAA-T. A layer of PVAm was first pre-adsorbed to the cellulose, and then the surface was oxidized by PAA-T in the presence of laccase. The results demonstrated that cellulose was oxidized, and that strong wet adhesion of cellulose was achieved. However, the mechanism of polymer grafted TEMPO as mediator during cellulose oxidation in the presence of laccase is unknown.

This thesis focuses on developing an understanding of the role of polymer grafted TEMPO as mediator for cellulose oxidation in the presence of laccase. In the following sections, background information about polyvinylamine, TEMPO-mediated oxidation, and polymers bearing TEMPO groups are reviewed; research objectives and the thesis outline are also presented.

1.1 Literature Review

1.1.1 Polyvinylamine

Polyvinylamine (PVAm) is a weak base polyelectrolyte which has the highest primary amine content of any polyelectrolyte. PVAm cannot be directly prepared from polymerization of vinylamine due to the instability of vinylamine[14]. Several routes have been developed to synthesize PVAm[15] and the two most widely used are the hydrolysis of poly(N-vinylformamide) and the Hofmann rearrangement of polyacrylamide (see Figure 1- 1). Preparing homo-polyvinylamine is difficult and there are usually some formamide or amide groups left.

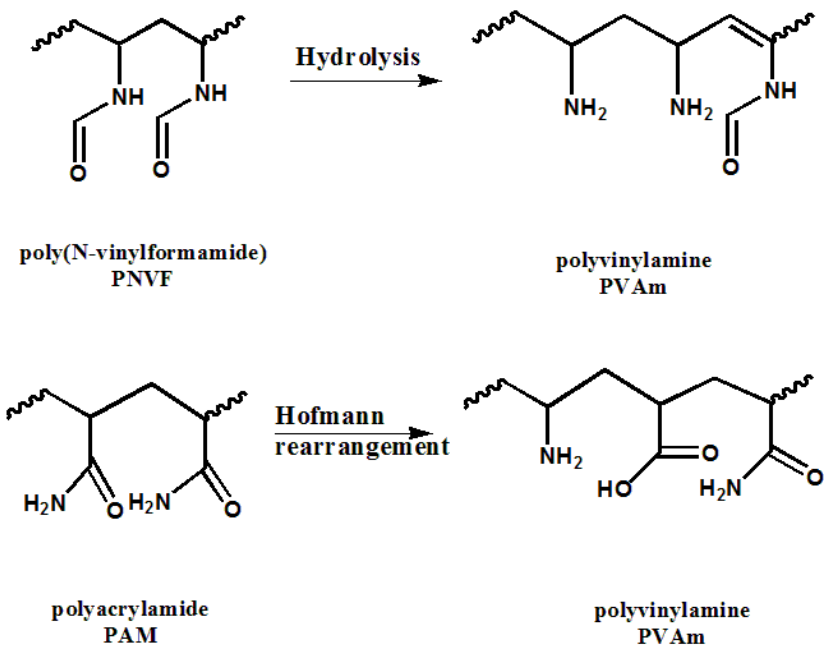

Figure 1- 1. Synthesis of PVAm from poly(N-vinylformamide) and from polyacrylamide (Figure adapted from Ref[14])

Recently, Pelton[15] reviewed the properties of PVAm and its derivatives, with specific attention focusing on modification of solid surfaces. In this section, the key properties of PVAm are summarized and relevant studies of PVAm are reviewed.

PVAm is partially ionized from pH < 2 to pH >12 due to the interaction between neighboring amine groups[16-17], also known as the polyelectrolyte effect. PVAm is highly charged at low pH, and the charge density decreases with increasing pH. PVAm is very hydrophilic, and it is not surface active without hydrophobic modification. Chen *et al.*[18] modified PVAm with hydrophobic benzyls and alkyls of different chain length, and the surface tension values of the hydrophobically modified PVAm fell on a master curve when plotting the surface tension values as a function of hydrophobicity. The hydrophobic association increased with increasing degree of hydrophobic substitution and alkyl chain length.

As a highly charged polycation, PVAm forms polyelectrolyte complexes with negatively charged polyelectrolytes, both natural and synthetic. Turro and coworkers[19] investigated

the polyelectrolyte complexes formed between PVAm and pyrene-substituted poly(acrylic acid) using photo physical techniques. Complexes were formed at both low and high pH. At low pH, hydrogen bonding was dominating whereas at high pH electrostatic interaction was the main force within the complexes. Polyelectrolyte complexes formed between PVAm and other oppositely charged polyelectrolytes, such as carboxymethyl cellulose[20-21], DNA[22], and protein[23] have also been reported. Most of these complexes show a behavior similar to other common polyelectrolyte complexes.

PVAm adsorbs on negatively charged surfaces such as silica[24], glass[25] and cellulose[26] through electrostatic interaction. The adsorption is an irreversible and kinetically controlled process[27]. The adsorbed amount is influenced by PVAm molecular weight, concentration, pH, ionic strength and presence of formamide moieties.

Amine groups on PVAm could interact with a variety of electrophilic reagents through either chemical reactions or electrostatic interaction. Various structures have been grafted onto PVAm alone or in combination with each other, such as fluorochemical chains[28], hydrophobes[29], PEG[30], dextran[31], galactose[32], p-nitrophenyl[33], nucleic acids[34], antibodies[35], phenylboronic acids[36], and peptide[37]. Some examples are shown in Figure 1-2.

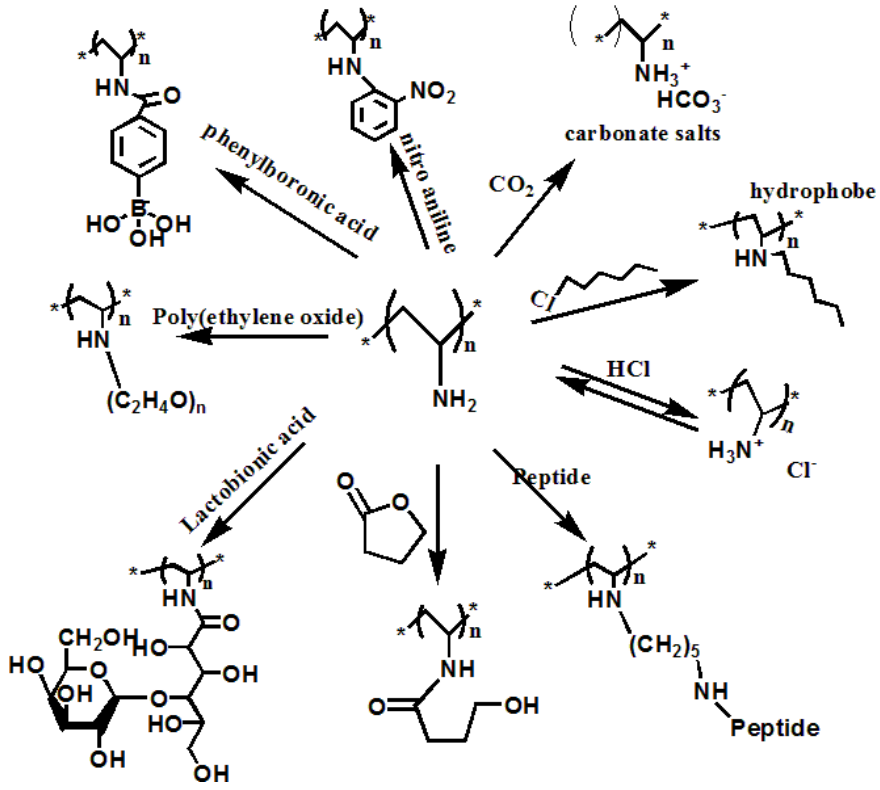

Figure 1- 2 PVAm and its derivatives (adapted from Ref [14])

At present the main commercial application of PVAm is in the papermaking industry. PVAm is mainly used as a flocculant and as a paper strength additive which improves cellulose fiber-fiber adhesion[38]. Tanaka's group[39] reported that both dry and wet tensile strength of paper increased with the addition of PVAm. Isogai and coworkers[8, 40] compared PVAm and other cationic polymers as paper wet strength additives and found that the wet strength was remarkably enhanced when cellulose fibers were oxidized by 2,2,6,6-Tetramethyl-1-piperidinyloxy (TEMPO). Zhang *et al.*[41] prepared a polymeric UV-absorber for cotton through grafting benzotriazole type UV absorber onto cationic polyvinylamine. Pelton's group has a series of publications describing PVAm and its derivatives as paper wet strength additives. DiFlavio *et al.*[3, 42] systematically investigated PVAm as a wet strength additive for paper and confirmed the covalent bond formation between amines of PVAm and aldehydes of the oxidized cellulose. Li *et al.*[11] and Kurosu *et al.*[37] compared the wet strength performance of PVAm with proteins and polypeptide containing amine groups and found that the higher the amine content the stronger the wet strength. Feng *et al.*[43-44] applied polyelectrolyte complexes of carboxymethyl cellulose

(CMC) and PVAm as cellulose wet adhesives. Chen *et al.*[45-46] grafted phenylboronic acid to PVAm, which resulted in strong adhesion to never-dried cellulose surfaces. Miao *et al.*[47-48] synthesized PVAm microgels, and compared the wet strength enhancement of PVAm microgels with linear PVAm. Wen *et al.*[49-50] designed microgels with PVAm physically absorbed on the surfaces, and found that only a monolayer of PVAm was enough to provide strong cellulose wet adhesion.

Wagberg's group has reported that antibacterial cellulose fibers can be obtained by modifying them with PVAm and its derivatives. Westman *et al.*[29] assessed the antibacterial properties of PVAm and alkyl modified PVAm against gram-negative *E. coli* and gram-positive bacillus subtilis. The antibacterial activity of PVAm depends on PVAm concentration and the type of bacteria. PVAm modified with a six carbon long alkyl chain was potent against *E. coli* while PVAm with an eight carbon long chain was more active against *B. subtilis*. Illergard *et al.*[51-52] continued this work and evaluated the antibacterial properties of fibers modified by polyelectrolyte multilayers. The number of bacteria was reduced by 99.9% even in the presence of nutrients. Griffiths' group[53] designed an antibacterial cellulose film by attaching the head of a bacteriophage onto pre-adsorbed polyvinylamine through electrostatic interaction. The net positively charged tails of the bacteriophage were left free to capture and lyse bacteria.

1.1.2 Cellulose Oxidation with small molecular TEMPO

2, 2, 6, 6-tetramethyl-1-piperidinoxy (TEMPO) is a typical free nitroxyl radical which has an unpaired electron between the nitrogen and oxygen atom. TEMPO is very stable at room temperature and as a result, the storage and transportation of TEMPO are less limited by moisture, temperature, or atmosphere than other radicals[54-56]. TEMPO is a typical redox species which can be both oxidized and reduced by chemical and electrochemical reactions. The oxidized form is called oxoammonium cation (TEMPO+) and the reduced form is called hydroxylamine (TEMPOH). TEMPO, TEMPO+ and TEMPOH transform into each other[57] (see Figure 1- 3).

More interestingly, TEMPO takes part in disproportionation reactions at acidic conditions (pH <3), producing the TEMPO oxoammonium cation and hydroxylamine[55, 58] (see Figure 1- 4). The acid-catalyzed disproportionation reaction is reversible, and when pH > 3 the equilibrium shifts to the left, TEMPO+ and TEMPOH+ disappear and TEMPO is reformed. It is worth noting that acid plays an important role in the disproportionation of TEMPO. TEMPOH and TEMPOH+ are electrochemically inactive under acidic conditions[59]. They are usually converted into TEMPO in applications, such as alcohol

oxidation. The disproportionation of TEMPO under acid conditions is applied to design redox functional materials, which will be discussed in chapter 2.

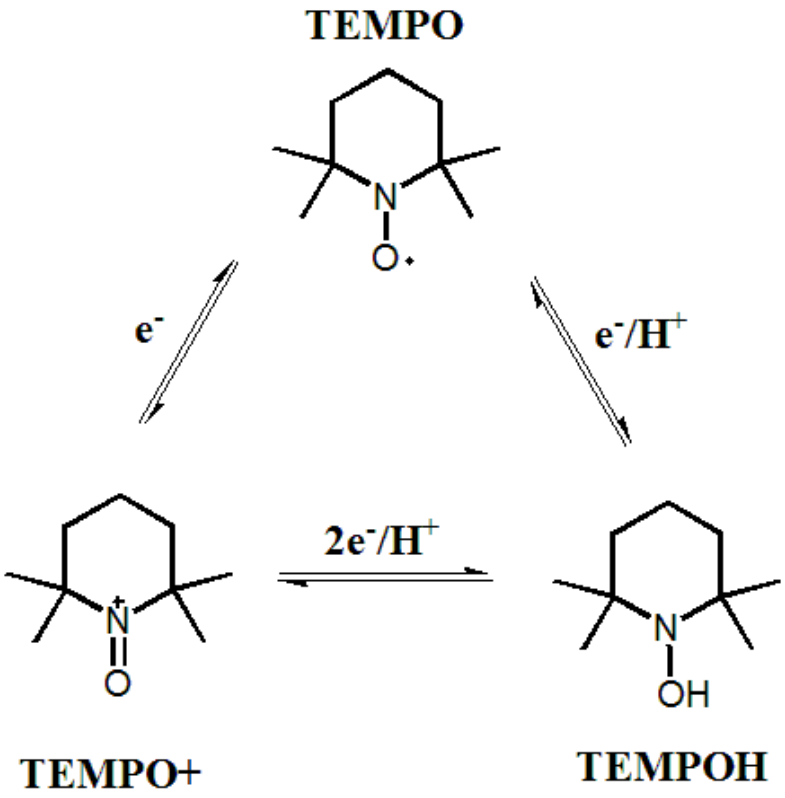

Figure 1- 3. TEMPO, TEMPO+ and TEMPOH (Figure reproduced from Ref[57])

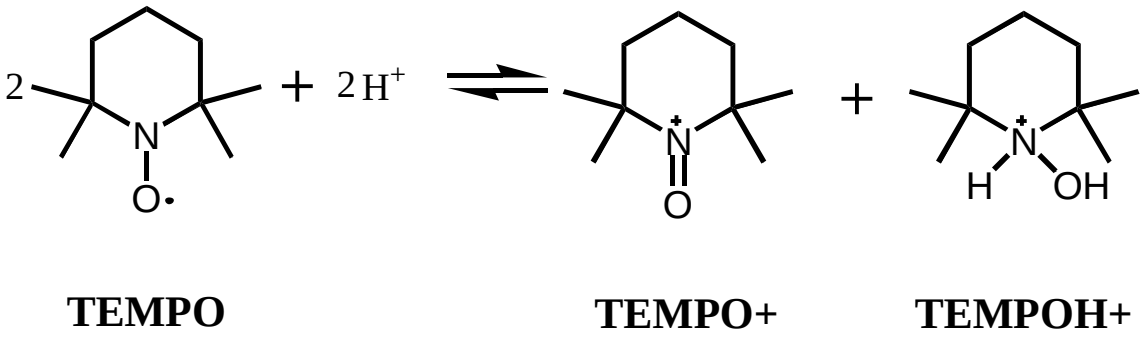

Figure 1- 4. Acid-catalyzed disproportionation of TEMPO (Figure reproduced from Ref[56])

The use TEMPO in the oxidation of small alcohols has a long history[60]. In 1994 De Nooy *et al.*[61] for the first time reported the use of TEMPO for the oxidation of primary alcohols of some water-soluble polysaccharides. Over the past 20 years TEMPO has been extensively investigated for the oxidation of various polysaccharides, both water-soluble[62-63] and water-insoluble[64]. Among these investigations, TEMPO-mediated oxidation of cellulose has received most attention. Today, the research around TEMPO-mediated oxidation of cellulose mainly focuses on two areas: activation of cellulose surfaces through introduction of aldehyde and carboxyl groups[65] and the preparation of nanocellulose[66]. In this thesis, attention is focused on the activation of cellulose surfaces.

The most outstanding characteristic of TEMPO-mediated oxidation is its high selectivity towards primary alcohols in the presence of secondary alcohols[62]. TEMPO itself cannot oxidize alcohol groups; it first needs to be converted to its corresponding oxoammonium cation using a primary oxidant. TEMPO-mediated oxidation systems for cellulose oxidation are briefly introduced in the following section, and the benefits and drawbacks of each system are summarized.

Figure 1- 5 shows a schematic of cellulose oxidation by the TEMPO/NaClO/NaBr system. TEMPO+ is continuously regenerated *in situ* by NaClO/NaBr. TEMPO+ contacts a primary alcohol of cellulose, and form an adduct. The formed adduct decomposes to an aldehyde group and a TEMPOH. The TEMPOH molecule is re-oxidized to TEMPO, forming a cycle. The aldehyde groups can be further oxidized to carboxyl groups by a similar cycle. The TEMPO/NaClO/NaBr system is most efficient at pH 10-11. Lower pH limits the oxidation rate, whereas too high pH lowers the conversion of hypochlorite to

hypobromite, which might also become rate limiting[67-68]. Isogai's group has extensively investigated the oxidation of cellulose and other polysaccharides using the TEMPO/NaClO/NaBr system[63-64, 69-71]. The ratio of aldehyde and carboxyl groups in the oxidized products is influenced by many factors including pH, NaClO concentration, NaBr concentration, oxidation time, and the nature of the substrates[69, 72-73]. The carboxyl content in TEMPO-oxidized cellulose fibers is usually in the range of 0.1-1 mmol/g and the aldehyde content in the range of 0.05-0.3 mmol/g[69]. Oxidation usually takes less than two hours, and slight depolymerisation of cellulose fibers occurs.

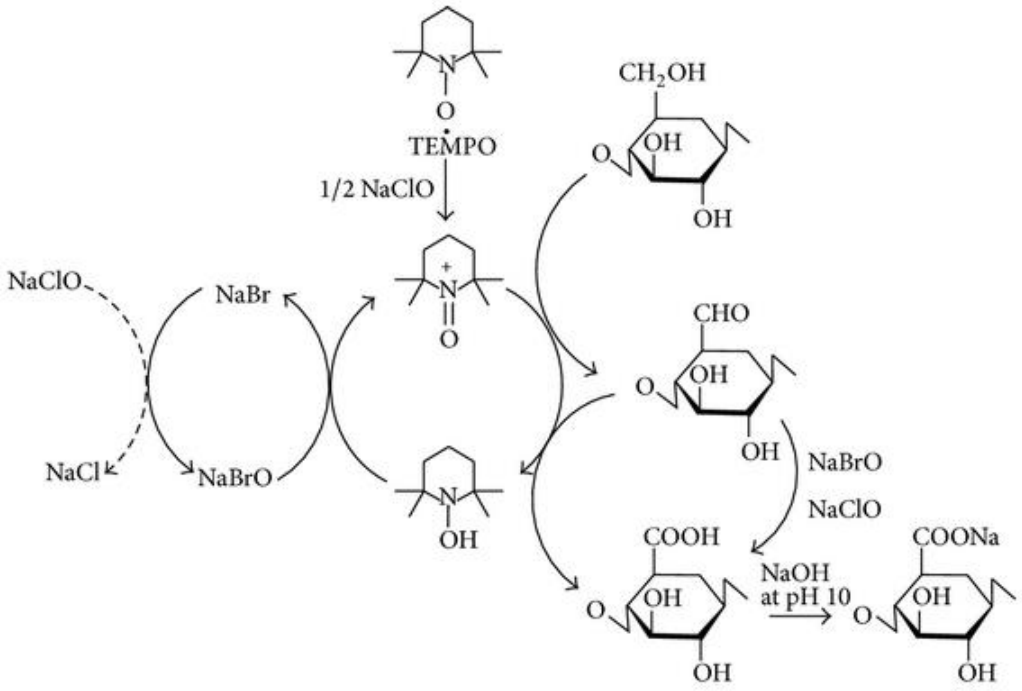

Figure 1- 5. Schematic of cellulose oxidation by the TEMPO/NaClO/NaBr (Figure reproduced from Ref[74])

In 1999 Zhao *et al.*[75] reported the use of TEMPO/NaClO/$NaClO_2$ for oxidation of primary alcohols of small organic substrates and Isogai *et al.*[76-77] later adapted this method for the oxidation of polysaccharides. The oxidation procedure is similar to TEMPO/NaClO/NaBr (see Figure 1- 6). However, compared to the conventional TEMPO/NaClO/NaBr system, the TEMPO/NaClO/$NaClO_2$ system reacts at acidic and neutral conditions (pH 3-7). More importantly, all aldehyde groups produced in the

intermediate stage are further oxidized to carboxyl groups, thus no aldehyde groups remain in the final products. The carboxyl content after this reaction is usually in the range of 0.3-1 mmol/g for bleached wood pulp[78]. The oxidation usually takes 1-3 days, and the oxidized cellulose maintains higher degree of polymerization than when oxidized by the conventional TEMPO/NaClO/NaBr system.

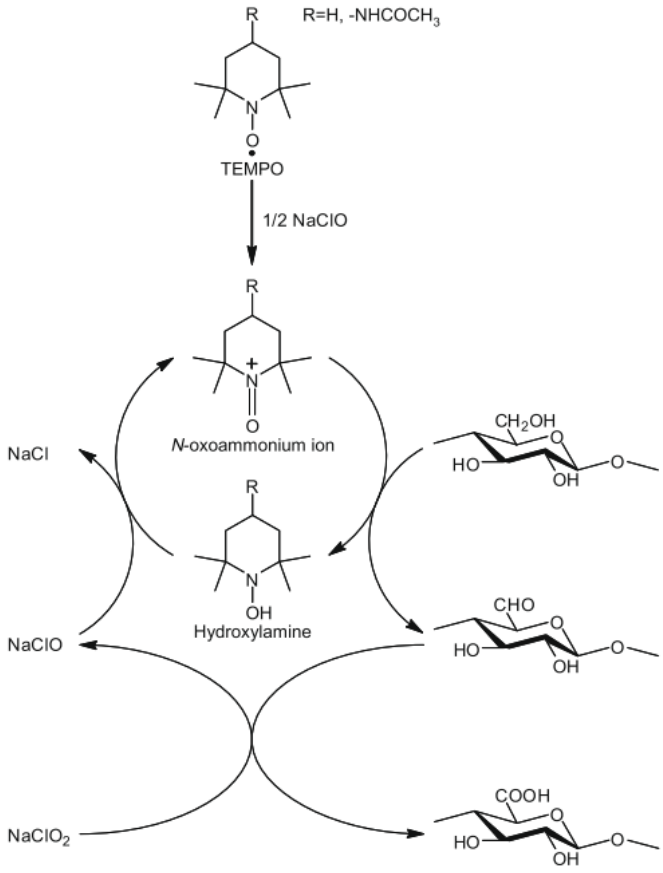

Figure 1- 6. Schematic of cellulose oxidation by TEMPO/NaClO/$NaClO_2$ (Figure reproduced from Ref[77])

Some oxidizing enzymes, for example laccase, can take the place of sodium hypochlorite as the oxidant[62] in TEMPO-mediated oxidation. Laccase is a multi-copper oxidase present in many plants, fungi, and microorganisms. It has various potential applications in the pulp and paper industry including delignification, pitch removal, pulp biografting and deinking of old newsprint[79]. During laccase oxidation of polysaccharides (see Figure 1-

7), TEMPO diffuses into the laccase enzyme pocket, where TEMPO+ is continuously regenerated *in situ* by the enzyme. The oxoammonium cation then diffuses out of the enzyme and contact a primary hydroxyl groups of cellulose, resulting in an aldehyde group and a TEMPOH. The TEMPOH is converted to TEMPO through oxidation or reaction with a TEMPO+. As in the case with TEMPO/NaClO/NaBr, the aldehyde group can be further oxidized to a carboxyl group by a similar procedure. Oxygen is consumed and the only side product is water. The oxidation is usually performed at pH 4-6 and both aldehyde and carboxyl groups are obtained in the oxidized products. The ratio of aldehyde to carboxyl groups in the oxidized product depends on the source of laccase and the substrate. Mathew *et al.*[80] oxidized granular potato starch using the TEMPO/laccase/O_2 system and showed that the primary alcohols are more easily converted to aldehyde groups than further converted to carboxyl groups. Aracri *et al.*[81-82] systematically investigated the oxidation of sisal cellulose fibers by laccase in the presence of three different mediators: sinapyl aldehyde, ferulic acid, and TEMPO. The results demonstrated that TEMPO was the most effective mediator. The aldehyde content was 0.1-0.2 mmol/g and the carboxyl content was 0.2-0.3 mmol/g of sisal cellulose fibers, both of which increased by 100%-200% compared to the untreated sisal cellulose fibers. The increased aldehyde and carboxyl group content contributed to the dry and wet strength of handsheet prepared from the oxidized sisal cellulose fibers[83]. However, some degradation of the cellulose fibers was also observed[83]. The main drawbacks of the laccase oxidation system are slow reaction rate, and low conversion rate. Laccase oxidation usually takes 18-48 h[84].

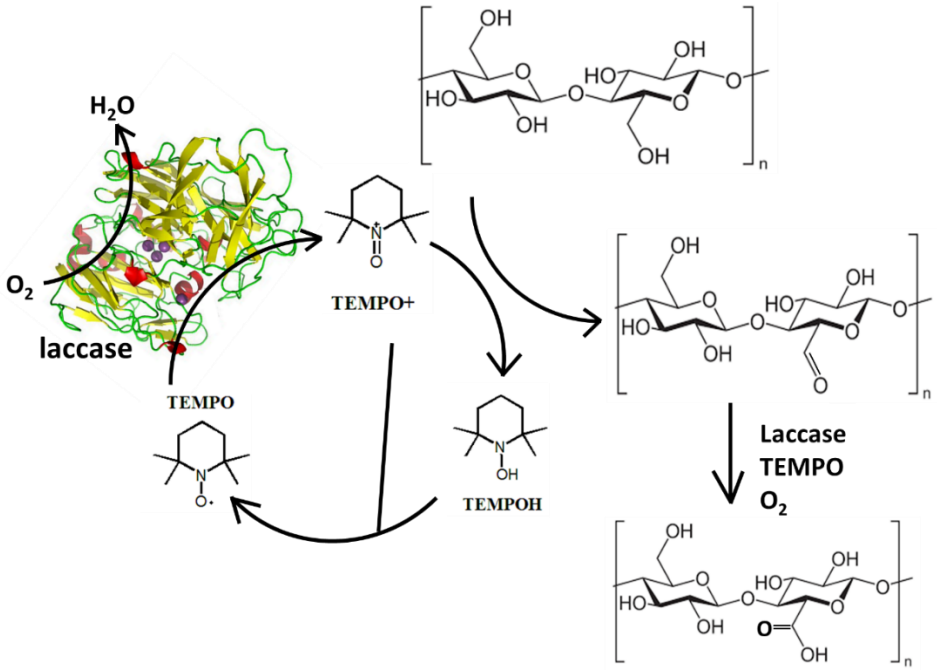

Figure 1- 7 Schematic of cellulose oxidation by TEMPO/laccase/O_2 system (Figure adapted from Ref[62])

Recently, Isogai's group[85-86] developed an electro-mediated TEMPO oxidation system (see Figure 1- 8). In this reaction TEMPO or one of its derivatives, such as 4-acetamido-TEMPO, is continuously oxidized to the corresponding oxoammonium cation at the electrode surface under a suitable potential. The oxoammonium cation can then oxidize the primary alcohols of cellulose. TEMPOH is formed which is re-oxidized to TEMPO at the electrode. The electro-mediated TEMPO oxidation is usually performed at neutral or alkaline pH. The aldehyde content in the oxidized regenerated cellulose fibers was 0.2-0.6 mmol/g and the carboxyl content was 0.3-1.1 mmol/g of regenerated cellulose fibers[86]. Electro-mediated TEMPO oxidation is more environmental friendly since less chemicals are used and the oxidation process can be controlled by the reaction potential. However, the reaction is very slow and usually takes 1-2 days.

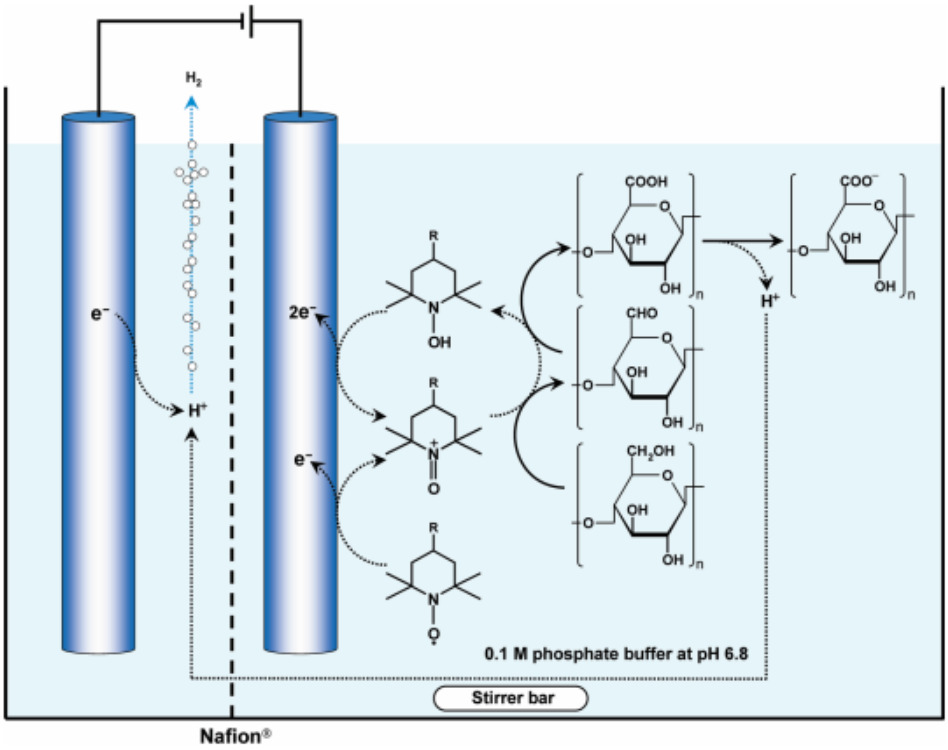

Figure 1- 8 Schematic of cellulose oxidation by electro-mediated TEMPO oxidation system (Figure reproduced from Ref[86])

Table 1-1 summarizes the comparison of cellulose oxidation by different TEMPO-mediated oxidation systems. TEMPO-mediated oxidation has many benefits, such as high selectivity towards primary alcohols, high reaction yield, catalytic usage of TEMPO, and only slightly degradation of polysaccharides[62]. However, the practical utility of TEMPO in the papermaking industry is challenged by two difficulties. First, large volumes of TEMPO solutions in wood pulp fiber processing would have a financial and environmental impact. Second, though NaClO is cheap and has already been used in pulp bleaching, the requirement of pH 10-11 for TEMPO/NaClO/NaBr is not compatible with current papermaking technologies.

Table 1-1. Comparison of different TEMPO-mediated oxidation systems for cellulose oxidation

TEMPO-mediated oxidation system	Primary oxidant	pH	Oxidation time	Example of oxidation substrate, carboxyl and aldehyde contents in products
TEMPO NaBr NaClO	NaClO	10-11	<2h	regenerated cellulose fibers[69]: carboxyl: 0.1-1 mmol/g aldehyde: 0.05-0.3 mmol/g
TEMPO $NaClO_2$ NaClO	NaClO	3-7	1-3days	bleached wood pulp[78] carboxyl: 0.3-1 mmol/g aldehyde content: 0
TEMPO laccase O_2	O_2	4-6	18 hr-2 days	sisal cellulose fibers[82]: carboxyl: 0.2-0.3 mmol/g aldehyde: 0.1-0.2 mmol/g
TEMPO electrode	electron	6-10	1-2 days	regenerated cellulose fibers[86] carboxyl: 0.2-1.1 mmol/g aldehyde: 0.1-0.6 mmol/g

1.1.3 Cellulose Oxidation with immobilized TEMPO

TEMPO recovery and reuse is a way to reduce cost. For that purpose, TEMPO has been immobilized onto polymers[87], silica gels[88], and other carriers[89-90]. Compared to homogenous oxidation systems, immobilized TEMPO oxidation offers several benefits including convenient product isolation and purification, reusing of bound TEMPO, and lower toxicity of TEMPO[62]. However, the immobilized TEMPO seems more appropriate in the oxidation of small molecular organic substrates than large polymeric substrates. There are few reports of cellulose oxidation using immobilized TEMPO. Araki and Iida[91] reported the recovery and recycling of monomethoxy poly(ethylene glycol) grafted TEMPO after oxidation of cellulose nanowhiskers. 80% of the monomethoxy poly(ethylene glycol) grafted TEMPO could be recovered after every cycle but the oxidation efficiency decreased with the number of reusing cycles of the immobilized TEMPO. However, it is still a challenge to recover the immobilized TEMPO from large volumes of TEMPO solutions in papermaking industry.

Instead of recovering and recycling TEMPO from solutions, the strategy of our group is to reduce the total TEMPO requirement. As mentioned in the above section, TEMPO needs to contact a primary alcohol on cellulose in order to initiate oxidation. In the case of small molecular TEMPO, TEMPO molecules in the bulk have to diffuse to the surface of the substrate to contact and oxidize a primary alcohol. Our strategy has been to graft TEMPO onto a PVAm, forming PVAm-T. The cationic PVAm-T spontaneously adsorbs onto negatively charged surfaces of cellulose through electrostatic interaction. As a result, the TEMPO concentration at the cellulose surfaces is much higher than in the bulk solution, and therefore the total TEMPO requirement is reduced. Ren and Liu[12-13] oxidized regenerated cellulose membranes with PVAm-T at pH 10.5 in the presence of NaClO/NaBr. A TEMPO substitution of 0.9 mol% was enough to efficiently oxidize regenerated cellulose membranes and give strong wet cellulose adhesion[13].

In order to lower the reaction pH, Liu *et al.*[13] replaced NaClO and NaBr with the enzyme laccase and O_2 and used PVAm-T to oxidize regenerated cellulose membranes at pH is 5. For the PVAm-T/laccase/O_2 system about 10 mol% TEMPO substitution was required to reach a similar level of wet adhesion as for NaClO/NaBr. Shi *et al.*[10] grafted TEMPO onto anionic poly(acrylic acid), forming PAA-T. Also for this TEMPO-grafted polymer it was found that around 10 mol% TEMPO substitution was required to achieve strong wet adhesion in combination with PVAm. The discrepancy between the level of grafting required for efficient oxidation using NaClO/NaBr and laccase/O_2 is yet to be explained.

The topic of this thesis is to develop an understanding of the role of polymer grafted TEMPO as mediator for cellulose oxidation in the presence of laccase, and to help to control cellulose oxidation. Thorough characterization of the properties of polymer grafted TEMPO is essential to understand their role as oxidation mediator.

1.1.4 Polymers bearing TEMPO groups

In addition to serving as oxidation mediator, TEMPO is also widely used in polymer science as free radical catcher[92] in controlled radical polymerization and as spin-label/probe[93-94] in measurements of polymer chain mobility. The application of polymers bearing TEMPO groups in organic electronic devices[95] has also recently received great attention. TEMPO-grafting to a variety of polymer backbones have been reported including poly(meth)acrylate[96], polystyrene[97], DNA [98], cellulose derivatives [99], and polyacrylamide[100].

TEMPO has also been grafted to polymers to design redox responsive materials. Bergbreiter and coworkers[101] grafted TEMPO onto poly(N-isopropylacrylamide)

(PNIPAM), and found that the lower critical solution temperature (LCST) of the new polymer could be tuned between 18° and 35-40 °C by oxidation ($NaClO/H_2O$) and reduction (ascorbic acid). The authors claimed that tuning of the LCST close to human body temperature makes it interesting for in vivo drug delivery. Schattling *et al.*[102] designed thermo-, light- and redox triple responsive polymers by introducing TEMPO and azobenzene moieties to PNIPAM. The LCST of the new polymers could be controlled independently by temperature, light, and redox chemicals. Bertrand *et al.*[103] designed a new homopolymer, poly(TEMPO methacrylate), which exhibits upper critical solution temperature (UCST) behavior in alcohol-water mixtures. The UCST could be tuned by either chemical or electrical stimuli. Yoshida *et al.*[104-105] designed a diblock copolymer, poly(4-vinylbenzyloxy-TEMPO)-block-polystyrene, which showed oxidation-induced micellization properties in carbon tetrachloride due to the acid-catalyzed disproportionation of TEMPO moieties.

Polymer bearing TEMPO groups is a typical redox polymer. Redox polymer refers to a polymer containing redox species which can be reversibly oxidized and reduced. Cyclic voltammetry is the most frequently used technique to study the redox properties of redox polymers[106]. In this technique, a working electrode potential is linearly scanned between an initial value, E_1, and a predetermined limit value, E_2, where the direction of the scan is reversed (Figure 1- 9). The cyclic voltammogram can be obtained when plotting the current at the working electrode as a function of the applied potential.

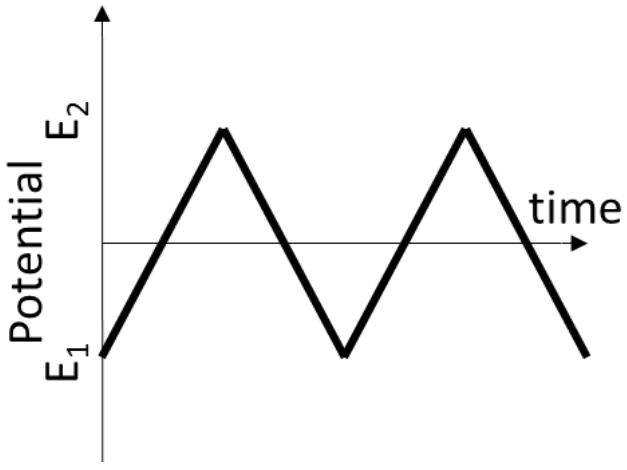

Figure 1- 9 Cyclic voltammetry potential waveform

Unlike free redox species in solution, cyclic voltammograms of redox polymer films deposited on an electrode may display two completely different behaviors. Figure 1- 10 shows cyclic voltammogramms of redox polymer films in two ideal cases. In the first ideal case, two symmetrical peaks can be seen. The peak potential separation (i.e. E_{pc} - E_{pa}, where E_{pc} is the cathodic peak potential, and E_{pa} is the anodic peak potential) is 0 mV[142] and the half-peak width (FWHM) is 90.6/n mV, where n is the number of electron difference between the oxidized and reduced states of redox species. The cathodic peak current (i_{pc}) equals the anodic peak current (i_{pa}). This behavior is called thin layer behavior[106] which is also the characteristic of "surface-confined behavior". In the second ideal case, the peak potential separation (E_{pc} - E_{pa}) in the cyclic voltammogram is 59/n mV and the cathodic peak current (i_{pc}) equals the anodic peak current (i_{pa}). This behavior is called "semi-infinite diffusion behavior"[106], which is well-known from studies of free redox species in solution. In most situations, redox polymer films show an intermediate behavior between the two ideal cases.

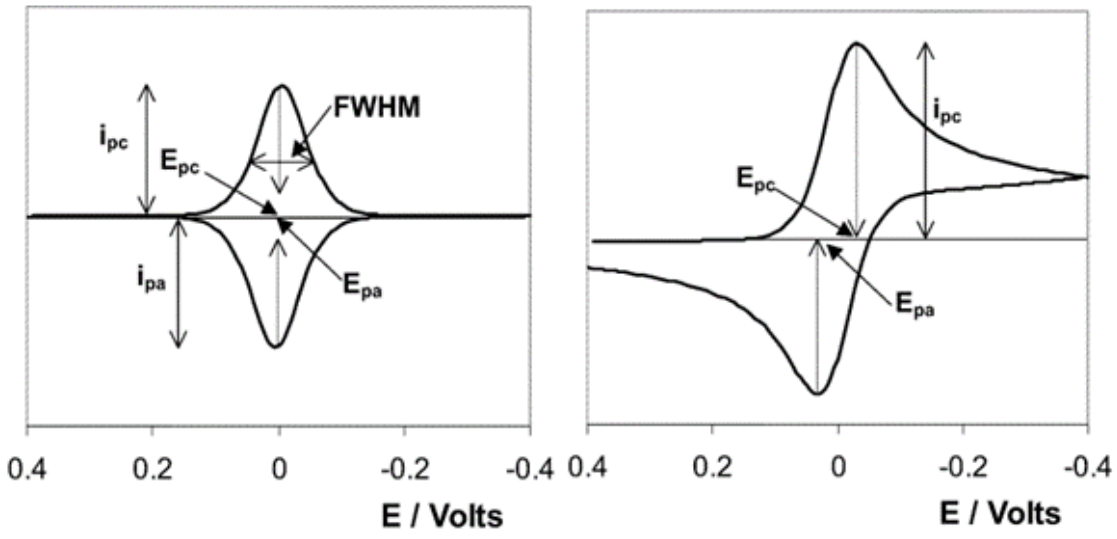

Figure 1- 10 Cyclic voltammograms of redox polymer films deposited on electrode surface. Left, thin layer (surface-confined) behavior. Right, semi-infinite diffusion behavior. (Figure adapted from Ref[107])

Charge transport does not only take place between the electrode and the nearby redox species, but also within the redox polymer films deposited on the electrode. The charge

transport within redox polymer films follows the laws of diffusion. The charge transport is usually considered to occur through physical displacement of redox species, electron hopping between neighboring redox species, or through a combination of both[108]. For example, when free redox species are physically entrapped in oppositely charged polyelectrolyte films, both processes occur. However, when redox species are covalently bound to polymer chains, the physical displacement of redox species contribute little to the charge transport, and the electron hopping between neighboring redox species dominate the charge transport in the films. The charge transport in the redox polymer films can be estimated by the charge transport diffusion coefficient D[109].

If the potential scan rate is very slow and the redox polymer film is sufficiently thin and has a large charge transport diffusion coefficient, the active redox species in the redox polymer films are rapidly electrolyzed when the applied external potential is changed. This results in a thin layer behavior of the cyclic voltammogram. The peak potential separation is 0 V under ideal conditions and the behavior can be expressed by the following equation[107]:

$$i_p = \frac{n^2 F^2 \Gamma}{4RT} \nu \tag{1-1}$$

where i_p is the peak current, F is the Faraday constant, R is the gas constant, n is the number of charge difference between the oxidized and reduced states of a redox species, Γ is the coverage of the redox-active species, T is the temperature, and ν is the scan rate. Γ can be determined by

$$\Gamma = \frac{Q}{nFA} \tag{1-2}$$

Where Q is the Faradaic charge passed during oxidation or reduction of redox species.

If the potential scan rate is fast and the redox polymer film is very thick, with a small charge transport diffusion coefficient, the response of redox species at the film's outer boundary is much slower than near the electrode surface. In this case a semi-infinite charge diffusion prevails and the Randles-Sevcik equation is applicable[110], as in the case of the semi-infinite diffusion of redox species in solutions.

$$i_p = 0.4463nFAC\left(\frac{nF\nu D}{RT}\right)^{\frac{1}{2}} \tag{1-3}$$

Where A is the surface area of the working electrode, C is the concentration of redox species.

In most situations an intermediate behavior can be observed. The type of the behavior can be predicted by the relationship between i_p and ν. $i_p \propto \nu$ means the redox process in redox films exhibits mainly thin layer (surface-confined) behavior, whereas $i_p \propto \sqrt{\nu}$ means that the redox process exhibits a mainly semi-infinite diffusion behavior.

1.1.5 Cellulose wet strength measurements

To investigate the adhesion of PVAm and other polymers to wet cellulose, Pelton's group have developed a 90° peel test[3] where regenerated cellulose dialysis membranes are used as model cellulose. The sample preparation and the peel test are illustrated in Figure 1-11. Cellulose laminates are prepared by adding a known amount of polymer between two pieces of regenerated cellulose membranes. The laminates are attached on a freely rotating aluminum wheel by double sided tape. The top membrane is peeled off and the peel force is recorded. The laminate of cellulose membranes with the added PVAm is assumed as a macroscopic model of fiber-fiber adhesion[111].

The wet peel test has several advantages compared to traditional paper testing methods[111], including rapid and reproducible measurements and the ability to accurately control the amount of polymer in the contact zone. The cellulose membranes can be chemically or physically modified prior to the addition of the adhesive polymer and thus the impact various surface groups can be systematically evaluated. The cellulose membranes can easily be characterized before and after peeling using e.g. microscopy and spectroscopic techniques in order to correlate morphology and chemical composition of the interface to the wet adhesion.

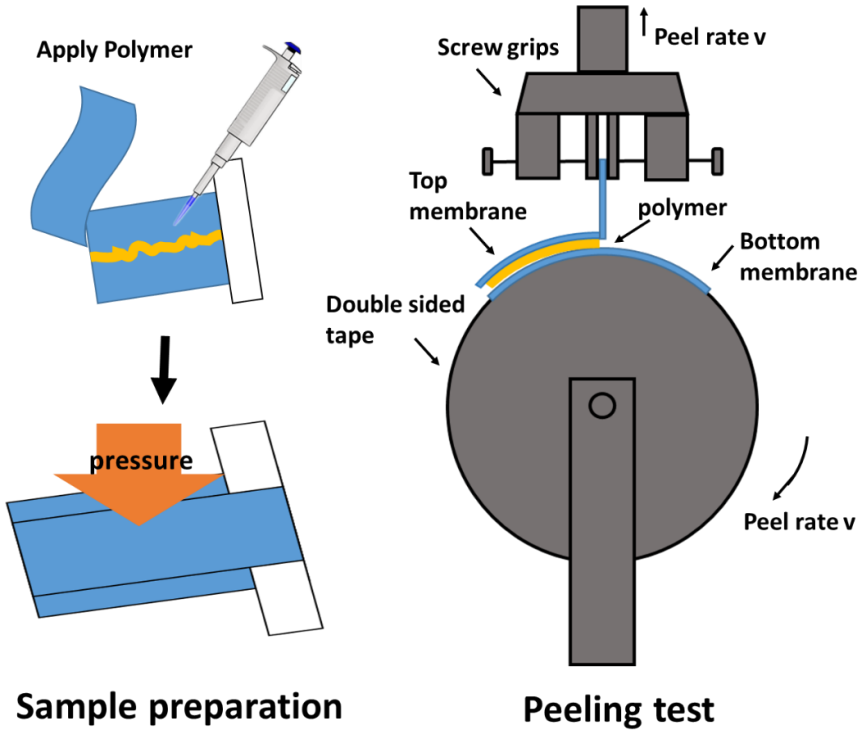

Figure 1- 11 Schematic of sample preparation and cellulose wet adhesion peel test (Figure adapted from Ref[111])

1.2 Objectives

As mentioned in the cellulose oxidation section, our previous results demonstrate that polymer grafted TEMPO can oxidize cellulose well in the presence of laccase and facilitate forming strong wet adhesion between cellulose membranes with the help of PVAm. The present view of the TEMPO/laccase/O_2 oxidation mechanism is that the reaction is mediated by small molecular TEMPO that is diffusing between the active enzyme site on the laccase, where it is oxidized to TEMPO+, and a primary alcohol on the cellulose surface, where it is forms an adduct that decomposes to TEMPOH and an aldehyde group. However, by grafting TEMPO to a polymer backbone the TEMPO mobility is greatly reduced and a diffusion based model is no longer plausible.

The overall objective of this work is to establish an alternative mechanism that can describe the polymer grafted TEMPO mediated oxidation in the presence of laccase, and

to control cellulose oxidation with the polymer grafted TEMPO. The specific objectives are listed below:

1. Characterize the properties of poly(acrylic acid-g-TEMPO) and polyvinylamine-g-TEMPO(PVAm-T). Properties of poly(acrylic acid-g-TEMPO) and polyvinylamine-g-TEMPO are important for their functions as oxidation mediator. The results can provide information of grafted TEMPO, on the interaction between TEMPO and TEMPO moieties, and the interaction between TEMPO pendant groups and the polymer backbones.

2. Investigate the electron transport between TEMPO moieties of polymers. The result would help the understanding of the electron transport between laccase and cellulose.

3. Investigate the interaction of polyvinylamine-g-TEMPO and laccase, the redox properties of polyvinylamine-g-TEMPO/laccase complexesas well as the process of polyvinylamine-g-TEMPO adsorbing onto and oxidizing cellulose. The result would help understanding the mechanism of oxidation process, and the role of grafted TEMPO as the enzyme mediator.

4. Determine aldehyde groups on cellulose surfaces introduced by PVAm-T/laccase complexes, and identify relationships between PVAm-T and cellulose oxidation, redox properties of PVAm-T/laccase complexes and cellulose oxidation. The result would help to realize controlling cellulose oxidation with polymer grafted TEMPO.

1.3 Thesis outline

Chapter 1: Introduction. This chapter presents the thorough background of this project, including the literature review of polyvinylamine, cellulose oxidation and polymers bearing TEMPO groups.Research objectives and thesis outline are also listed in this chapter.

Chapter 2: This chapter investigates the phase behavior of aqueous poly(acrylic acid-g-TEMPO) (PAA-T). PAA-T was characterized by FTIR and conductometric titration. The phase behavior, intrinsic viscosity, ionization, and surface activity of PAA-T aqueous solutions were investigated. This chapter has been published in *Macromolecules*[112].

Chapter 3: This chapter investigates redox properties of polyvinylamine-g-TEMPO (PVAm-T) in multilayer films with sodium poly(styrene sulfonate) (PSS). The solution properties of PVAm-T were studied. The redox properties of PVAm-T/PSS multilayer films and their stability upon external electro stimuli were studied. The electron transport between TEMPO moieties within the redox films was also investigated. This chapter is submitted to *ACS Applied Materials & Interfaces*.

Chapter 4: This chapter investigates PVAm-T/laccase complexes adsorbing onto, oxidizing, and promoting wet adhesion of cellulose. The PVAm-T/laccase complexes phase behavior, stability, adsorption properties, and redox properties were studied. The electron transport between TEMPO moieties within PVAm-T/laccase complexes adsorbed on an electrode was studied. The aldehyde density on oxidized cellulose surfaces was measured and the relationship between redox-active TEMPO and aldehyde density produced by PVAm-T/laccase complexes adsorbed on cellulose was built. This chapter is under preparation for publication.

Chapter 5: This chapter summarizes the major contributions of this study.

References

(1) Espy, H. H. The Mechanism of Wet-Strength Development in Paper - a Review. *Tappi Journal* **1995,** *78* (4), 90-99.

(2) Delgado-Fornue, E.; Contreras, H. J.; Toriz, G.; Allan, G. G. Adhesion between Cellulosic Fibers in Paper. *Journal of Adhesion Science and Technology* **2011,** *25* (6-7), 597-614.

(3) DiFlavio, J.-L.; Bertoia, R.; Pelton, R.; Leduc, M. *The Mechanism of Polyvinylamine Wet-Strengthing* 2005. p 1293-1316.

(4) Xu, G. G. Z.; Yang, C. Q. X.; Deng, Y. L. Applications of Bifunctional Aldehydes to Improve Paper Wet Strength. *Journal of Applied Polymer Science* **2002,** *83* (12), 2539-2547.

(5) Gustafsson, E.; Pelton, R.; Wågberg, L. Rapid Development of Wet Adhesion between Carboxymethylcellulose Modified Cellulose Surfaces Laminated with Polyvinylamine Adhesive. *Acs Applied Materials & Interfaces* **2016,** *8* (36), 24161-24167.

(6) Linhart, F. The Practical Application of Wet-Strength Resins. In *Applications of Wet-End Paper Chemistry*; Springer, 1995, pp 102-119.

(7) Ginebreda, A.; Guillén, D.; Barceló, D.; Darbra, R. M. Additives in the Paper Industry. In *Global Risk-Based Management of Chemical Additives I*; Springer, 2011, pp 11-34.

(8) Saito, T.; Isogai, A. Wet Strength Improvement of TEMPO-Oxidized Cellulose Sheets Prepared with Cationic Polymers. *Industrial & Engineering Chemistry Research* **2007,** *46* (3), 773-780.

(9) DiFlavio, J.-L. The Wed Adhesion of Polyvinylamine to Cellulose. *PhD thesis* **2013**.

(10) Shi, S.; Pelton, R.; Fu, Q.; Yang, S. Comparing Polymer-Supported TEMPO Mediators for Cellulose Oxidation and Subsequent Polyvinylamine Grafting. *Industrial & Engineering Chemistry Research* **2014,** *53* (12), 4748-4754.

(11) Li, X.; Pelton, R. Enhancing Wet Cellulose Adhesion with Proteins. *Industrial & Engineering Chemistry Research* **2005,** *44* (19), 7398-7404.

(12) Pelton, R.; Ren, P.; Liu, J.; Mijoloyic, D. Polyvinylamine-Graft-TEMPO Adsorbs onto, Oxidizes, and Covalently Bonds to Wet Cellulose. *Biomacromolecules* **2011,** *12* (4), 942-948.

(13) Liu, J.; Pelton, R.; Obermeyer, J. M.; Esser, A. Laccase Complex with Polyvinylamine Bearing Grafted TEMPO Is a Cellulose Adhesion Primer. *Biomacromolecules* **2013,** *14* (8), 2953-60.

(14) Pinschmidt, R. K., Jr. Polyvinylamine at Last. *Journal of Polymer Science Part a-Polymer Chemistry* **2010,** *48* (11), 2257-2283.

(15) Pelton, R. Polyvinylamine: A Tool for Engineering Interfaces. *Langmuir* **2014,** *30* (51), 15373-82.

(16) Katchalsky, A.; Mazur, J.; Spitnik, P. Section Ii: Polybase Properties of Polyvinylamine. *Journal of Polymer Science* **1957,** *23* (104), 513-532.

(17) Lewis, E. A.; Barkley, J.; Stpierre, T. Calorimetric Titration of Poly(Vinylamine) and Poly(Iminoethylene) *Macromolecules* **1981,** *14* (3), 546-551.

(18) Chen, X. N.; Wang, Y.; Pelton, R. pH-Dependence of the Properties of Hydrophobically Modified Polyvinylamine. *Langmuir* **2005,** *21* (25), 11673-11677.

(19) Arora, K. S.; Turro, N. J. Photophysical Investigations of Interpolymer Interactions in Solutions of a Pyrene Substituted Poly(Acrylic Acid), Polyvinylamine, Poly(1-Aminoacrylic Acid), and Poly(1-Acetylaminoacrylic Acid). *Journal of Polymer Science Part B-Polymer Physics* **1987,** *25* (2), 243-262.

(20) Feng, X.; Pelton, R. Carboxymethyl Cellulose: Polyvinylamine Complex Hydrogel Swelling. *Macromolecules* **2007,** *40* (5), 1624-1630.

(21) Feng, X.; Pelton, R.; Leduc, M.; Champ, S. Colloidal Complexes from Poly(vinyl amine) and Carboxymethyl Cellulose Mixtures. *Langmuir* **2007,** *23* (6), 2970-2976.

(22) Slita, A.; Kasyanenko, N.; Nazarova, O.; Gavrilova, I.; Eropkina, E.; Sirotkin, A.; Smirnova, T.; Kiselev, O.; Panarin, E. DNA–Polycation Complexes Effect of Polycation Structure on Physico-Chemical and Biological Properties. *Journal of Biotechnology* **2007,** *127* (4), 679-693.

(23) Scorilas, A.; Diamandis, E. P. Polyvinylamine-Streptavidin Complexes Labeled with a Europium Chelator: A Universal Detection Reagent for Solid-Phase Time Resolved Fluorometric Applications. *Clinical Biochemistry* **2000,** *33* (5), 345-350.

(24) Meszaros, R.; Thompson, L.; Bos, M.; de Groot, P. Adsorption and Electrokinetic Properties of Polyethylenimine on Silica Surfaces. *Langmuir* **2002,** *18* (16), 6164-6169.

(25) Widmaier, J.; Shulga, A.; Pefferkorn, E.; Champ, S.; Auweter, H. Reconformation of Polyvinylamine Adsorbed on Glass Fibers. *Journal of Colloid and Interface Science* **2003,** *264* (1), 277-283.

(26) Geffroy, C.; Labeau, M. P.; Wong, K.; Cabane, B.; Stuart, M. A. C. Kinetics of Adsorption of Polyvinylamine onto Cellulose. *Colloids and Surfaces a-Physicochemical and Engineering Aspects* **2000,** *172* (1-3), 47-56.

(27) Shulga, A.; Widmaier, J.; Pefferkorn, E.; Champ, S.; Auweter, H. Kinetics of Adsorption of Polyvinylamine on Cellulose Fibers ii. Adsorption from Electrolyte Solutions. *Journal of Colloid and Interface Science* **2003,** *258* (2), 228-234.

(28) Wang, S. W.; Marchant, R. E. Fluorocarbon Surfactant Polymers: Effect of Perfluorocarbon Branch Density on Surface Active Properties. *Macromolecules* **2004,** *37* (9), 3353-3359.

(29) Westman, E.-H.; Ek, M.; Enarsson, L.-E.; Wagberg, L. Assessment of Antibacterial Properties of Polyvinylamine (PVAm) with Different Charge Densities and Hydrophobic Modifications. *Biomacromolecules* **2009,** *10* (6), 1478-1483.

(30) Holland, N. B.; Xu, Z.; Vacheethasanee, K.; Marchant, R. E. Structure of Poly(ethylene oxide) Surfactant Polymers at Air-Water and Solid-Water Interfaces. *Macromolecules* **2001,** *34* (18), 6424-6430.

(31) Sen Gupta, A.; Wang, S.; Link, E.; Anderson, E. H.; Hofmann, C.; Lewandowski, J.; Kottke-Marchant, K.; Marchant, R. E. Glycocalyx-Mimetic Dextran-Modified Poly(vinyl amine) Surfactant Coating Reduces Platelet Adhesion on Medical-Grade Polycarbonate Surface. *Biomaterials* **2006,** *27* (16), 3084-3095.

(32) Mokhtari, H.; Pelton, R.; Jin, L. Q. Polyvinylamine-g-Galactose Is a Route to Bioactivated Silica Surfaces. *Journal of Colloid and Interface Science* **2014,** *413,* 86-91.

(33) Roth, I.; Simon, F.; Bellmann, C.; Seifert, A.; Spange, S. Fabrication of Silica Particles Functionalized with Chromophores and Amino Groups Using Synergism of Poly(Vinylamine) Adsorption and Nucleophilic Aromatic Substitution with Fluoroaromatics. *Chemistry of Materials* **2006,** *18* (20), 4730-4739.

(34) Overberger, C. G.; Chen, C. C. The Reaction of Optically - Active Nucleic-Acid Base Derivative with Polyvinylamine in Nonaqueous Media- Grafting Reaction. *Journal of Polymer Science Part C-Polymer Letters* **1985,** *23* (6), 345-348.

(35) Rupp, S.; von Schickfus, M.; Hunklinger, S.; Eipel, H.; Priebe, A.; Enders, D.; Pucci, A. A Shear Horizontal Surface Acoustic Wave Sensor for the Detection of Antigen-Antibody Reactions for Medical Diagnosis. *Sensors and Actuators B-Chemical* **2008,** *134* (1), 225-229.

(36) Chen, W.; Cui, Y.; Pelton, R. The Remarkable Adhesion of Cellulose Hydrogel to Polyvinylamine Bearing Pendent Phenylboronic Acid. *Journal of Adhesion Science and Technology* **2011,** *25* (6-7), 543-555.

(37) Kurosu, K.; Pelton, R. Simple Lysine-Containing Polypeptide and Polyvinylamine Adhesives for Wet Cellulose. *Journal of Pulp and Paper Science* **2004,** *30* (8), 228-232.

(38) Hubbe, M. A. Prospects for Maintaining Strength of Paper and Paperboard Products While Using Less Forest Resources: A Review. *Bioresources* **2014,** *9* (1), 1634-1763.

(39) Wu, Z. H.; Chen, S. P.; Tanaka, H. Function Mechanisms of Polyamines in Rosin Sizing under Neutral Papermaking Conditions. *Journal of Applied Polymer Science* **2001,** *80* (12), 2185-2190.

(40) Uematsu, T.; Matsui, Y.; Kakiuchi, S.; Isogai, A. Cellulose Wet Wiper Sheets Prepared with Cationic Polymer and Carboxymethyl Cellulose Using a Papermaking Technique. *Cellulose* **2011,** *18* (4), 1129-1138.

(41) Ma, W.; Jiang, X.; Liu, Y.; Tang, B. T.; Zhang, S. F. Synthesis of a Novel Water-Soluble Polymeric Uv-Absorber for Cotton. *Chinese Chemical Letters* **2011,** *22* (12), 1489-1491.

(42) DiFlavio, J.-L.; Pelton, R.; Leduc, M.; Champ, S.; Essig, M.; Frechen, T. The Role of Mild TEMPO-NaBr-NaClO Oxidation on the Wet Adhesion of Regenerated Cellulose Membranes with Polyvinylamine. *Cellulose* **2007,** *14* (3), 257-268.

(43) Feng, X.; Pouw, K.; Leung, V.; Pelton, R. Adhesion of Colloidal Polyelectrolyte Complexes to Wet Cellulose. *Biomacromolecules* **2007,** *8* (7), 2161-2166.

(44) Feng, X.; Zhang, D.; Pelton, R. Adhesion to Wet Cellulose - Comparing Adhesive Layer-by-Layer Assembly to Coating Polyelectrolyte Complex Suspensions. *Holzforschung* **2009,** *63* (1), 28-32.

(45) Chen, W.; Leung, V.; Kroener, H.; Pelton, R. Polyvinylamine-Phenylboronic Acid Adhesion to Cellulose Hydrogel. *Langmuir* **2009,** *25* (12), 6863-6868.

(46) Chen, W.; Lu, C.; Pelton, R. Polyvinylamine Boronate Adhesion to Cellulose Hydrogel. *Biomacromolecules* **2006,** *7* (3), 701-702.

(47) Miao, C.; Leduc, M.; Pelton, R. The Influence of Polyvinylamine Microgels on Paper Strength. *Journal of Pulp and Paper Science* **2008,** *34* (1), 69-75.

(48) Miao, C.; Chen, X.; Pelton, R. Adhesion of Poly(Vinylamine) Microgels to Wet Cellulose. *Industrial & Engineering Chemistry Research* **2007,** *46* (20), 6486-6493.

(49) Wen, Q.; Pelton, R. Design Rules for Microgel-Supported Adhesives. *Industrial & Engineering Chemistry Research* **2012,** *51* (28), 9564-9570.

(50) Wen, Q.; Pelton, R. Microgel Adhesives for Wet Cellulose: Measurements and Modeling. *Langmuir* **2012,** *28* (12), 5450-5457.

(51) Illergard, J.; Wagberg, L.; Ek, M. Bacterial-Growth Inhibiting Properties of Multilayers Formed with Modified Polyvinylamine. *Colloids and Surfaces B-Biointerfaces* **2011,** *88* (1), 115-120.

(52) Illergard, J.; Romling, U.; Wagberg, L.; Ek, M. Biointeractive Antibacterial Fibres Using Polyelectrolyte Multilayer Modification. *Cellulose* **2012,** *19* (5), 1731-1741.

(53) Anany, H.; Chen, W.; Pelton, R.; Griffiths, M. W. Biocontrol of Listeria Monocytogenes and Escherichia Coli O157:H7 in Meat by Using Phages Immobilized on Modified Cellulose Membranes. *Applied and Environmental Microbiology* **2011,** *77* (18), 6379-6387.

(54) Tebben, L.; Studer, A. Nitroxides: Applications in Synthesis and in Polymer Chemistry. *Angewandte Chemie-International Edition* **2011,** *50* (22), 5034-5068.

(55) Sen, V. D.; Golubev, V. A. Kinetics and Mechanism for Acid-Catalyzed Disproportionation of 2,2,6,6-Tetramethylpiperidine-1-oxyl. *Journal of Physical Organic Chemistry* **2009,** *22* (2), 138-143.

(56) Golubev, V. A.; Sen, V. D.; Kulyk, I. V.; Aleksandrov, A. L. Mechanism of the Oxygen Disproportionation of Ditert-Alkylniteoxyl Radicals. *Bulletin of the Academy of Sciences of the USSR, Division of chemical science* **1975,** *24* (10), 2119-2126.

(57) Ma, Y.; Loyns, C.; Price, P.; Chechik, V. Thermal Decay of TEMPO in Acidic Media Via an N-Oxoammonium Salt Intermediate. *Organic & biomolecular chemistry* **2011,** *9* (15), 5573-5578.

(58) Ponedel'kina, I. Y.; Khaibrakhmanova, E. A.; Odinokov, V. N. Nitroxide-Catalyzed Selective Oxidation of Alcohols and Polysaccharides. *Russian Chemical Reviews* **2010,** *79* (1), 63-75.

(59) Coseri, S.; Biliuta, G.; Simionescu, B. C.; Stana-Kleinschek, K.; Ribitsch, V.; Harabagiu, V. Oxidized Cellulose-Survey of the Most Recent Achievements. *Carbohydrate Polymers* **2013,** *93* (1), 207-215.

(60) Anelli, P. L.; Biffi, C.; Montanari, F.; Quici, S. Fast and Selective Oxidation of Primary Alcohols to Aldehydes or to Carboxylic-Acids and of Secondary

Alcohols to Ketones Mediated by Oxoammonium Salts under 2-Phase Conditions. *Journal of Organic Chemistry* **1987,** *52* (12), 2559-2562.

(61) De Nooy, A.; Besemer, A.; Van Bekkum, H. Highly Selective TEMPO Mediated Oxidation of Primary Alcohol Groups in Polysaccharides. *Recueil des Travaux Chimiques des Pays-Bas* **1994,** *113* (3), 165-166.

(62) Bragd, P. L.; van Bekkum, H.; Besemer, A. C. TEMPO-Mediated Oxidation of Polysaccharides: Survey of Methods and Applications. *Topics in Catalysis* **2004,** *27* (1-4), 49-66.

(63) Kato, Y.; Matsuo, R.; Isogai, A. Oxidation Process of Water-Soluble Starch in TEMPO-Mediated System. *Carbohydrate Polymers* **2003,** *51* (1), 69-75.

(64) Saito, T.; Isogai, A. TEMPO-Mediated Oxidation of Native Cellulose. The Effect of Oxidation Conditions on Chemical and Crystal Structures of the Water-Insoluble Fractions. *Biomacromolecules* **2004,** *5* (5), 1983-1989.

(65) Watanabe, E.; Tamura, N.; Saito, T.; Habu, N.; Isogai, A. Preparation of Completely C6-Carboxylated Curdlan by Catalytic Oxidation with 4-Acetamido-TEMPO. *Carbohydrate Polymers* **2014,** *100*, 74-79.

(66) Kuramae, R.; Saito, T.; Isogai, A. TEMPO-Oxidized Cellulose Nanofibrils Prepared from Various Plant Holocelluloses. *Reactive & Functional Polymers* **2014,** *85*, 126-133.

(67) de Nooy, A. E. J.; Besemer, A. C.; van Bekkum, H. Highly Selective Nitroxyl Radical-Mediated Oxidation of Primary Alcohol Groups in Water-Soluble Glucans. *Carbohydrate Research* **1995,** *269* (1), 89-98.

(68) deNooy, A. E. J.; Besemer, A. C.; vanBekkum, H. On the Use of Stable Organic Nitroxyl Radicals for the Oxidation of Primary and Secondary Alcohols. *Synthesis-Stuttgart* **1996,** (10), 1153-1174.

(69) Isogai, A.; Kato, Y. Preparation of Polyglucuronic Acid from Cellulose by TEMPO-Mediated Oxidation. *Cellulose* **1998,** *5* (3), 153-164.

(70) Kitaoka, T.; Isogai, A.; Onabe, F. Chemical Modification of Pulp Fibers by TEMPO-Mediated Oxidation. *Nordic Pulp & Paper Research Journal* **1999,** *14* (4), 279-284.

(71) Saito, T.; Isogai, A. A Novel Method to Improve Wet Strength of Paper. *Tappi Journal* **2005,** *4* (3), 3-8.

(72) Saito, T.; Okita, Y.; Nge, T. T.; Sugiyama, J.; Isogai, A. TEMPO-Mediated Oxidation of Native Cellulose: Microscopic Analysis of Fibrous Fractions in the Oxidized Products. *Carbohydrate Polymers* **2006,** *65* (4), 435-440.

(73) Saito, T.; Shibata, I.; Isogai, A.; Suguri, N.; Sumikawa, N. Distribution of Carboxylate Groups Introduced into Cotton Linters by the TEMPO-Mediated Oxidation. *Carbohydrate Polymers* **2005,** *61* (4), 414-419.

(74) Isogai, A.; Saito, T.; Fukuzumi, H. TEMPO-Oxidized Cellulose Nanofibers. *Nanoscale* **2011,** *3* (1), 71-85.

(75) Zhao, M.; Li, J.; Mano, E.; Song, Z.; Tschaen, D. M.; Grabowski, E. J.; Reider, P. J. Oxidation of Primary Alcohols to Carboxylic Acids with Sodium Chlorite Catalyzed by Tempo and Bleach. *The Journal of Organic Chemistry* **1999,** *64* (7), 2564-2566.

(76) Hirota, M.; Tamura, N.; Saito, T.; Isogai, A. Surface Carboxylation of Porous Regenerated Cellulose Beads by 4-Acetamide-TEMPO/NaClO/NaClO(2) System. *Cellulose* **2009,** *16* (5), 841-851.

(77) Hirota, M.; Tamura, N.; Saito, T.; Isogai, A. Oxidation of Regenerated Cellulose with NaClO2 Catalyzed by TEMPO and NaClO under Acid-Neutral Conditions. *Carbohydrate Polymers* **2009,** *78* (2), 330-335.

(78) Saito, T.; Hirota, M.; Tamura, N.; Isogai, A. Oxidation of Bleached Wood Pulp by TEMPO/NaClO/NaClO2 System: Effect of the Oxidation Conditions on Carboxylate Content and Degree of Polymerization. *Journal of Wood Science* **2010,** *56* (3), 227-232.

(79) Mayer, A. M.; Staples, R. C. Laccase: New Functions for an Old Enzyme. *Phytochemistry* **2002,** *60* (6), 551-565.

(80) Mathew, S.; Adlercreutz, P. Mediator Facilitated, Laccase Catalysed Oxidation of Granular Potato Starch and the Physico-Chemical Characterisation of the Oxidized Products. *Bioresource Technology* **2009,** *100* (14), 3576-3584.

(81) Aracri, E.; Valls, C.; Vidal, T. Paper Strength Improvement by Oxidative Modification of Sisal Cellulose Fibers with Laccase-TEMPO System: Influence of the Process Variables. *Carbohydrate Polymers* **2012,** *88* (3), 830-837.

(82) Aracri, E.; Barneto, A. G.; Vidal, T. Comparative Study of the Effects Induced by Different Laccase-Based Systems on Sisal Cellulose Fibers. *Industrial & Engineering Chemistry Research* **2012,** *51* (10), 3895-3902.

(83) Aracri, E.; Vidal, T.; Ragauskas, A. J. Wet Strength Development in Sisal Cellulose Fibers by Effect of a Laccase-TEMPO Treatment. *Carbohydrate Polymers* **2011,** *84* (4), 1384-1390.

(84) Aracri, E.; Vidal, T. Enhancing the Effectiveness of a Laccase-TEMPO Treatment Has a Biorefining Effect on Sisal Cellulose Fibres. *Cellulose* **2012,** *19* (3), 867-877.

(85) Isogai, T.; Saito, T.; Isogai, A. Wood Cellulose Nanofibrils Prepared by TEMPO Electro-Mediated Oxidation. *Cellulose* **2011,** *18* (2), 421-431.

(86) Isogai, T.; Saito, T.; Isogai, A. TEMPO Electromediated Oxidation of Some Polysaccharides Including Regenerated Cellulose Fiber. *Biomacromolecules* **2010,** *11* (6), 1593-1599.

(87) Pozzi, G.; Cavazzini, M.; Quici, S.; Benaglia, M.; Dell'Anna, G. Poly(Ethylene Glycol)-Supported TEMPO: An Efficient, Recoverable Metal-Free Catalyst for the Selective Oxidation of Alcohols. *Organic Letters* **2004,** *6* (3), 441-443.

(88) Fey, T.; Fischer, H.; Bachmann, S.; Albert, K.; Bolm, C. Silica-Supported TEMPO Catalysts: Synthesis and Application in the Anelli Oxidation of Alcohols. *The Journal of Organic Chemistry* **2001,** *66* (24), 8154-8159.

(89) Geneste, F.; Moinet, C.; Ababou-Girard, S.; Solal, F. Covalent Attachment of TEMPO onto a Graphite Felt Electrode and Application in Electrocatalysis. *New Journal of Chemistry* **2005,** *29* (12), 1520-1526.

(90) Brunel, D.; Fajula, F.; Nagy, J. B.; Deroide, B.; Verhoef, M. J.; Veum, L.; Peters, J. A.; van Bekkum, H. Comparison of Two Mcm-41 Grafted TEMPO Catalysts in Selective Alcohol Oxidation. *Applied Catalysis A: General* **2001,** *213* (1), 73-82.

(91) Araki, J.; Iida, M. Surface Carboxylation of Cellulose Nanowhiskers Using Mpeg-TEMPO: Its Recovery and Recycling. *Polymer Journal* **2016**.

(92) Nicolas, J.; Guillaneuf, Y.; Lefay, C.; Bertin, D.; Gigmes, D.; Charleux, B. Nitroxide-Mediated Polymerization. *Progress in Polymer Science* **2013,** *38* (1), 63-235.

(93) Lappan, U.; Wiesner, B.; Scheler, U. Rotational Dynamics of Spin-Labeled Polyacid Chain Segments in Polyelectrolyte Complexes Studied by Cw Epr Spectroscopy. *Macromolecules* **2015,** *48* (11), 3577-3581.

(94) Tan, L.; Chen, S.; Ping, Z.; Shen, Y. Nitroxide Spin Probe Study of Probe Size, Hydrogen Bonding and Polymer Matrix Rigidity Effects on Poly (Acrylic Acid)/Poly (Ethylene Oxide) Complexes. *Magnetic Resonance in Chemistry* **2003,** *41* (7), 481-488.

(95) Janoschka, T.; Hager, M. D.; Schubert, U. S. Powering up the Future: Radical Polymers for Battery Applications. *Advanced Materials* **2012,** *24* (48), 6397-6409.

(96) Vlad, A.; Rolland, J.; Hauffman, G.; Ernould, B.; Gohy, J. F. Melt-Polymerization of Tempo Methacrylates with Nano Carbons Enables Superior Battery Materials. *Chemsuschem* **2015,** *8* (10), 1692-1696.

(97) Suga, T.; Sugita, S.; Ohshiro, H.; Oyaizu, K.; Nishide, H. P‐and N‐Type Bipolar Redox‐Active Radical Polymer: Toward Totally Organic Polymer‐Based Rechargeable Devices with Variable Configuration. *Advanced Materials* **2011,** *23* (6), 751-754.

(98) Qu, J.; Morita, R.; Satoh, M.; Wada, J.; Terakura, F.; Mizoguchi, K.; Ogata, N.; Masuda, T. Synthesis and Properties of DNA Complexes Containing 2, 2, 6, 6‐Tetramethyl‐1‐Piperidinoxy (TEMPO) Moieties as Organic Radical Battery Materials. *Chemistry–A European Journal* **2008,** *14* (11), 3250-3259.

(99) Qu, J.; Khan, F. Z.; Satoh, M.; Wada, J.; Hayashi, H.; Mizoguchi, K.; Masuda, T. Synthesis and Charge/Discharge Properties of Cellulose Derivatives Carrying Free Radicals. *Polymer* **2008,** *49* (6), 1490-1496.

(100) Koshika, K.; Chikushi, N.; Sano, N.; Oyaizu, K.; Nishide, H. A TEMPO-Substituted Polyacrylamide as a New Cathode Material: An Organic Rechargeable Device Composed of Polymer Electrodes and Aqueous Electrolyte. *Green Chemistry* **2010,** *12* (9), 1573-1575.

(101) Fu, H.; Policarpio, D. M.; Batteas, J. D.; Bergbreiter, D. E. Redox-Controlled 'Smart'polyacrylamide Solubility. *Polymer Chemistry* **2010,** *1* (5), 631-633.

(102) Schattling, P.; Jochum, F. D.; Theato, P. Multi-Responsive Copolymers: Using Thermo-, Light-and Redox Stimuli as Three Independent Inputs Towards Polymeric Information Processing. *Chemical Communications* **2011,** *47* (31), 8859-8861.

(103) Bertrand, O.; Vlad, A.; Hoogenboom, R.; Gohy, J. F. Redox-Controlled Upper Critical Solution Temperature Behaviour of a Nitroxide Containing Polymer in Alcohol-Water Mixtures. *Polymer Chemistry* **2016,** *7* (5), 1088-1095.

(104) Yoshida, E.; Tanaka, T. Oxidation-Induced Micellization of a Diblock Copolymer Containing Stable Nitroxyl Radicals. *Colloid and Polymer Science* **2006,** *285* (2), 135-144.

(105) Yoshida, E. Control of Micellization Induced by Disproportionation of 2, 2, 6, 6-Tetramethylpiperidine-1-Oxyl Supported on Side Chains of a Block Copolymer. *Colloid and Polymer Science* **2009,** *287* (11), 1365-1368.

(106) Bott, A. W. Electrochemical Techniques for the Characterization of Redox Polymers. *Current Separations* **2001,** *19* (3), 71-75.

(107) Rusling, J. F.; Forster, R. J. Electrochemical Catalysis with Redox Polymer and Polyion–Protein Films. *Journal of Colloid and Interface Science* **2003,** *262* (1), 1-15.

(108) Calvo, E. Electrochemically Active Lbl Multilayer Films: From Biosensors to Nanocatalysts. *Multilayer Thin Films: Sequential Assembly of Nanocomposite Materials, Second Edition* **2012**, 1003-1038.

(109) Murray, R. W. Chemically Modified Electrodes. *Electroanalytical chemistry* **1984,** *13*, 191-368.

(110) Casado, N.; Hernández, G.; Sardon, H.; Mecerreyes, D. Current Trends in Redox Polymers for Energy and Medicine. *Progress in Polymer Science* **2016,** *52*, 107-135.

(111) wen, q. Microgel Based Adhesives for Wet Paper Strength. *PhD thesis* **2012**.

(112) Fu, Q.; Gray, Z. R.; van der Est, A.; Pelton, R. H. Phase Behavior of Aqueous Poly(Acrylic Acid-g-TEMPO). *Macromolecules* **2016,** *49* (13), 4935-4939.

Chapter 2 Phase Behavior of Aqueous Poly(acrylic acid-g-TEMPO)

In chapter 2, all experiments were conducted by myself. Zachary R. Gray (undergraduate student) helped me with polymer synthesis, and Professor Art van der Est (Department of Chemistry, Brock University) helped me with the electron paramagnetic resonance spectroscopy measurement. I plotted the experimental data and Dr. Robert Pelton helped to analyze the data. The paper was initially drafted by myself, and edited later to final version by Dr. Robert Pelton. This chapter has been published in *Macromolecules*, 2016, 49 (13), pp 4935-4939.

Macromolecules

Article

pubs.acs.org/Macromolecules

Phase Behavior of Aqueous Poly(acrylic acid-*g*-TEMPO)

Qiang Fu,[†] Zachary Russell Gray,[†] Art van der Est,[‡] and Robert H. Pelton*[,†]

[†]Department of Chemical Engineering, McMaster University, Hamilton, Ontario, Canada L8S 4L7

[‡]Department of Chemistry, Brock University, St. Catharines, Ontario, Canada L2S 3A1

Supporting Information

ABSTRACT: Poly(acrylic acid) with grafted TEMPO moieties, PAA-T, phase separates over the pH range 2−4, whereas at lower and higher pH, the polymer is water-soluble. The pH range of the two-phase region increases linearly with the content of grafted TEMPO moieties. As evidenced by surface tension measurements, the PAA-T molecules have little hydrophobic character. We propose that at low pH PAA-T is an amphoteric polymer that, in addition the anionic carboxyl groups, contains cationic species resulting from the disproportion of TEMPO at low pH. Furthermore, we propose that two-phase regions occur near the isoelectric points of the polymer, suggesting that phase separation is due to electrostatically driven association of polymer molecules.

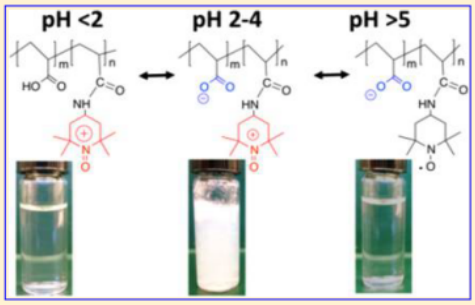

INTRODUCTION

TEMPO (2,2,6,6-tetramethylpiperidine-1-oxyl) is a stable nitroxyl radical that is widely used in polymer science in controlled radical polymerizations,[1−3] and as a spin-label, facilitating measurements of polymer chain mobility.[4,5] TEMPO-grafted water-soluble polymers are redox-active and have potential applications in energy storage.[6−8] TEMPO is also widely used as an oxidation mediator for polysaccharides because it selectively oxidizes primary alcohols to the corresponding aldehydes and carboxylic acids.[9,10] Our work has focused on the use of TEMPO grafted to water-soluble polymers to oxidize cellulose. In one variation we have shown that polyvinylamine with grafted TEMPO (PVAm-T) adsorbs onto cellulose and induces oxidation to generate surface aldehydes, which then form covalent linkages with amine groups on the PVAm-T chains.[11,12] Thus, oxidation and grafting occur in a single step. In another variation, we prepared poly(acrylic acid-*g*-TEMPO) (PAA-T) and showed that it could be a useful oxidant for cellulose.[13] Although the oxidative properties of PAA-T have been long known,[14] there has been no reported studies of PAA-T's unusual phase behaviors.

In ongoing work with PAA-T, we measured the water solubility characteristics across the pH range. We were surprised to observe the reversible phase separation of PAA-T polymers under acidic conditions (pH 2−4.5), depending upon the polymer concentration and the degree of TEMPO substitution. At pH values less than 2 and above 4.5, the PAA-T was soluble. To us, these behaviors were surprising, and the explanation was not obvious. Herein we present a systematic series of experiments describing PAA-T phase behaviors in water and after evidence for our explanation of the driving force for phase separation.

EXPERIMENTAL SECTION

Materials. Poly(acrylic acid) (M_w 100 kDa, 35 wt % in H_2O), 4-amino-TEMPO, 1-ethyl-3-(3-(dimethylamino)propyl)carbodiimide (EDC), and *N*-hydroxysulfosuccinimide sodium salt (sulfo-NHS) were all purchased from Sigma-Aldrich and used as received. All experiments were performed with water from a Millipore Milli-Q system.

Preparation of PAA-T. Scheme 1 shows the carbodiimide facilitated conjugation of 4-amino-TEMPO PAA carboxyl groups

Scheme 1. Preparation of PAA-T

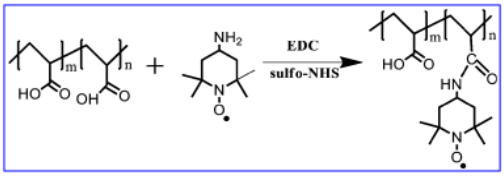

following the method we described previously.[13] Table 1 summarizes the grafting conditions and resulting PAA-T compositions. In a typical experiment, 2.0 g of PAA solution (35 wt %) was dissolved in 200 mL of water in a beaker. 2.84 g of EDC and 0.1 g of sulfo-NHS were added to initiate the reaction. The reaction was stirred for 30 min at room temperature, and the pH was maintained at 6.0 with 0.1 M HCl and 0.1 M NaOH solutions. 0.81 g of 4-amino-TEMPO dissolved in 100 mL of water was slowly dropped into above solution, and the pH of the mixed solution was maintained at 6.0 for 4 h with 0.1 M HCl and 0.1 M NaOH solutions. The resulting solution was dialyzed (MWCO 12−14 kDa) against water for 2 weeks. The purified polymer was

Received: May 11, 2016
Revised: June 14, 2016
Published: June 22, 2016

DOI: 10.1021/acs.macromol.6b00977
Macromolecules 2016, 49, 4935−4939

Table 1. Grafting Conditions and the Resulting PAA-T Compositions Where the Degree of Substitution Is the Mole Percentage of Substituted Carboxyl Groups

designation	PAA (35 wt %) (g)	4-amino-TEMPO (g)	EDC (g)	sulfo-NHS (g)	deg of substitution (DS) (%)
PAA-T18	1.0	0.25	0.87	0.05	18
PAA-T23	1.0	0.52	1.82	0.05	23
PAA-T40	2.0	0.81	2.84	0.1	40
PAA-T50	2.0	1.0	3.51	0.1	50

freeze-dried and stored in a desiccator. Conductometric titration was used to determine the carboxyl contents before and after TEMPO grafting. The grafted TEMPO contents were calculated from the change in carboxyl contents. An example of a titration curve and TEMPO contents calculation is shown in Supporting Information Figure S2 along with a description of the method.

Phase Behavior Measurements. PAA-T solutions were prepared in 5 mM KCl, and the pH was adjusted with NaOH or HCl. After 24 h aging at 25 °C, the solutions were placed in 10 mm silica cuvettes, and the optical transmittances at 600 nm were measured with a Beckman DU800 UV−vis spectrophotometer. The polymer solutions were considered single phase if the transmittance was greater than 95%, colloidal (stable and unstable) when transmittance was 90−95%, and precipitated for transmittance values less than 90%.[15]

Viscosity Measurements. The viscosity of polymer solutions was measured with a viscometer (Vibro viscometer SV-10, Japan). A water bath was used to maintain the temperature at 25 °C. Intrinsic viscosity measurements were determined using an Ubbelohde capillary viscometer (size 50, Cannon Instrument Co.). Measurements were made as functions of pH of PAA-T as functions of pH in 0.1 M KCl solutions at 25 °C. Example plots for determining intrinsic viscosity are given in the Supporting Information (Figure S3).

Electrophoresis Measurements. The electrophoretic mobility values of PAA-T copolymers at different pH were measured by a ZetaPlus Analyzer (Brookhaven Instruments Corp.) with PALS (phase analysis light scattering) Software Version 2.5. To facilitate the measurement, the copolymers were adsorbed onto 200 nm cationic, surfactant-free polystyrene latex. The samples were prepared by dropping 0.01 g/L cationic polystyrene latex into 0.2 g/L copolymer. All measurements were carried out in 5 mM KCl aqueous solution at 25 °C. The standard deviation of 10 measurements was used as an estimate of the error bars.

Normaly, PAA-T copolymers were purified by exhaustive dialysis against pure water. However, to remove possible cationic contaminates, PAA-T40 was first dialyzed against 1 M NaCl. For this, 10 mg of dried PAA-T40 sample was dissolved in 10 mL of 1 M NaCl solution and dialyzed against 1 M NaCl for 4 days and then Milli-Q water for 3 days, with changing both 1 M NaCl and Milli-Q water three times a day. After dialyzing, the polymer solution was freeze-dried to get solid sample.

Dynamic Light Scattering Measurements. Hydrodynamic diameters of the PAA-T solutions were measured by DLS with a Malven Zetasizer instrument. The laser source was 633 nm He−Ne, and the detection angle was 173°. The data were analyzed with the dispersion technology software (version 6.0). In a typical experiment 0.9 mL of 0.1 g/L PAA-T18 solution, pH 5.7, was added into a cuvette with 10 mm path length, and then the cuvette was placed in the cuvette holder. Each sample was performed 10 runs with 8 repetitions. The Z-average diameter was reported in the present work as the hydrodynamic diameter. All experiment was performed at 25 °C.

Electron Paramagnetic Resonance Spectroscopy (EPR). EPR spectroscopy was performed at room temperature on a Bruker Elexsys E580 instrument operating in CW mode. To compare the effect of pH on the intensity of the EPR signal, a 0.5 g/L PAA-T aqueous solution was prepared as described above and divided into aliquots of equal volume. The pH of each sample was then adjusted by adding concentrated HCl. The solutions were bubbled with N_2 before filling into an EPR flat cell. The relative intensities of the EPR spectra were estimated by double integration.

Surface Tension Measurements. The surface tensions of PAA and PAA-T were measured with the pendant drop method using the Kruss drop shape analysis system DSA 10. The temperature and the relative humidity were kept at 23 °C and 100% with an environmental chamber. In a typical experiment 0.3 wt % PAA-T solutions were prepared in 10 mM KCl solution at various pH. Drops were formed using a syringe with a 1.22 mm o.d. flat needle, and the drop volumes varied from 15 to 19 μL.

RESULTS

Four poly(acrylic acid-*g*-TEMPO) polymers (PAA-T) were prepared by EDC-mediated conjugation of 4-amino-TEMPO to poly(acrylic acid). The copolymer structures are shown in Scheme 1, and Table 1 summarizes the properties of four PAA-T polymers. The TEMPO contents are expressed as the mole percentage of the carboxyl groups substituted with TEMPO moieties; PAA-T40 has TEMPO groups on 40% of the acrylates (i.e., DS = 40%).

The phase behaviors of the four PAA-T polymers are summarized in Figure 1 as functions of pH and polymer

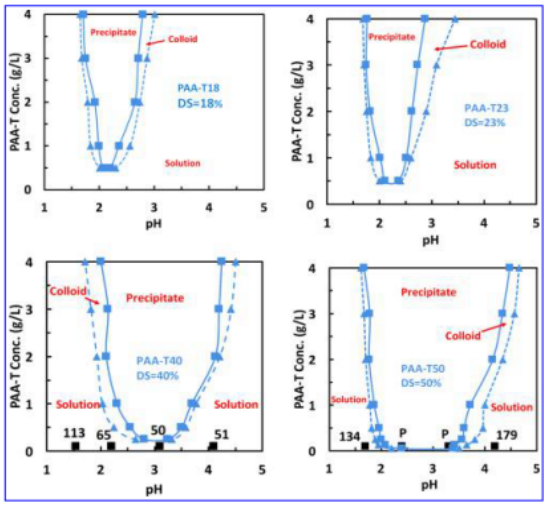

Figure 1. Phase boundaries of PAA-T as functions of pH, polymer concentration, and the degree of substitution. The black squares and numbers give average particle diameters in nm, measured by dynamic light scattering. Samples labeled "P" had no colloidal phase All measurements were carried out in 5 mM KCl aqueous solution at 25 °C.

concentrations. The phase boundary lines denote two transitions based upon the optical transmittance of the solutions: (1) the dashed line showing the transition between a true solution (transmittance at 600 nm >95%) and a colloidal dispersion (90% < %*T* < 95%), and (2) the transition between the colloidal phase and macroscopic precipitate formation (solid lines). When we first observed the precipitation at low pH, we were concerned that the amide linkages in PAA-T were hydrolyzing. To confirm our polymers were stable, a PAA-T40 copolymer solution was stirred under pH 1.5 for 4 days at room temperature, followed by dialysis and lyophilization. FTIR and conductometric titration of the 4-day-aged polymer showed no changes compared to the initial polymer.

DOI: 10.1021/acs.macromol.6b00977
Macromolecules 2016, 49, 4935−4939

The parent poly(acrylic acid) was soluble over whole pH range,[16] whereas each of the four PAA-T polymers phase separated at low pH. Precipitation was reversible. Either increasing or decreasing the pH of a suspension of precipitated polymer resulted in a single phase solution. The lower pH boundary for all of the PAA-T polymers was between pH 1.5 and 2 depending upon polymer concentration. By contrast, the pH range for the upper pH boundary was sensitive to TEMPO content. With only an 18% DS, 1 g/L PAA-T18 showed the onset of turbidity at pH 2.6 whereas the onset of phase separation for 1 g/L PAA-T50 was at pH 4. A few particles sizes from dynamic light scattering are plotted on the phase diagrams. The size distributions are broad.

The influence of TEMPO DS on phase separation is further illustrated in Figure 2 which shows ΔpH, the width of the

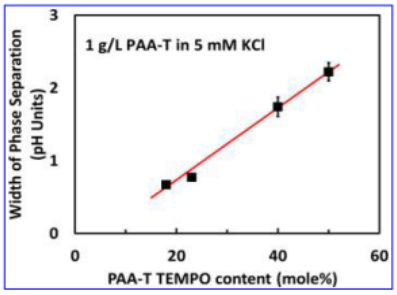

Figure 2. Width of the two phase region for 1 g/L polymer solutions as functions of the TEMPO degree of substitution. The *y*-axis error bars show the range of three measurements.

precipitation zone along the pH axis for 1 g/L PAA-T solutions as a function of TEMPO cotent. ΔpH increased linearly with TEMPO content. By contrast, we have reported the solution properties of TEMPO derivatized polyvinylamine-*g*-TEMPO.[12] PVAm-T is the polyvinylamine analogue of PAA-T, and PVAm-T is water-soluble throughout the pH range. Therefore, the phase separation behavior of PAA-T is associated with the combined presence of TEMPO and carboxyl moieties. Herein we explore the origins of the phase separation behaviors.

Changes in PAA-T chemical properties are driving phase separation at low pH and redissolution at very low pH. The following section describes disproportionation, which we propose is one of the important reactions.

TEMPO Disproportionation. A number of studies have shown that at low pH TEMPO undergoes a reversible disproportionation reaction. The stoichiometry of the reaction is shown in Scheme 2. Free TEMPO undergoes disproportionation at pH < 3.[17,18] From the perspective of influencing phase behavior, a TEMPO disproportion reaction converts two neutral species to cationic nitrogen species.

Scheme 2. Disproportionation of TEMPO under Acid Condition

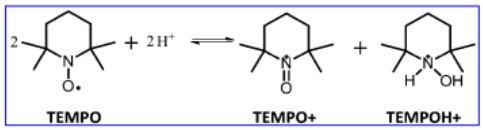

We have found only one group reporting the disproportionation of polymer-bound TEMPO; Yoshida et al. prepared block copolymer, poly(4-vinylbenzyloxy-TEMPO)-*block*-polystyrene, which was soluble in dioxane but formed micelles with acid introduction.[19,20] If TEMPO−TEMPO molecular contact is required for disproportionation, the reduced mobility of tethered TEMPO in PAA-T could inhibit disproportionation. Therefore, we performed the following experiment to verify disproportionation at low pH.

Disproportionation consumes nitroxyl radicals, and this is reflected in the intensity of the EPR spectra. Figure 3 compares

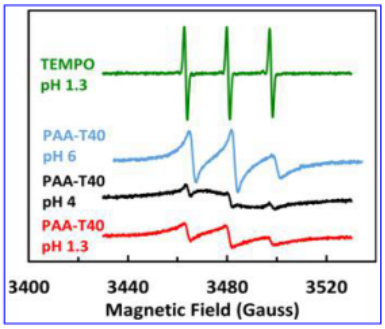

Figure 3. EPR spectra of PAA-T40 (0.5 g/L) at low and neutral pH at 25 °C.

the EPR spectra of PAA-T40 at three pH values and free TEMPO at pH 1.3. Several effects are apparent in these spectra. First, those of the PAA-T40 samples are broadened compared to the spectrum of free TEMPO as a result of the restricted motion of the polymer. At pH 4 in the colloidal phase, the broadening is greater, but there is a minor fraction of spin-labels with greater mobility. Because of the difference in line shape and the inhomogeneity of the colloidal sample, a reliable comparison of the amplitude of its EPR spectrum is difficult. However, the shapes of the spectra at pH 1.3 and pH 6 are the same, and both samples are isotropic solutions of the same concentration. It is apparent in the figure that the intensity at pH 1.3 is significantly lower. Double integration of the spectra indicates that the intensity at pH 1.3 is about 50% of that at pH 6, suggesting that roughly half of the nitroxides have disproportionated at this pH.

In an effort to obtain more evidence for the disproportionation of PAA-T at low pH, we measured the electrophoretic mobility of PAA-T40 adsorbed on a polystyrene latex. This surfactant-free latex has a sparse coating of amidine cationic groups, sufficient to promote colloidal stability and to promote the adsorption of highly anionic polymers such as PAA.[21] Figure 4 compares PAA-T40 with the parent PAA. Below pH 3, PAA-T40 had a net positive charge, supporting the proposal that many of the pendant TEMPO moieties underwent disproportionation at pH < 3, converting uncharged TEMPO into cationic $TEMPO^+$ and $TEMPOH^+$ (see Scheme 2). Following the suggestions of a reviewer, we initially dialyzed PAA-T40 against 1 M NaCl to remove possible cationic impurities from the coupling chemistry. The electrophoresis data from the two dialysis procedures were the same, suggesting contamination was not a problem.

To summarize, the PAA-T phase separation occurs under acidic conditions with a lower limit of pH 1.5−2, where

DOI: 10.1021/acs.macromol.6b00977
Macromolecules 2016, 49, 4935−4939

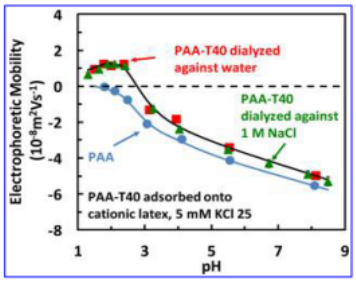

Figure 4. Electrophoretic mobility as a function of pH for 0.2 g/L PAA-T40 adsorbed onto 0.01 g/L 200 nm diameter cationic polystyrene latex. All measurements were carried out in 5 mM KCl aqueous solution at 25 °C.

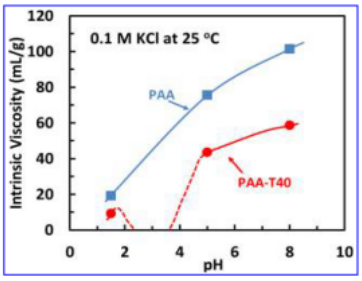

Figure 5. Intrinsic viscosity of PAA and PAA-T40 in 0.1 M KCl at 25 °C. The dashed line crosses two phase regions.

disproportionation converts some of the TEMPO moieties to cationic species (see Scheme 2). The upper limit, pH 2.5−4.5, corresponds to the significant ionization of the PAA backbone. The next sections describe PAA-T properties in the one-phase regime at neutral and alkaline pH.

Solution Properties of PAA-T. Figure 4 compares the intrinsic viscosity of PAA-T40 and PAA at three different pH values. At every pH value PAA is more expanded than PAA-T40. TEMPO substitution lowers the anionic charge density, and TEMPO is more hydrophobic than acrylate moieties—a less expanded configuration of PAA-T versus PAA seems reasonable. Viscosity measurements were also performed for the PAA-T solutions as functions of concentration. The results shown in Figure S4 of the Supporting Information show that viscosity decreased with increasing TEMPO derivatization.

PAA-T Surface Tension. The possible role of hydrophobic interactions was probed by surface tension measurements. Figure 6 shows the surface tension of PAA-T40 as a function of pH along with PAA data from the literature.[22] The main conclusion is that PAA-T40 is not very hydrophobic at all pH values. PAA-T40 is more surface active than PAA; the lowest surface tensions correspond to the phase separation pH range. Approaching very low pH, the surface tension increased, again supporting the disproportionation mechanism (Scheme 2).

The influence of TEMPO content on surface tension at pH 5.5 is shown in Figure 7. The surface tension decreases linearly with TEMPO content; however, none of the polymers are very surface active in water.

The surface tension measurements suggests that PAA-T has little hydrophobic character.

■ DISCUSSION

We were surprised to observe PAA-T phase separation at low pH followed by redissolution as the pH was lowered through pH 2 (Figure 1). We propose that two phenomena can drive phase separation. First, the PAA-T is fundamentally less hydrophilic than PAA, and as the degree of ionization decreases with lowering pH, PAA-T solubility decreases. The intrinsic viscosity behaviors in Figure 5 support this explanation. At neutral pH the intrinsic viscosity of PAA-T is less than PAA, and the intrinsic viscosity decreases with lowering pH, reflecting the decreasing degree of carboxyl ionization.

The second phenomenon driving phase separation is electrostatic attraction between cationic $TEMPO^+$ or $TEMPOH^+$ (Scheme 2) and anionic, ionized carboxylate groups. The electrophoretic behavior of PAA-T as a function of pH, shown in Figure 4, shows the amphoteric nature of PAA-T. At neutral pH it is negatively charged due to the high concentration of carboxylate ions, whereas at very low pH the $TEMPO^+$ and $TEMPOH^+$ dominate. At intermediate pH ~ 2.5−3.5, the PAA-T40 passes through an isoelectric point where we expect a minimum in solubility.

Which of these two mechanisms dominates? The surface tension data as a function of pH (Figure 6) or as a function of

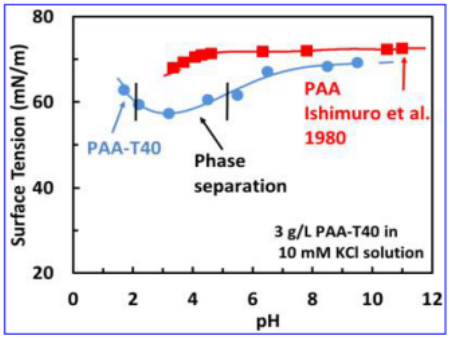

Figure 6. pH-dependent surface tension of PAA-T40 (3 g/L in 10 mM KCl at 23 °C) compared to PAA results from the literature.[22]

the extent of TEMPO substitution (Figure 7) suggest that PAA-T is not very hydrophobic even at low pH. Therefore, we propose that electrostatically driven intermolecular and intramolecular association of PAA-T drives phase separation.

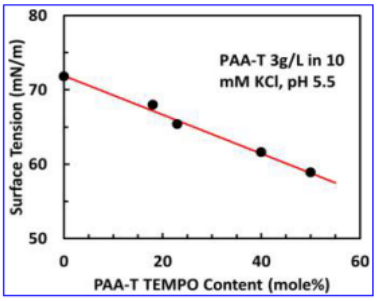

Figure 7. Surface tension of PAA-T as a function of TEMPO substitution degree at pH 5.5 in 10 mM KCl at 23 °C.

DOI: 10.1021/acs.macromol.6b00977
Macromolecules 2016, 49, 4935−4939

PAA-T is a redox-sensitive polymer that can act as an oxidation mediator for the oxidation of primary alcohols to aldehydes and ketones.[13] These oxidation reactions require a primary oxidant that activates the TEMPO moieties. Since the oxidations are usually carried out either at high pH with NaClO/NaBr as a primary oxidant or at neutral pH with enzyme/oxygen primary oxidants, phase separation at low pH is not an issue. However, the phase behavior may be exploited to separate PAA-T in solution oxidation processes or to drive desorption of PAA-T adsorbed on cationic surfaces.

■ CONCLUSIONS

The major conclusions of this work are as follows:

1. PAA-T phase separates between a lower limit of pH 1.5−2 and an upper limit of pH 2.5−4.5. The pH range of the two-phase region increases with the TEMPO content.
2. PAA-T has a more compact configuration in solution compared to the parent PAA.
3. PAA-T is only slightly surface active, with the maximum surface activity occurring at the pH near the phase separation boundary.
4. We propose that phase separation at low pH is the combined result of the low degree of PAA ionization, the hydrophobic contributions of the TEMPO moieties, and electrostatic interactions between the cationic TEMPO species, resulting from disproportionation at low pH (see Scheme 2), and anionic ionized carboxyl groups.

■ ASSOCIATED CONTENT

Supporting Information

The Supporting Information is available free of charge on the ACS Publications website at DOI: 10.1021/acs.macromol.6b00977.

Figures S1−S4 (PDF)

■ AUTHOR INFORMATION

Corresponding Author

*(R.P.) E-mail: peltonhr@mcmaster.ca.

Notes

The authors declare no competing financial interest.

■ ACKNOWLEDGMENTS

BASF Canada is acknowledged for funding this project. We also thank the Canadian Foundation for Innovation and the Ontario Ministry of Research and Innovation for Infra-structure funding to the Biointerfaces Institute. R.H.P. holds the Canada Research Chair in Interfacial Technologies.

■ REFERENCES

(1) Nicolas, J.; Guillaneuf, Y.; Lefay, C.; Bertin, D.; Gigmes, D.; Charleux, B. Nitroxide-Mediated Polymerization. *Prog. Polym. Sci.* **2013**, *38*, 63−235.

(2) Fukuda, T.; Terauchi, T.; Goto, A.; Ohno, K.; Tsujii, Y.; Miyamoto, T.; Kobatake, S.; Yamada, B. Mechanisms and Kinetics of Nitroxide-Controlled Free Radical Polymerization. *Macromolecules* **1996**, *29*, 6393−6398.

(3) Hawker, C. J.; Barclay, G. G.; Orellana, A.; Dao, J.; Devonport, W. Initiating Systems for Nitroxide-Mediated "Living" Free Radical Polymerizations: Synthesis and Evaluation. *Macromolecules* **1996**, *29*, 5245−5254.

(4) Lappan, U.; Wiesner, B.; Scheler, U. Rotational Dynamics of Spin-Labeled Polyacid Chain Segments in Polyelectrolyte Complexes Studied by Cw Epr Spectroscopy. *Macromolecules* **2015**, *48*, 3577−3581.

(5) Pilar, J.; Labsky, J. Epr Study of Chain Rotational Dynamics in Dilute Aqueous Solutions of Spin-Labeled Poly(Acrylic Acid) at Different Degrees of Neutralization. *Macromolecules* **1994**, *27*, 3977−3981.

(6) Takahashi, Y.; Hayashi, N.; Oyaizu, K.; Honda, K.; Nishide, H. Totally Organic Polymer-Based Electrochromic Cell Using Tempo-Substituted Polynorbornene as a Counter Electrode-Active Material. *Polym. J.* **2008**, *40*, 763−767.

(7) Janoschka, T.; Morgenstern, S.; Hiller, H.; Friebe, C.; Wolkersdorfer, K.; Haupler, B.; Hager, M. D.; Schubert, U. S. Synthesis and Characterization of Tempo- and Viologen-Polymers for Water-Based Redox-Flow Batteries. *Polym. Chem.* **2015**, *6*, 7801−7811.

(8) Bugnon, L.; Morton, C. J. H.; Novak, P.; Vetter, J.; Nesvadba, P. Synthesis of Poly(4-Methacryloyloxy-Tempo) Via Group-Transfer Polymerization and Its Evaluation in Organic Radical Battery. *Chem. Mater.* **2007**, *19*, 2910−2914.

(9) Bragd, P. L.; Van Bekkum, H.; Besemer, A. C. Tempo-Mediated Oxidation of Polysaccharides: Survey of Methods and Applications. *Top. Catal.* **2004**, *27*, 49−66.

(10) Isogai, A.; Saito, T.; Fukuzumi, H. Tempo-Oxidized Cellulose Nanofibers. *Nanoscale* **2011**, *3*, 71−85.

(11) Pelton, R.; Ren, P. R.; Liu, J.; Mijolovic, D. Polyvinylamine-Graft-Tempo Adsorbs onto, Oxidizes and Covalently Bonds to Wet Cellulose. *Biomacromolecules* **2011**, *12*, 942−948.

(12) Liu, J.; Pelton, R.; Obermeyer, J. M.; Esser, A. Laccase Complex with Polyvinylamine Bearing Grafted Tempo Is a Cellulose Adhesion Primer. *Biomacromolecules* **2013**, *14*, 2953−60.

(13) Shi, S.; Pelton, R.; Fu, Q.; Yang, S. Comparing Polymer-Supported Tempo Mediators for Cellulose Oxidation and Subsequent Polyvinylamine Grafting. *Ind. Eng. Chem. Res.* **2014**, *53*, 4748−4754.

(14) Osa, T.; Akiba, U.; Segawa, I.; Bobbitt, J. M. Electrocatalytic Oxidation of Nerol with Nitroxyl Radical Covalently Immobilized to Poly(Acrylic Acid) Coated on Carbon Electrodes. *Chem. Lett.* **1988**, *17*, 1423−1426.

(15) Chen, W.; Pelton, R.; Leung, V. Solution Properties of Polyvinylamine Derivatized with Phenylboronic Acid. *Macromolecules* **2009**, *42*, 1300−1305.

(16) Ishimuro, Y.; Ueberreiter, K. The Surface Tension of Poly (Acrylic Acid) in Sodium Chloride Solutions. *Colloid Polym. Sci.* **1980**, *258*, 1052−1054.

(17) Golubev, V. A.; Sen, V. D.; Kulyk, I. V.; Aleksandrov, A. L. Mechanism of the Oxygen Disproportionation of Ditert-Alkylniteoxyl Radicals. *Bull. Acad. Sci. USSR, Div. Chem. Sci.* **1975**, *24*, 2119−2126.

(18) Sen', V. D.; Tikhonov, I. V.; Borodin, L. I.; Pliss, E. M.; Golubev, V. A.; Syroeshkin, M. A.; Rusakov, A. I. Kinetics and Thermodynamics of Reversible Disproportionation−Comproportionation in Redox Triad Oxoammonium Cations − Nitroxyl Radicals − Hydroxylamines. *J. Phys. Org. Chem.* **2015**, *28*, 17−24.

(19) Yoshida, E.; Tanaka, T. Oxidation-Induced Micellization of a Diblock Copolymer Containing Stable Nitroxyl Radicals. *Colloid Polym. Sci.* **2006**, *285*, 135−144.

(20) Yoshida, E.; Ogawa, H. Micelle Formation Induced by Disproportionation of Stable Nitroxyl Radicals Supported on a Diblock Copolymer. *J. Oleo Sci.* **2007**, *56*, 297−302.

(21) Goodwin, J. W.; Ottewill, R. H.; Pelton, R. Studies on the Preparation and Characterization of Monodisperse Polystyrene Lattices 0.5. Preparation of Cationic Lattices. *Colloid Polym. Sci.* **1979**, *257*, 61−69.

(22) Ishimuro, Y.; Ueberreiter, K. The Surface Tension of Poly (Acrylic Acid) in Aqueous Solution. *Colloid Polym. Sci.* **1980**, *258*, 928−931.

DOI: 10.1021/acs.macromol.6b00977
Macromolecules 2016, 49, 4935−4939

Appendix: Supporting Information for Chapter 2

Supporting information for the phase behaviour of aqueous poly(acrylic acid-g-TEMPO)

Qiang Fu[1], Zachary Russell Gray[1], Arthur van der Est[2], and Robert H. Pelton[1]

[1] Department of Chemical Engineering, McMaster University, Hamilton, Canada, L8S 4L7
[2] Department of Chemistry, Brock University, St. Catharines, Ontario, L2S 3A1

Synthesis of PAA-T

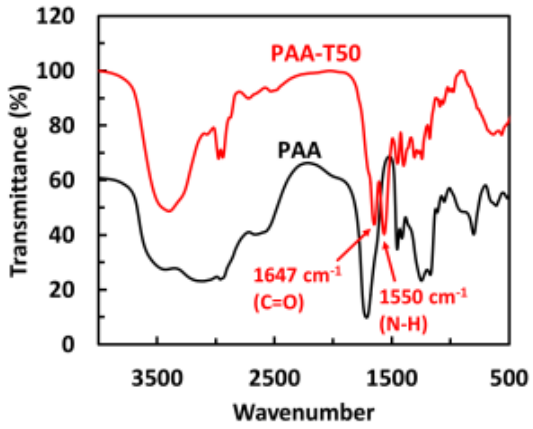

Figure S1 FTIR spectrum of PAA and PAA-T50. The peaks at 1647 cm^{-1} (amide I, C=O) and 1550 cm^{-1} (amide II, N-H) confirming synthesis of PAA-T.

Example conductometric titrations and TEMPO content calculation.

The conductometric titrations were performed with a PC Titrate (Mantech Inc.), and the carboxyl contents in PAA and PAA-T samples were determined by conductometric titration. In a typical experiment, 7.0 mg of freeze-dried PAA was dissolved in 100 mL of 5 mM NaCl solution. The initial pH of the sample solution was adjusted to 3 with 2.0 M HCl, and then the sample solution was titrated with 0.1 M NaOH at room temperature until the pH reached 11. The TEMPO degree of substitution was calculated from the change in carboxyl contents.

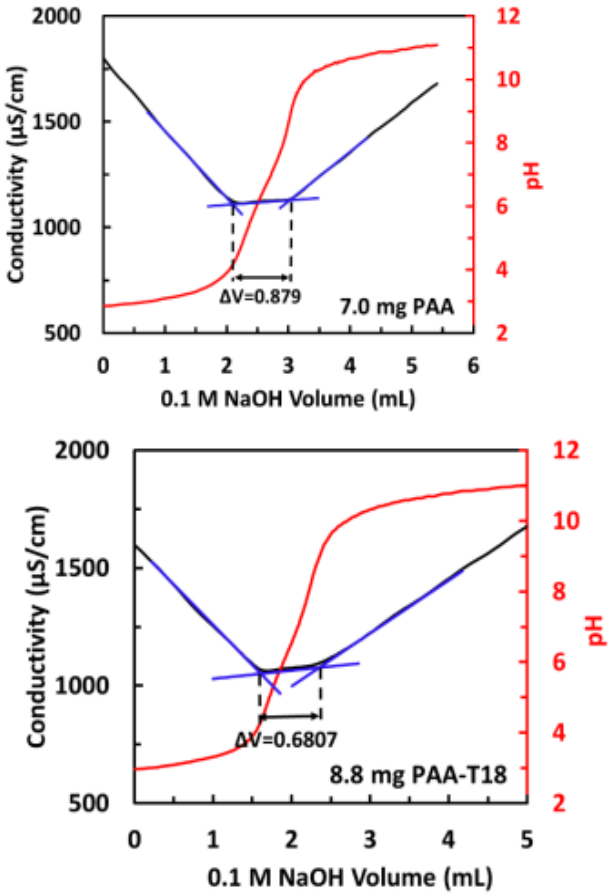

Figure S2 Conductometric titration of PAA and PAA-T18

$$n_{PCOOH} = \frac{0.879\ mL*0.1M}{7.0\ mg} = 12.56\ \frac{mmol}{g}$$ npcooh carboxyl mole content per gram PAA

$$n_{TCOOH} = \frac{0.6807\ mL*0.1M}{8.8\ mg} = 7.74\ \frac{mmol}{g}$$ ntcooh carboxyl mole content per gram PAA-T18

$$DS = \frac{1-\frac{n_{TCOOH}}{n_{PCOOH}}}{1+n_{TCOOH}*(MW_{aTEMPO}-MW_H-MW_H-MW_O)} * 100\%$$

DS : TEMPO degree of substitution

MWatempo: molecular weight of amino-TEMPO

MWh: atomic weight of hydrogen H

MWo: atomic weight of oxygen O

Example of intrinsic viscosity calculation.

Experiment conditions: pH 5, 0.1M KCl solution, temperature 23 °C.
Original data of flow through time with three times measurement.

sample	flow through time (s)			average flow through time (s)
	t1	t2	t3	
0.1 M KCl	150.51	150.50	150.51	150.51

PAA Conc. (g/L)	Flow through time (s)			average flow through time (s)
	t1	t2	t3	
10	276.38	276.48	276.57	276.48
8	249.81	248.60	250.0	249.81
6.667	232.14	232.00	232.28	232.14
5.708	219.63	219.61	219.77	219.63
4.444	203.42	203.29	203.16	204.29
2.684	182.1	182.15	182.05	182.1

PAA-T40 Conc. (g/L)	Flow through time (s)			average flow through time (s)
	t1	t2	t3	
10	226.98	226.88	227.06	226.97
8	209.82	209.66	209.50	209.66
6.667	199.30	199.35	199.33	199.33
5.708	191.52	191.40	191.28	191.40
4.444	181.62	182.0	181.81	181.81
2.684	169.01	168.79	168.9	168.90

Calculation:

For PAA-T40, 10 g/L in 0.1 M KCl, pH 5, 23 °C

Through Huggins Equation method

$\eta_{sp} = \frac{t_{PAA-T40}}{t_{sol}} - 1 = \frac{226.97\ s}{150.51\ s} - 1 = 0.508$ η_{sp} is specific viscosity

$t_{PAA-T40}$ is the flow through time of PAA-T40 solution

t_{sol} is the flow through time of pure 0.1 M KCl solution

$\eta_{red} = \frac{\eta_{sp}}{c} = \frac{0.83629}{10\ g/L} = 0.0508\frac{L}{g}$ η_{red} is reduced viscosity

The intrinsic viscosity is obtained by extending reduced viscosity vs polymer concentration curve to the y-axis.

Through Kraemer Equation method

$\eta_{rel} = \frac{t_{PAA-T40}}{t_{sol}} = \frac{226.97}{150.51} = 1.508$ η_{rel} is the relative viscosity

$\eta_{inh} = \frac{\ln(\eta_{rel})}{c} = \frac{\ln(1.508)}{10\ g/L} = 0.04108$ η_{inh} is the inherent viscosity

c is concentration of PAA-T40

The intrinsic viscosity is obtained by extending inherent viscosity vs polymer concentration curve to the y-axis.

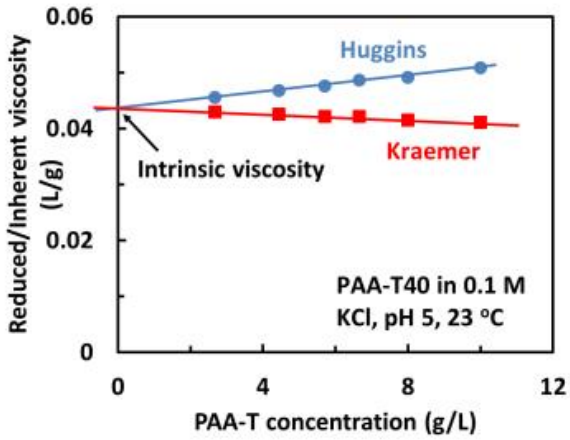

Figure S3 Determination of intrinsic viscosity of PAA-T40

Viscosity measurement

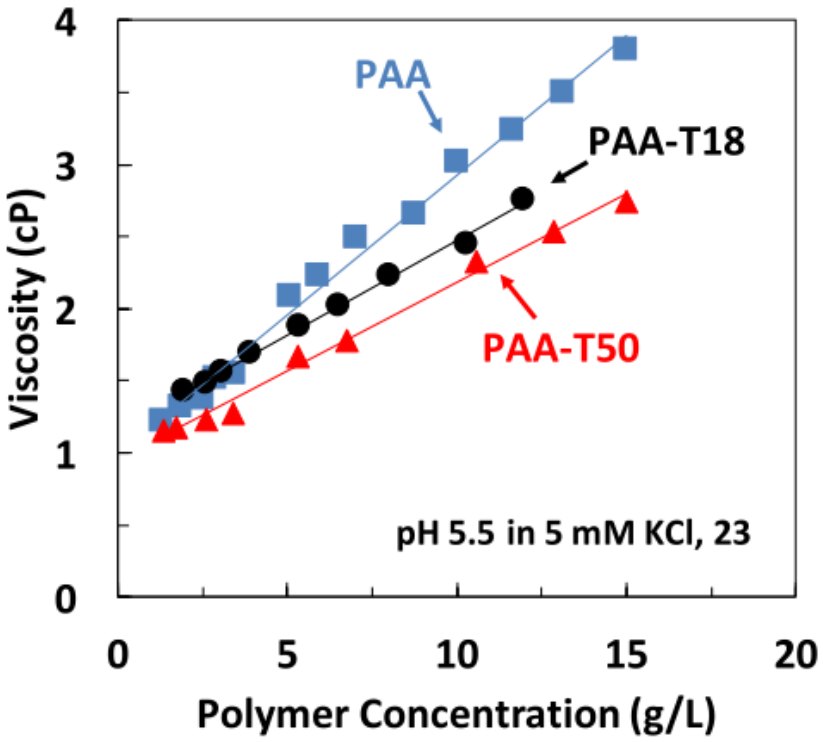

Figure S4 Viscosity of PAA-T and the parent PAA solutions at various concentrations. Viscosity was measured with Vibro viscometer SV-10 in 5 mM KCl, pH 5.5, 23 ^{o}C.

Viscosity of PAA-T and the parent PAA solutions at various concentrations were measured. Under the measurement conditions, all polymer solutions showed as one phase. The viscosity decreased with increasing TEMPO derivatization.

Chapter 3 Redox Properties of Polyvinylamine-g-TEMPO in Multilayer Films with Sodium Poly(styrene sulfonate)

I conduced most of the experiments in chapter 3. Igor Zoudanov (undergraduate student) helped me with polymer synthesis, surface tension and viscosity measurements. Dong Yang (PhD student) helped me with EQCM-D measurement. Dr. Emil Gustafsson helped me with ellipsometry measurement and discussion about surface tension properties of polymers. They will be coauthors on the publication along with Professor Soleymani. I plotted the experimental data and Dr. Robert Pelton helped to analyze the data. The paper was initially written by me, and edited later by Dr. Robert Pelton.

Chapter 3 Redox properties of polyvinylamine-g-TEMPO in multilayer films with sodium poly(styrene sulfonate)

3.1 Introduction

Cellulose is an important platform in the push to more sustainable products and processes. However, cellulose must be modified for most applications. TEMPO (2, 2, 6, 6,-tetramethyl-1-piperidinoxy) mediated oxidation is one of the most widely used approaches to functionalizing cellulose by virtue of the selective oxidation of C6 primary hydroxyls to aldehydes and acids. Our interests involve using TEMPO to oxidize cellulose to facilitate the covalent coupling of polyvinylamine (PVAm) to cellulose surfaces. PVAm grafted "primer" coatings on cellulose [1] provides amine-rich surfaces that readily modified, providing wide variety of functions including bioactive surfaces, redox active surfaces, and surfaces giving exceptionally high cellulose/cellulose wet adhesion. Although TEMPO chemistry offers many advantages, its use in some industrial operations is inhibited by the cost, the environmental impact of TEMPO, and the difficulty in recycling TEMPO. For our applications we have solved these limitations by grafting TEMPO onto PVAm to give polyvinylamine-g-TEMPO (PVAm-T) – see structure in Figure 3-1. In water, this very cationic polymer spontaneously adsorbs onto cellulose, and, in the presence of a primary oxidant such as bleach, the cellulose is oxidized to aldehydes and the amine groups subsequently form imine and aminal bonds after drying. [2] More recently, we have shown that ~500 nm colloidal complexes formed between PVAm-T and the redox enzyme laccase, also oxidize cellulose surfaces. [3] We explained this by hypothesizing that TEMPO-to-TEMPO electron transfer occurred in PVAm-T, even when only 10% of the amine repeat units bore a grafted TEMPO.

The goals of the work described herein include confirming that PVAm-T polymers with relatively low TEMPO contents were able support TEMPO-to-TEMPO electron transport. By combining quartz crystal microbalance measurements with cyclic voltammetry (EQCM-D) and with ellipsometric characterization of the dried layer-by-layer (LbL) multilayer films, we were able to estimate the fraction of TEMPO moieties that could be oxidized by a gold electrode.

Polymers with grafted TEMPO moieties are not new. TEMPO has been grafted to water insoluble polymers giving a supported catalyst for the oxidation of soluble molecules[4]. Grafted TEMPO probes have also been widely used for electron spin resonance studies of polymers. There appears to be a resurgence in polymer grafted TEMPO based on potential applications in energy storage. [5-7] Many of studies involve redox polymers deposited on electrode surfaces using LbL assembly. In one of the earlier LbL redox studies, Laurent and Schlenoff showed that the extent of interpenetration between polymer layers in LbL constructs could be probed by placing non-redox active pairs of blocking layers between the electrode and the redox polymer layers. [8] They reported that 4 pairs of blocking layers were required to prevent electron transfer to the redox polymers; we report herein similar results.

Closest to our work was a publication by Anzai's group [9] that described LbL films based on alternating layers of anionic poly(acrylic acid) with 46 mole percent of the carboxyls bearing grafted TEMPO substitution and cationic poly(ethyleneimine). They reported that their multilayer films decomposed when the TEMPOs were oxidized. By contrast, our work involves lower levels of TEMPO grafted on the cationic polymer, PVAm, and we have used polystyrene sulfonate as the anionic polymer. Our polymers were chemically stable and the multilayers remained intact during cyclic voltammetry.

Finally, our work is focused on PVAm-T oxidation of and subsequent grafting to cellulose of adhesion applications. However, the ability of PVAm-T to spontaneously adsorb onto negatively charged surfaces in water, gives a simple route to TEMPO-rich surfaces for other applications.

3.2 Experimental section

Materials. Two different polyvinylamine samples were obtained from BASF Canada Inc. PVAm 5095, Mw 45 kDa, hydrolysis degree 75% and PVAm 9095, Mw 340 KDa, hydrolysis degree 95%. We completely hydrolyzed the PVAm following Gu *et al.*'s method.[10] All experiments were performed with water from a Millipore system with a

resistivity of 18.2 MΩ cm The PVAm was dialyzed against deionized water and freeze-dried before use. 4-carboxy-TEMPO, sodium 3-mercapto-1-propanesulfonate (MPS), sodium poly(styrene sulfonate) (PSS), Mw 70 kDa (density 0.801 g/mL), 1-ethyl-3-(3-dimethylaminopropyl) carbodiimide (EDC), and N-hydroxysulfosuccinimide sodium salt (sulfo-NHS) were purchased from Sigma-Aldrich and used as received..

Preparation of PVAm-T. A series of PVAm-T were synthesized as previously reported by our group[11]. In a typical experiment, 55 mg 4-carboxy-TEMPO was dissolved in 100 mL deionized water and 157 mg EDC was reacted with the 4-carboxy-TEMPO. 170 mg Sulfo-NHS was further added. The reaction was stirred for 20 min at pH 5.5 at room temperature. PVAm solution (100 mg PVAm in 40 mL deionized water) was slowly dropped into the above 4-carboxy-TEMPO solution and the solution pH was maintained at 7.0 for four hours with 0.1 M HCl and 0.1 M NaOH solutions. The resulting solution was dialyzed (MWCO 3 kDa) against deionized H_2O for two weeks. Purified and dried PVAm-T samples were obtained through lyophilisation and stored in a desiccator. The amine contents of PVAm-T were determined by potentiometric and conductometric titration method. The degree of TEMPO substitution was calculated from the change in amine contents. Table 3-1 summarized the properties of PVAm-T copolymers.

Table 3- 1 Properties of PVAm-T copolymers – see structure in Figure 3- 1. DH is the percentage of N-vinylformamide groups hydrolyzed to amine groups in the parent PVAm. DS is the mole fraction of PVAm amine groups bearing pendant TEMPOs. EW_T is the TEMPO equivalent weight at pH 7.5 and EW_N is the amine equivalent weight at pH 7.5

Designation	PVAm DH (mole %)	PVAm MW (kDa)	TEMPO DS (mole %)	EW_T (Da)	EW_N (Da)
PVAm-T4L	75	45	4	2260	94.0
PVAm-T10L	75	45	10	1000	111
PVAm-T13L	75	45	13	809	121
PVAm-T25L	75	45	25	500	167
PVAm-T5H	100	340	5	1360	71.8
PVAm-T12H	100	340	12	665	90.7
PVAm-T22H	100	340	22	438	123
PVAm-T35H	100	340	35	337	181

Electrochemical Quartz Crystal Microbalance with Dissipation (EQCM-D). The EQCM-D measurements were carried out with an electrochemical QCM-D cell (E401

model from Q-Sense, Sweden). A QSX301 gold sensor served as the working electrode. The counter electrode was platinum and a low leakage "Dri-Ref 2SH" Ag|AgCl (3 M KCl) electrode (World Precision Instruments, USA) was the reference electrode. The QSX301 gold sensor and the platinum electrode were cleaned with piranha solution at 75 ^{o}C for 5 minutes and then thoroughly rinsed with deionized water, and dried by N_2. Note piranha is dangerous and appropriate precautions must be taken when working with it. Sulfonate groups were grafted to the gold surface by immersing the electrode into 3 mM sodium 3-mercapto-1-propanesulfonate (MPS) ethanol solution for 24h at room temperature, followed by rinsing with ethanol, and finally by deionized water, and dried with N_2.

Using the traditional LbL approach alternating layers of cationic PVAm-T and anionic PSS were adsorbed on the gold sulfate electrode. For example, PVAm-T25L solution (0.1 g/L in 0.1 M NaCl with pH 7.5) was pumped through the EQCM-D cell at a rate of 0.100 mL/min for 15 minutes. The cell was then rinsed with NaCl solution (0.1M with pH 7.5) for another 15 minutes, followed by PSS (0.1 g/L in 0.1M NaCl with pH 7.5) for 15 minutes again followed rinsing with salt solution. All measurements were performed at 23 ^{o}C. The buildup of polymer layers was followed by QCM-D and the electrochemical properties of completed multilayers were measured by cyclic voltammetry performed with a Palmsens potentiostat (PalmSens, Amsterdam, Netherlands) in a conventional three-electrode configuration. For most experiments the potential was varied between 0.3 and 0.8 V at rates between 5 and 100 mV/s. Generally under each condition, measurements were performed over 20 minutes. In addition to voltammograms, the instruments software PSTrace 4.7 was used to extract peak voltages and the areas under the oxidation curves. The errors associated with the area measurements were estimated from the variation over three measurements. Finally, the density of redox active TEMPO moieties was calculated from the CV results – see example calculation in the supporting information.

Ellipsometry. The quantity of TEMPO moieties in the multilayers were estimated from ellipsometric characterization of the dried multilayer. The thickness of the dry multilayer films was measured using a Nanofilm EP3W imaging ellipsometer (Accurion Inc., Germany) fitted with wavelength 658 nm solid state laser. The Ellipsometry data were analyzed with modeling software EP4 (Accurion Inc).

The refractive index of multilayer films is calculated as the average refractive index of PVAm-T and PSS. The refractive index of PSS was 1.484[12]. The refractive indices of PVAm-Ts were measured from thick films, which were prepared by spin coating 0.1 wt%

aqueous solutions at 3000 rpm on piranha-cleaned silicon wafers. The thick (~100 nm) PVAm-T polymer films were annealed at 50 ºC for overnight before determining the refractive index with the ellipsometer. The refractive index of PVAm-T25L was 1.462 ± 0.021, where the error estimate was based on three measurements.

In some cases, after each layer of polymer was deposited, the EQCM-D sensor surfaces were air-dried and layer thickness was determined on the ellipsometer. For this analysis we assumed that overall refractive index was the average of the PVAm-T and PSS (1.473). The coverage (dry mass/area) of PVAm-T in each layer was estimated from the incremental ellipsometric thickness and the density of PVAm-T (1.08 g/mL, assumed to be the same as PVAm[13]).

3.3 Results

PVAm-T Compositions. A series of PVAm-T copolymers with varying TEMPO contents were prepared and the generic PVAm-T structure is shown in Figure 3- 1. In water, PVAm-T is mixture of four types of repeating units – see Figure 3- 1. Polyvinylamine can be prepared through acidic or basic hydrolysis of poly(N-vinylformamide) and most commercial PVAms are not completely hydrolyzed. We define PVAm-T compositions by: DH the degree of hydrolysis of the parent PVAm; DS, the fraction of amine groups coupled to TEMPO; and, α, the degree of ionization of amine groups.

The properties of the PVAm-T polymers used herein are summarized in Table 3-1. The copolymers are based on two parent PVAms, one with DH = 0.75, a value given by the supplier and one fully hydrolyzed by us to give DH = 1. The DS values were determined the difference in amine contents, measured by conductometric titration, before TEMPO grafting. Finally, α values were estimated by the Katchalsky model[14,15] that predicts α = 0.46 for PVAm in 0.1 M NaCl at pH 7.5, the main conditions used in this work.

Two other compositional parameters, useful for data manipulations are: EW_T the TEMPO equivalent weight (Da) and EW_N the equivalent weight of amine groups, both ionized and non-ionized. These equivalent weights were calculated from DS, DH and α values, are also tabulated in Table 3-1. The equivalent weights and other PVAm-T compositional details are and the detailed calculations, performed in Mathcad Prime are given in the SI file.

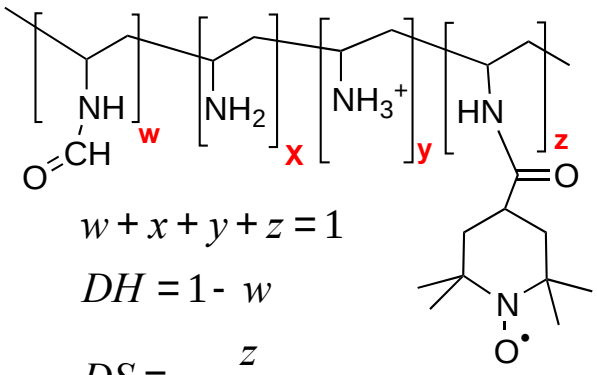

$$w + x + y + z = 1$$

$$DH = 1 - w$$

$$DS = \frac{z}{x + y + z}$$

$$a = \frac{y}{x + y}$$

Figure 3- 1 PVAm-T structure. The degree of hydrolysis, DH, the degree of TEMPO substitution based on amines, DS, and the degree of ionization, are functions of w, x, y, and z. The polymer properties are summarized in Table 3- 1.

Finally, we express the amount of TEMPO on surfaces as either a mass coverage of PVAm-T, $_T$ (mg/m^2) or as a molar coverage of TEMPO groups, $_T$ (mol/m^2). These two quantities are related by EW_T – see Eq 1.

$$g_T = \frac{G_T}{EW_T} \qquad \textit{Eq 1}$$

PVAm-T solution properties. PVAm-T is water soluble from pH 2 to 12. However, the TEMPO moieties in PVAm-T is more hydrophobic than PVAm alone. Therefore TEMPO substitution has two impacts; it lowers the surface tension (see Figure S3- 3) and TEMPO substituents causes the polymer coils in aqueous solutions to shrink (see Figure S3- 5).

PVAm-T/PSS multilayer films. Alternating layers of PVAm-T and polystyrene sulfonate (PSS) were formed on a QCM-D gold sensor surface. To facilitate adsorption of the first PVAm-T layer, the gold was treated with sodium 3-mercapto-1-propanesulfonate to give surface sulfonate groups.[16] Figure 3- 2 shows the EQCM-D frequency change with each additional adsorbed layer. The average frequency shift of PVAm-T25L layer was -20 Hz and the average frequency shift of PSS layer was -5 Hz. The total dissipation shift was less than 2×10^{-6} (see supporting information Figure S3- 6). The curves under different overtones overlapped well, and the ΔD was less than 10% in magnitude of Δf, indicating that the $(PVAm\text{-}T25L/PSS)_4$ multilayer film was rigid, and the absorbed mass can be calculated with Sauerbrey equation.[17-18]

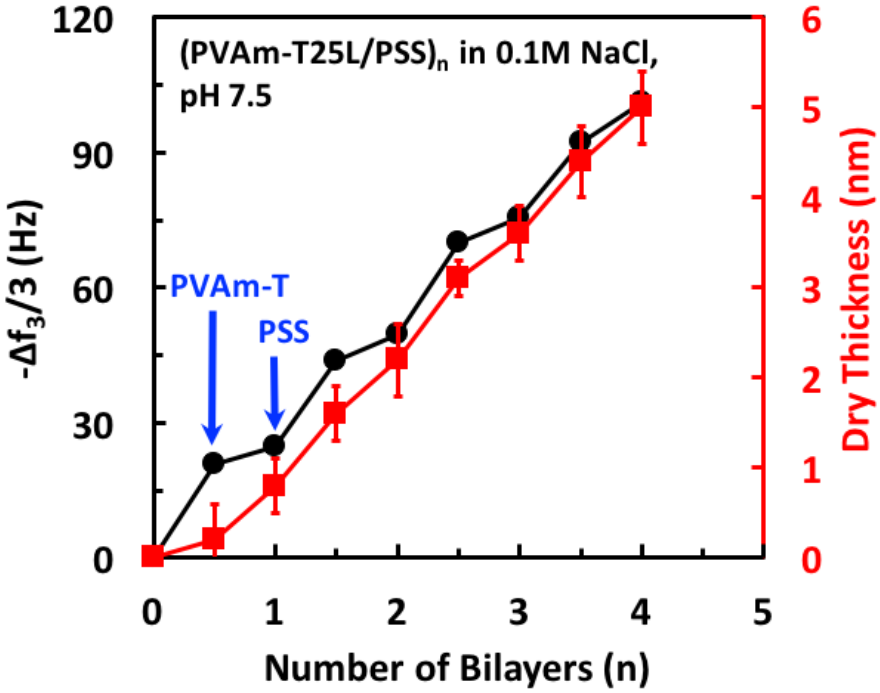

Figure 3- 2 QCM-D frequency changes with the buildup of (PVAm-T25L/PSS) multilayer together with the resulting dry film thicknesses measured by ellipsometry.

Figure 3- 2 also shows the dry thickness of PVAm-T25L/PSS multilayer films measured by ellipsometry. The average thickness of PVAm-T25L layer is 0.8 ± 0.2 nm, and the average thickness of PSS layer is 0.6 ± 0.2 nm. The mass of PVAm-T25L/PSS multilayer films was calculated from both EQCM-D and ellipsometry results. EQCM-D gave the

wet mass of the adsorbed polymer whereas ellipsometry gave dry film masses. Comparing these results, we estimated the water contents of the multilayer films and the results (see Figure 3- 3 and tabulated data in Table S3- 1) show that about 75 wt% of the multilayer films is water.

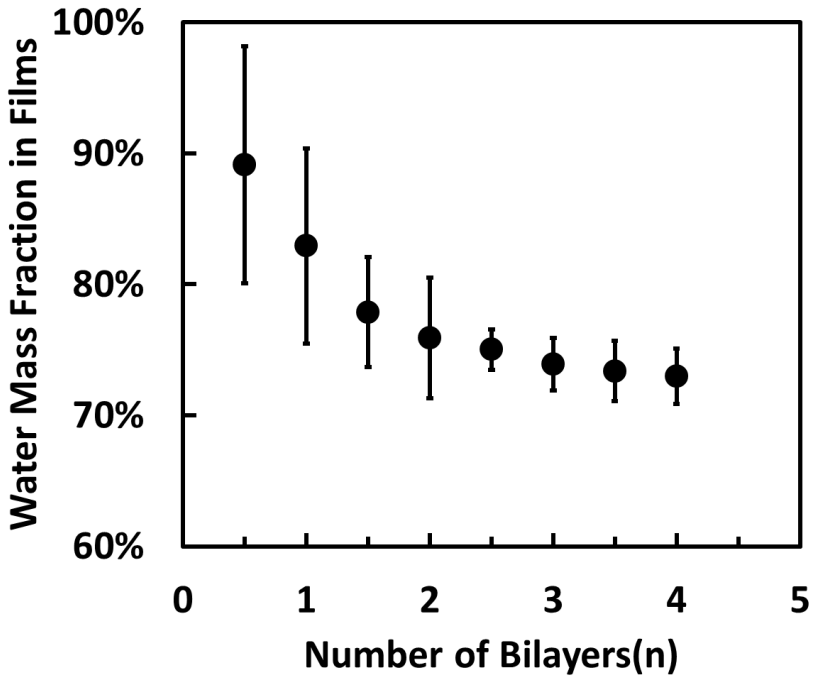

Figure 3- 3 The water content of PVAm-T25L/PSS multilayer films as a function of the number of polymer layers

Redox properties of PVAm-T/PSS multilayer films. Cyclic voltammetry was used to measure the content of redox-active TEMPO moieties in the multilayer films. In this technique, the electrical potential on a gold-sulfonate EQCM sensor is cycled and the resulting current is measured. Figure 3- 4A shows the cyclic voltammograms of $(PVAm\text{-}T25L/PSS)_4$ multilayer films at various scan rates. Under the scan rate 100 mV/s, the anodic peak was located at 0.61 V, which corresponds to oxidizing TEMPO to oxoammonium, and the cathodic peak at 0.560V, which corresponds to reducing oxoammonium to TEMPO. The peak separation (ΔE) between the anodic and the cathodic peaks was about 34 mV at scan rate 5 mV/s, and the ΔE increased to 52 mV at

scan rate 100 mV/s. In the case of free small TEMPO, the anodic peak potential was 0.54V, and the cationic peak potential was 0.43V under the same conditions. The peak potentials shifted ~0.1V towards the negative direction. Another characteristic of the cyclic voltammograms is that both the anodic and the cathodic peak currents increased linearly proportional to the scan rate (see Figure 3- 4B).The voltammograms show both surface-confined and diffusion-limited redox processes, and the surface-confined redox process dominated the behavior.[7]

The ratio of oxidative (positive) peak currents to the reductive (negative) peak currents ranged from 1 for the lowest two scan rates down to 0.74 for the highest two scan rates in Figure 3- 4; therefore the redox process was not completely reversible at high scan rate. Finally, the surface coverages of redox-active TEMPO moieties were estimated from areas under the voltammograms; these values will be discussed below.

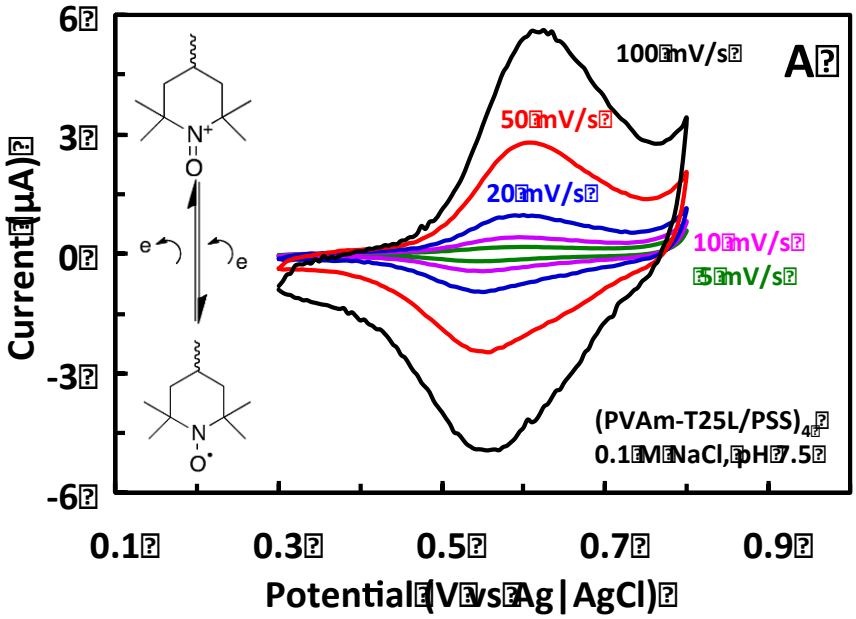

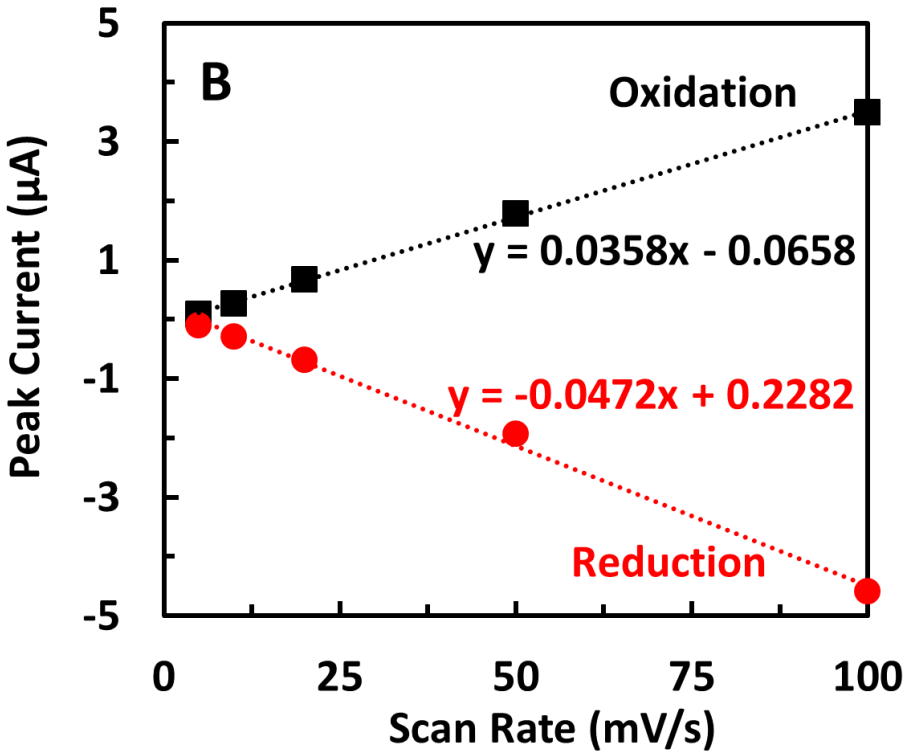

Figure 3- 4 (a) Cyclic voltammograms of $(PVAm\text{-}T25L/PSS)_4$ at various scan rates. (b) Dependence of the peak currents on scan rates for the $(PVAm\text{-}T25L/PSS)_4$ multilayer film.

TEMPO oxidation converts a neutral stable radical to the corresponding cationic oxoammonium ion (see structure in Figure 3- 4A). The multilayer film responds by shrinking, giving a decreased water content of approximately 10 %. The small swelling changes were reversible and examples data are shown in Figure S3- 7.

Figure 3- 5 shows the cyclic voltammograms of PVAm-T25L/PSS multilayer films as a function of the number of bilayers. Both the maximum oxidative and reductive peak currents increased with the number bilayer. This is an important observation because it indicates that TEMPO moieties far apart from the electrode surface are redox-active.

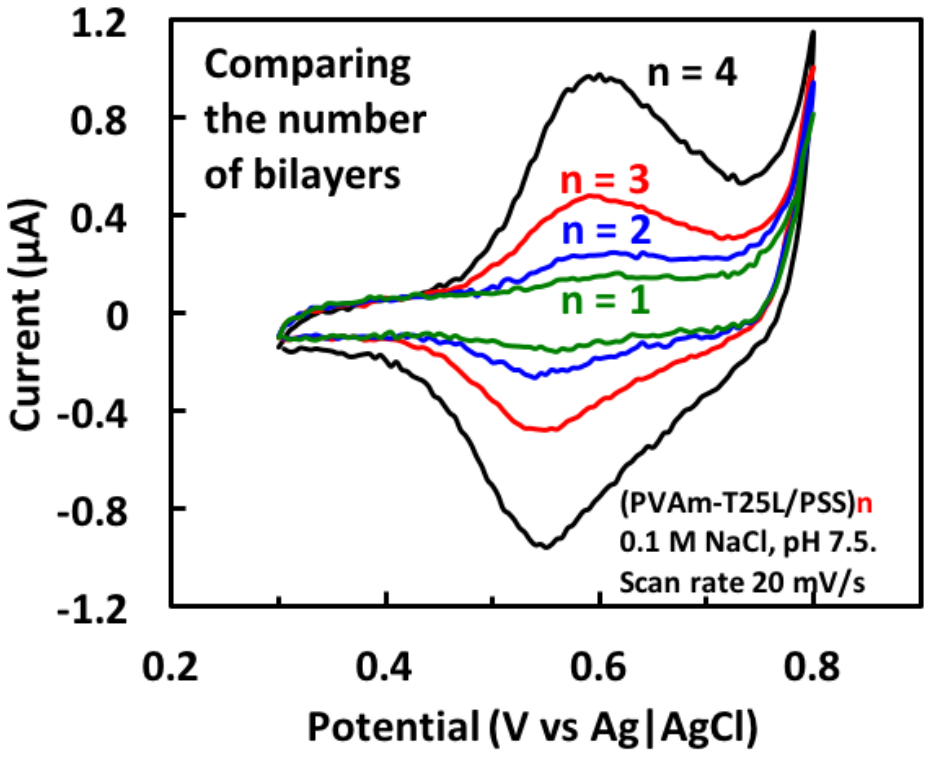

Figure 3- 5 Cyclic voltammograms of $(PVAm\text{-}T25L/PSS)_n$ multilayer films in 0.1M NaCl, pH 7.5. Scan rate 20 mV/s.

Redox-active TEMPO measurements. The areas under the oxidation curves were used to estimate the coverage of redox-active TEMPO moieties in the multilayer films. Example calculations performed Mathcad Prime are shown in the supporting information together with tabulated results in Table S3- 1. Figure 3- 6 shows the coverage of redox-active TEMPO moieties that are redox active as a function the number of PVAm-T layers. The straight lines were calculated with a model presented in the discussion section.

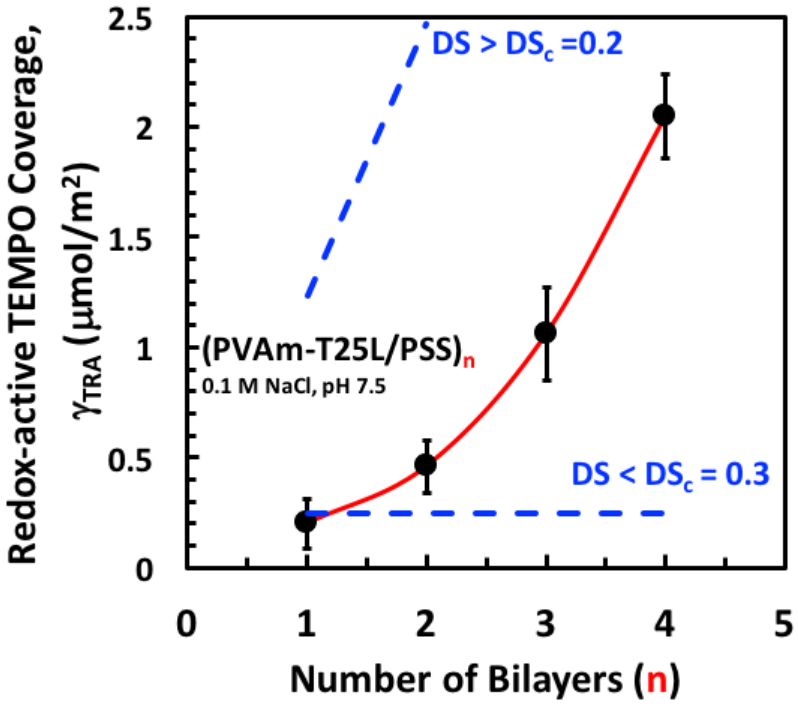

Figure 3- 6 The coverage of redox-active TEMPO in (PVAm-T25L/PSS)$_n$ multilayer films as a function of the number of bilayers. For model p = 0.2, $_1$ = 0.5 mg/m^2

The results in Figure 3- 5, Figure 3- 6 and in Table S3-1 show that the surface coverage of redox-active TEMPOs increases with the number of polyelectrolyte bilayers. Another way to vary the coverage of redox-active TEMPO is to vary the TEMPO DS in PVAm-T. Figure 3- 7 (data are tabulated in Table S3-2) shows the coverage of redox-active TEMPO for (PVAm-TxL/PSS)$_4$ for a series of PVAm-T where the DS varied from 4 to 25%. The results show a linear relationship between PVAm-T TEMPO DS and the redox-active TEMPO coverage in an assembly of four bilayers. The model curve will be addressed in the discussion section.

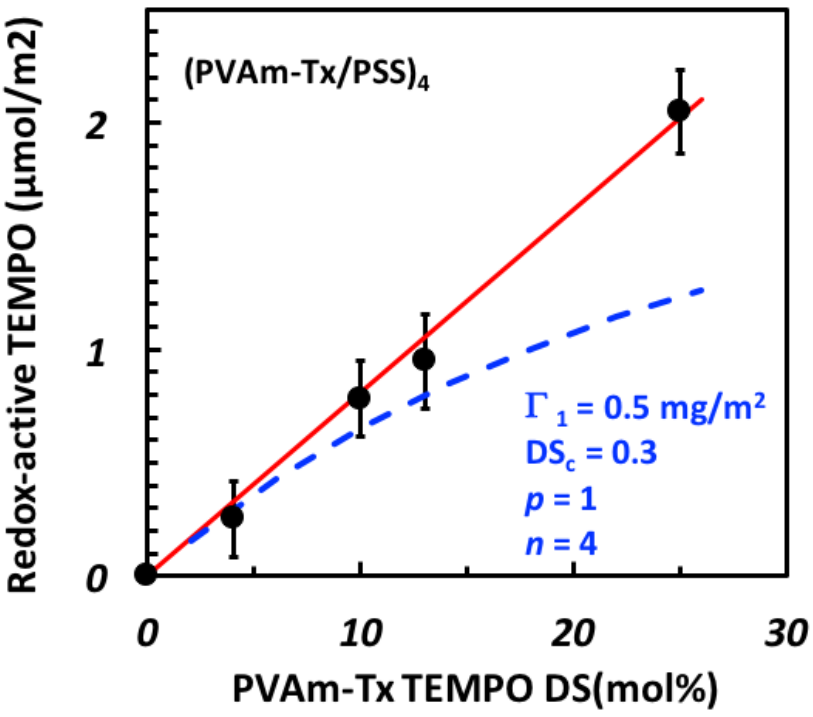

Figure 3- 7 The coverage of redox-active TEMPO moieties as a function of PVAm-T TEMPO DS in $(PVAm\text{-}TxL/PSS)_4$ multilayers. The polymers were based on the parent 45 kDa PVAm, 75% hydrolyzed.

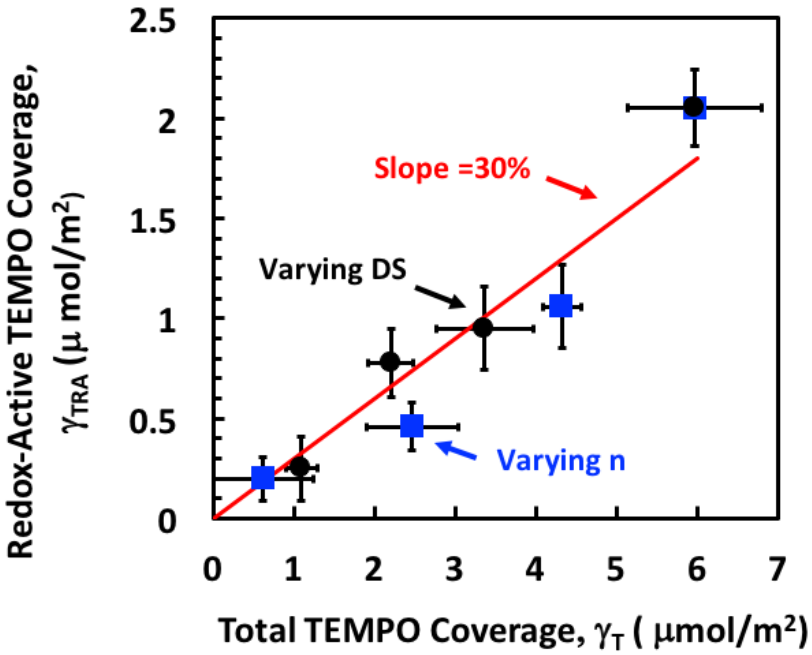

Figure 3- 8 Comparing the redox-reactive TEMPO coverage, measured by cyclic voltammetry to the overall TEMPO contents in LbL films. Approximately 30% of the TEMPOs are redox-reactive over the whole data set.

Figure 3- 8 compare the redox-active TEMPO coverage to the overall TEMPO coverage for the two data sets- varying the number of bilayers (Figure 3- 6) and varying the PVAm-T TEMPO DS (Figure 3- 7). Most of the data are close to the red line corresponding 30% of the TEMPOs being redox-active.

Blocking electron transport in polyelectrolyte multilayers. A series of polyelectrolyte multilayer films were prepared with the following compositions. Between 0 and 3 non-redox "blocking" bilayers based on PVAm/PSS were first deposited on gold sulfate sensor surfaces followed by two redox active PVAm-T25L bilayers. Figure 3- 9 shows the oxidative peak currents as a function of the number of blocking layers. Three pairs of non-redox blocking layers were required to completely prevent electron transport to the outer most two PVAm-T25L bilayers. This result is most likely a reflection of significant interpenetration of polymer chains between layers. A similar conclusion was made by earlier researchers working with other redox-active polyelectrolyte multilayers. [8 19]

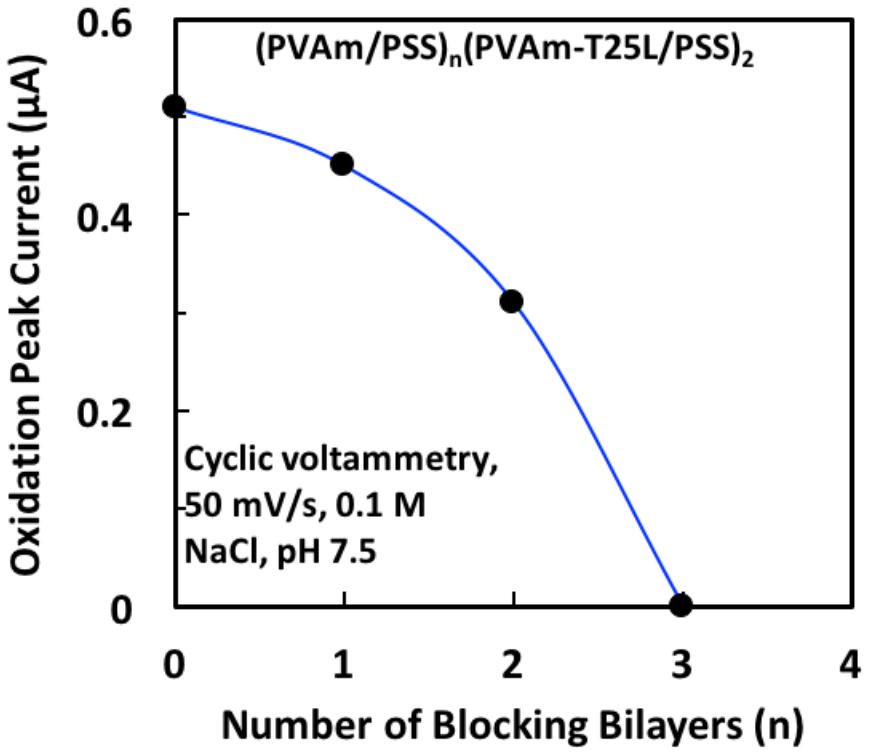

Figure 3- 9 Effect of blocking bilayers on oxidation peak current of (PVAm-T25L/PSS)$_2$ multilayers. 0.1 M NaCl, pH 7.5. Scan rate 50 mV/s.

3.4 Discussion

Published theoretical studies suggest that for electron hopping (transfer) between TEMPO groups, the distance between the TEMPO moieties must be less than ~ 0.6 nm. [5] One published estimate is that at least 60% of polymer repeat units must bear TEMPO groups for effective transfer in dilute polymer solutions. [6] By contrast, our results show that 30% of the TEMPO groups are redox active in multilayer films. This is remarkable because in our experiments, the PVAm-T should be rather immobile in multilayer films. In addition, we have used very short tethers between TEMPO and PVAm (see structure in Figure 3- 1). Nevertheless, our results seem consistent with other redox-active LbL systems – see examples in Table 3- 2.

Table 3- 2 Examples of redox LbL assemblies described in the literature where: PEI is poly(ethyleneimine); Fc is ferrocene; PVS is polyvinylsulfate; PAH is polyallylamine; and PGA is poly(L-glutamic acid).

LBL systems	Redox Species DS (%)	Fraction Redox-active (%)	ref
PAA-T/PEI	46	"most"	[9]
PAH-Fc/DNA	7.2	20-25	[20]
PEI-Fc/DNA	2.3	40-60	[20]
PAH-Fc/PVS	15%	56	[21]
PGA/PAH	10 mM ferrocyanide solution	~50%	[22]

We now consider the factors influencing the coverage of redox-active TEMPO groups. There are two relevant electron transport mechanisms: 1) transport between the gold-sulfonate surface and adsorbed TEMPOs; and, 2) transport between neighboring TEMPO moieties. In both cases the electron transfer partners must be within ~0.5 nm for efficient electron hopping. [5]

Consider first the PVAm-T adsorbed directly on the gold-sulfonate surface. Fleer *et al*. have discussed the configuration of adsorbed polymer in detail, and the relevant parameter is *p*, the fractions of polymer segments present as adsorbed trains; the remainder of the polymer chain is present as loops and tails, not in contact with the surface ($0<p\leq1$). [23] It seems reasonable to propose that for PVAm-T copolymers with low DS values, only those TEMPOs attached to trains would be redox-active.

$$\Gamma_{TRA} = p \times \Gamma_{TL1} \quad \text{for DS} \leq \text{DS}_c$$
$$\Gamma_{TRA} = \Gamma_T \quad \text{for DS} > \text{DS}_c \qquad \text{Eq 2}$$

The other limiting case is when the TEMPO DS is so high that, through TEMPO-to-TEMPO hopping, all TEMPO moieties are redox active. These two limiting cases are captured in Eq 2 where: Γ_{TRA}, the surface coverage of redox-active TEMPO; Γ_{TL1} is the total TEMPO coverage in the first PVAm-T layer adsorbed on gold; and, Γ_T is the total TEMPO coverage from all the layers in the multilayer films.

Eq 2 was use to simulate the results in Figure 3- 6 and in Figure 3- 7. We assumed that every PVAm-T layer had the same mass coverage $_{T1}$ = 0.5 mg/m^2 and the corresponding $_{TL1}$ was calculated from Eq 1. The detailed calculations are shown in the SI file.

Figure 3- 6 compares the model with the experimental redox-active TEMPO coverage versus the number of bilayers, n. The model predicts two straight lines; one is horizontal if the DS is below the critical value, DSc. In this case, only the first adsorbed layer accounts for all of the redox-active TEMPO coverage. The experimental values sit between these theoretical limiting cases.

When varying the TEMPO DS on PVAm-T for a 4 bilayer assembly (Figure 3- 7), the model curve corresponded to DS< DSc where only the first layer is redox active. In this case the plot is non-linear and the chosen model parameters give a reasonable fit to the experimental values. However, we present this analysis not as a useful fitting tool for the data, but instead to illustrate where the experimental results map onto two limiting cases.

From a more practical perspective, the results in Figure 3- 8 shows that the surface density of redox-active TEMPOs is a linear function of the overall TEMPO coverage for our system. This suggests a convenient route to control oxidation in practical applications.

3.5 Conclusions

The new conclusions from this work are:

1. Layer-by-layer PVAm-T/PSS films are stable and redox-active.

2. Only 20-30% of the TEMPOs in (PVAm-T25L/PSS)$_4$ multilayer films were redox-active, reflecting the requirement that TEMPO moieties must be closer than ~ 0.6nm for electron transfer to occur. This efficiency of electron transfer was maintained up to four bilayer pairs, the thickest assembly we examined.

3. The molar coverage (mol/m^2) of redox-active TEMPO moieties was a linear function of the TEMPO content in the (PVAm-Tx/PSS)$_4$ multilayer films. We did not observe a percolation threshold below which outer TEMPO groups could not be oxidized by the gold-sulfonate electrode.

4. The PVAm-T25L/PSS LbL multilayer films were about 75% water and small, reversible decreases in swelling were induced by oxidizing the TEMPO moieties.

5. There was significant interpenetration of polymer chains between the multilayers as evidenced by the need for three pairs of blocking layers to prevent electron transfer throughout the film. Similar results have been reported for other redox-active multilayer film types. [8] [19]

6. PVAm-T is slightly more hydrophobic than PVAm, as evidenced by decreasing surface tension with increasing TEMPO substitution. However, unlike TEMPO derivatives of polyacrylic acid, [24] PVAm-T with DS values up to 35% is water soluble over the pH range 1 to 9.

References

(1) Pelton, R. Polyvinylamine: A Tool for Engineering Interfaces. *Langmuir* **2014,** *30* (51), 15373-15382.

(2) Pelton, R.; Ren, P. R.; Liu, J.; Mijolovic, D. Polyvinylamine-G-TEMPO Adsorbs onto, Oxidizes and Covalently Bonds to Wet Cellulose. *Biomacromolecules* **2011,** *12*, 942–948.

(3) Liu, J.; Pelton, R.; Obermeyer, J. M.; Esser, A. Laccase Complex with Polyvinylamine Bearing Grafted TEMPO Is a Cellulose Adhesion Primer. *Biomacromolecules* **2013,** *14*, 2953−2960.

(4) Tanyeli, C.; Gümüş, A. Synthesis of Polymer-Supported TEMPO Catalysts and Their Application in the Oxidation of Various Alcohols. *Tetrahedron Letters* **2003,** *44* (8), 1639-1642.

(5) Kemper, T. W.; Larsen, R. E.; Gennett, T. Relationship between Molecular Structure and Electron Transfer in a Polymeric Nitroxyl-Radical Energy Storage Material. *The Journal of Physical Chemistry C* **2014,** *118* (31), 17213-17220.

(6) Bobela, D. C.; Hughes, B. K.; Braunecker, W. A.; Kemper, T. W.; Larsen, R. E.; Gennett, T. Close Packing of Nitroxide Radicals in Stable Organic Radical Polymeric Materials. *The Journal of Physical Chemistry Letters* **2015,** *6* (8), 1414-1419.

(7) Casado, N.; Hernández, G.; Sardon, H.; Mecerreyes, D. Current Trends in Redox Polymers for Energy and Medicine. *Progress in Polymer Science* **2016,** *52*, 107-135.

(8) Laurent, D.; Schlenoff, J. B. Multilayer Assemblies of Redox Polyelectrolytes. *Langmuir* **1997,** *13* (6), 1552-1557.

(9) Takahashi, S.; Aikawa, Y.; Kudo, T.; Ono, T.; Kashiwagi, Y.; Anzai, J.-i. Electrochemical Decomposition of Layer-by-Layer Thin Films Composed of TEMPO-Modified Poly(Acrylic Acid) and Poly(Ethyleneimine). *Colloid and Polymer Science* **2014,** *292* (3), 771-776.

(10) Gu, L.; Zhu, S.; Hrymak, A. N. Acidic and Basic Hydrolysis of Poly(N-Vinylformamide). *Journal of Applied Polymer Science* **2002,** *86* (13), 3412-3419.

(11) Pelton, R.; Ren, P.; Liu, J.; Mijoloyic, D. Polyvinylamine-Graft-TEMPO Adsorbs onto, Oxidizes, and Covalently Bonds to Wet Cellulose. *Biomacromolecules* **2011,** *12* (4), 942-948.

(12) Ruths, J.; Essler, F.; Decher, G.; Riegler, H. Polyelectrolytes I: Polyanion/Polycation Multilayers at the Air/Monolayer/Water Interface as Elements for Quantitative Polymer Adsorption Studies and Preparation of Hetero-Superlattices on Solid Surfaces. *Langmuir* **2000,** *16* (23), 8871-8878.

(13) Feng, X.; Zhang, D.; Pelton, R. Adhesion to Wet Cellulose - Comparing Adhesive Layer-by-Layer Assembly to Coating Polyelectrolyte Complex Suspensions. *Holzforschung* **2009,** *63* (1), 28-32.

(14) Katchalsky, A.; Mazur, J.; Spitnik, P. Section Ii: Polybase Properties of Polyvinylamine. *Journal of Polymer Science* **1957,** *23* (104), 513-532.

(15) Feng, X.; Pelton, R.; Leduc, M.; Champ, S. Colloidal Complexes from Poly(vinyl amine) and Carboxymethyl Cellulose Mixtures. *Langmuir* **2007,** *23* (6), 2970-2976.

(16) Hodak, J.; Etchenique, R.; Calvo, E. J.; Singhal, K.; Bartlett, P. N. Layer-by-Layer Self-Assembly of Glucose Oxidase with a Poly(Allylamine)Ferrocene Redox Mediator. *Langmuir* **1997,** *13* (10), 2708-2716.

(17) Voinova, M. V.; Jonson, M.; Kasemo, B. 'Missing Mass' Effect in Biosensor's Qcm Applications. *Biosensors and Bioelectronics* **2002,** *17* (10), 835-841.

(18) Sauerbrey, G. Use of Quartz Crystal Vibrator for Weighting Thin Films on a Microbalance. *Zeitschrift fur Physik* **1959,** *155*, 206-222.

(19) Liu, A.; Anzai, J.-i. Ferrocene-Containing Polyelectrolyte Multilayer Films: Effects of Electrochemically Inactive Surface Layers on the Redox Properties. *Langmuir* **2003,** *19* (9), 4043-4046.

(20) Sato, H.; Anzai, J.-i. Preparation of Layer-by-Layer Thin Films Composed of DNA and Ferrocene-Bearing Poly(Amine)s and Their Redox Properties. *Biomacromolecules* **2006,** *7* (6), 2072-2076.

(21) Liu, A. H.; Kashiwagi, Y.; Anzai, J. Polyelectrolyte Multilayer Films Containing Ferrocene: Effects of Polyelectrolyte Type and Ferrocene Contents in the Film on the Redox Properties. *Electroanalysis* **2003,** *15* (13), 1139-1142.

(22) Zahn, R.; Vörös, J.; Zambelli, T. Tuning the Electrochemical Swelling of Polyelectrolyte Multilayers toward Nanoactuation. *Langmuir* **2014,** *30* (40), 12057-12066.

(23) Fleer, G. J.; Cohen Stuart, M. A.; Scheutjens, J. M. H. M.; Cosgrove, T.; Vincent, B. *Polymers at Interfaces*; Chapman & Hall: London, 1993.

(24) Fu, Q.; Gray, Z. R.; van der Est, A.; Pelton, R. H. Phase Behavior of Aqueous Poly(Acrylic Acid-g-TEMPO). *Macromolecules* **2016,** *49* (13), 4935-4939.

(25) Chen, X. N.; Wang, Y.; Pelton, R. Ph-Dependence of the Properties of Hydrophobically Modified Polyvinylamine. *Langmuir* **2005,** *21* (25), 11673-11677.

Appendix: Supporting information for Chapter 3

Chapter 3 Redox properties of polyvinylamine-g-TEMPO in multilayer films with sodium poly(styrene sulfonate)

Polymer synthesis

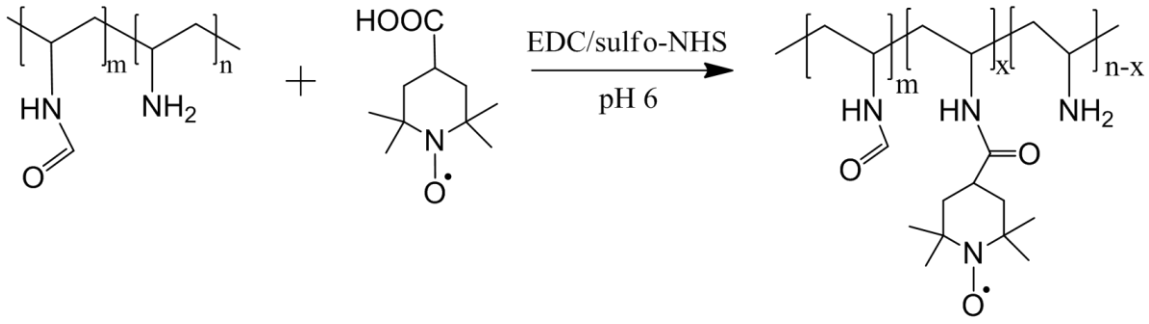

Figure S3- 1 Preparation of PVAm-T from PVAm

Surface Activity of PVAm-T

Surface tension measurement. Surface tension of PVAm and PVAm-T solutions was measured with the pendant drop method (Kruss GmbHdrop shape system DSA10, Hamburg, Germany). The temperature was maintained at 25 ^{o}C, and the humidity 100% with a closed glass chamber. In a typical experiment, 0.3 wt% PVAm-T was completely dissolved in a 5 mM KCl solution, and the pH of the PVAm-T solution were adjusted by 1 N NaOH and HCl. A syringe with a 1.22 mm flat needle was used to form drops. , and

the drop volumes varied from 15 to 19 μL. Surface tension values were recorded as a function of drop lifetime.

Figure S3- 2 shows surface tension of PVAm-T13L solution as functions of drop age and pH. A slow decrease of surface tension with aging time was observed. In fact, steady-state surface tension curves of PVAm derivatives have never been observed since 2005 Chen *et al*[1] studied the surface tension of hydrophobically modified polyvinylamine in our group. We followed Chen *et al.*[1] method, and studied the surface tension values at the break point where the dynamic surface tension curve switches from a rapid to slow changing rate regime.

Figure S3- 3 shows the break point surface tension values from Figure S3- 2 as functions of pH. The breakpoint surface tension decreased slightly at pH <5, which indicated that the PVAm-T was surface inactive in this pH range. In the pH range 5 to 7 an obvious decrease was observed, and the breakpoint surface tension rapidly decreased to 60 mN/m, whereas, further increasing pH the surface tension became stable at 60 mN/m. The PVAm-T was only slightly surface active at alkaline conditions (60 mN/m at pH above 9). And the surface tension of PVAm-T was collapsed well onto the single master curve "breakpoint surface tension vs hydrophobicity index" developed by Chen et al. [1] (see Figure S3- 4).

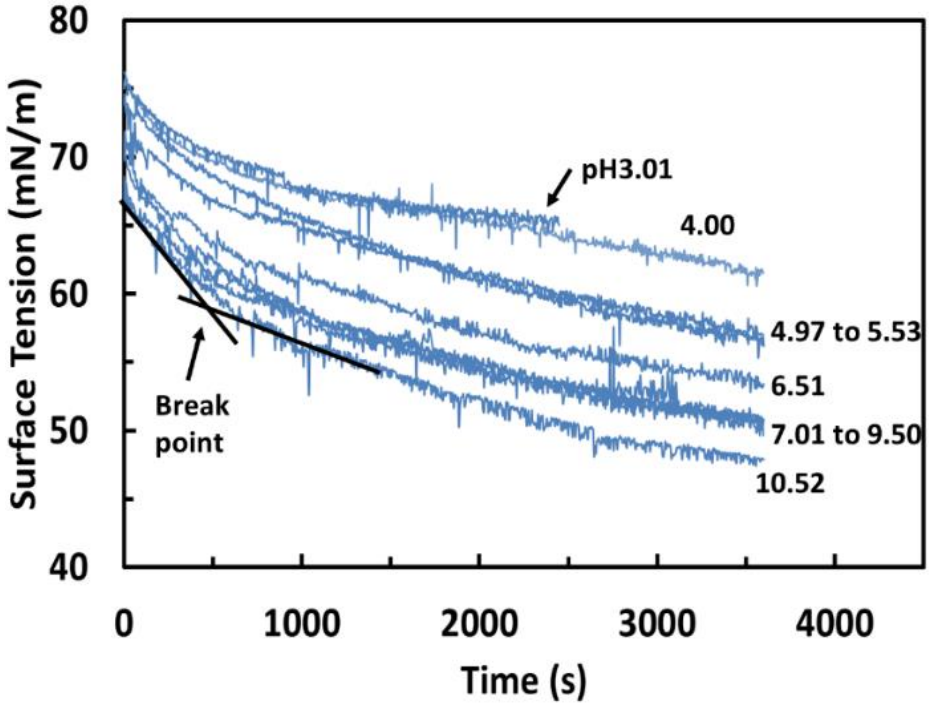

Figure S3- 2 Surface tension of 0.3wt% PVAm-T13L in 5 mM KCl as a function of pendant drop age at 25 ^{o}C.

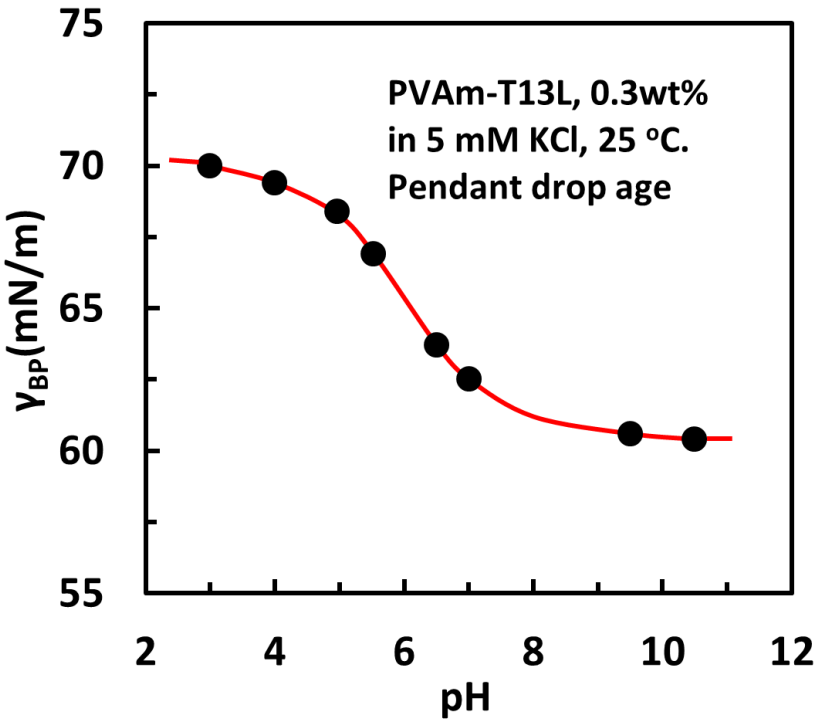

Figure S3-3 Break point surface tension (See Figure 1) as a function of pH for 0.3wt% PVAm-T13L in 5 mM KCl at 25 °C.

Chen et al. [1] developed a hydrophobicity index to study the surface tension of hydrophobically modified polyvinylamine at pH 9. According to Chen *et al.*[1] the hydrophobicity index "*was defined as DS*n, where DS is the number of hydrophobic substituents per nitrogen, and n is the number of hydrophobic carbon atoms in each substituent"*. It was found that the surface tension behaviors of both alkyl and benzyl substituted PVAm fell into a master curve when the surface tension values were plotted against hydrophobicity. TEMPO is more water soluble than alkyl chain and benzyl group due to the N-O bond in its structure. The hydrophobicity index was also applied to PVAm-T to study the surface tension of PVAm-T as functions of hydrophobicity index. As shown in Figure S1, the TEMPO pendant group has 9 carbon atoms. As a result the n in the hydrophobicity index was given as 9. Figure S3- 4 shows the breakpoint surface tension of modified PVAm as functions of hydrophobicity index at pH 9. The surface tension of PVAm-T was collapsed well onto the single master curve "breakpoint surface tension vs hydrophobicity index".

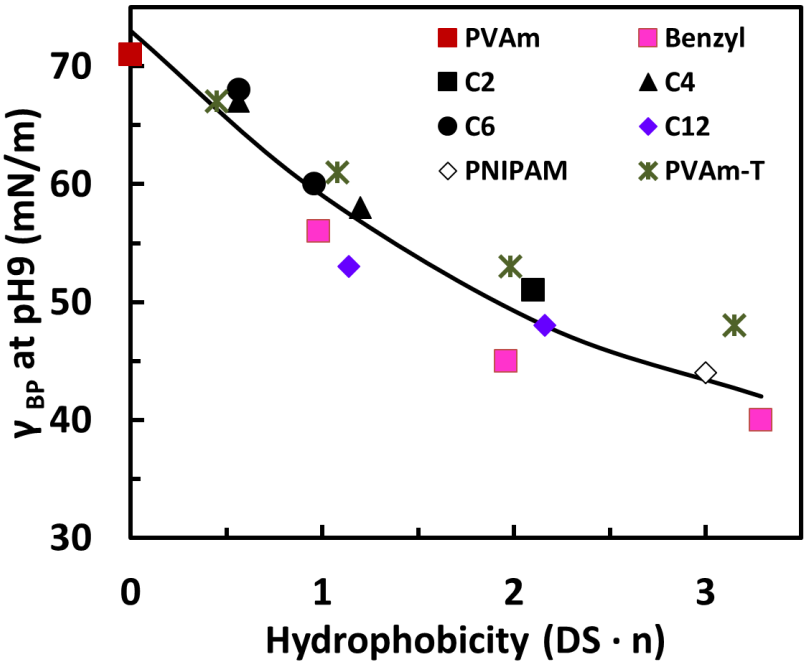

Figure S3- 4 Breakpoint surface tension as functions of hydrophobicity of modified PVAm. Measurement conditions: 0.3 wt% polymer in 1 mM KCl aqueous solution, polymer solution pH 9, and temperature 25 ^{o}C.

Intrinsic viscosity

Intrinsic viscosity measurements. The intrinsic viscosity of PVAm and PVAm-T solutions was determined from the extrapolation of specific and inherent viscosities under varied polymer concentrations. The viscosity of polymer solutions was measured with an Ubbelohde capillary viscometer (Size 75, Cannon Instrument Co. USA) at 25 ^{o}C. Figure S5 shows the intrinsic viscosity of PVAm and PVAm-T at three pH values. TEMPO substitution lowered the intrinsic viscosity of PVAm at pH 4 and 8, suggesting a more compact configuration of PVAm-T, whereas the effect of TEMPO substitution on intrinsic viscosity is negligible at pH 10.

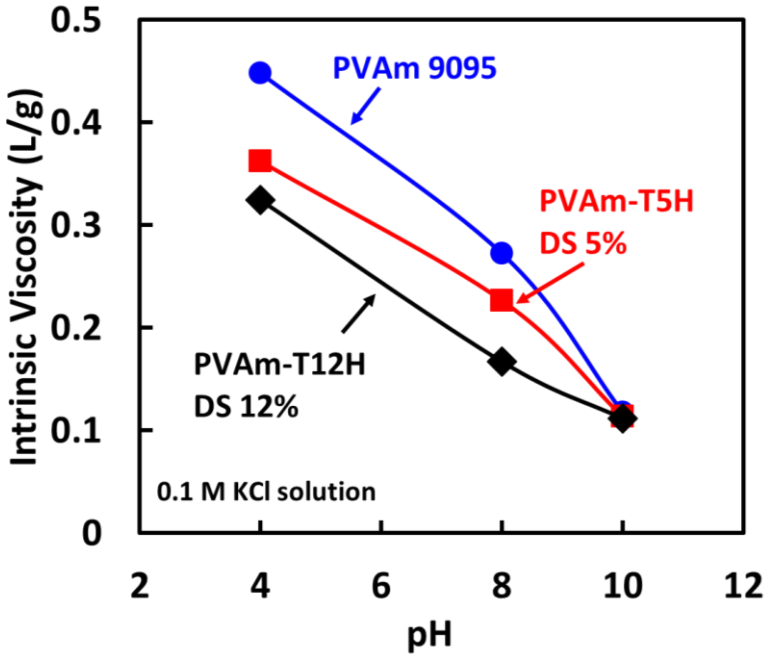

Figure S3- 5 Intrinsic viscosity of PVAm and PVAm-T in 0.1 M KCl at 25 °C.

QCM-D

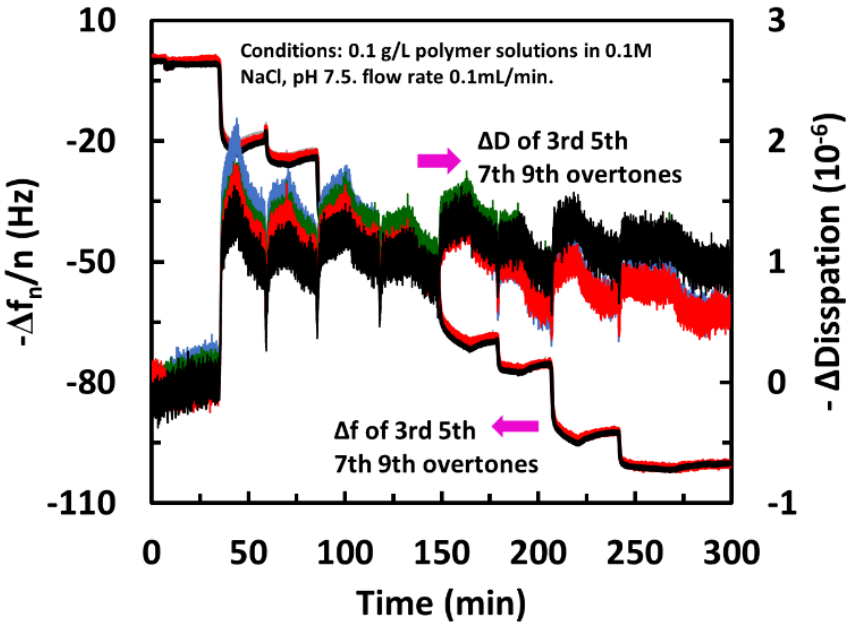

Figure S3- 6 QCM-D monitoring the formation process of $(PVAm\text{-}T25L/PSS)_4$ multilayer films

Reversible swelling of (PVAm-T/PSS) multilayer films under electro-stimuli

Upon exposure to electro-stimuli redox multilayer films usually show multiple responses, such as changes of film thickness, Young's elastic modulus, and permeability for ions and small molecules through the thin films[2]. Upon electro-stimuli, counter ions and solvent flux in or out, the osmotic pressure in the films changes respond to the flux, resulting in shrinking or swelling of films.

Figure S3- 7 (a) shows the electrochemical controlling the shrinking of $(PVAm\text{-}T25L/PSS)_4$ multilayer film with varied external potentials. Two features were observed. First, the film was very stable under the external potentials, and no decomposition was observed. Second, the change of Δf depends on the applied potentials. Three cycles of external potentials were applied (two cycles shown here), the response of the multilayer film to the external potentials showed good reproducibility. Figure S3- 7 (b) shows that about 10-15 wt% water and ions in the multilayer films were exchanged with the ambient NaCl solution under applied potentials.

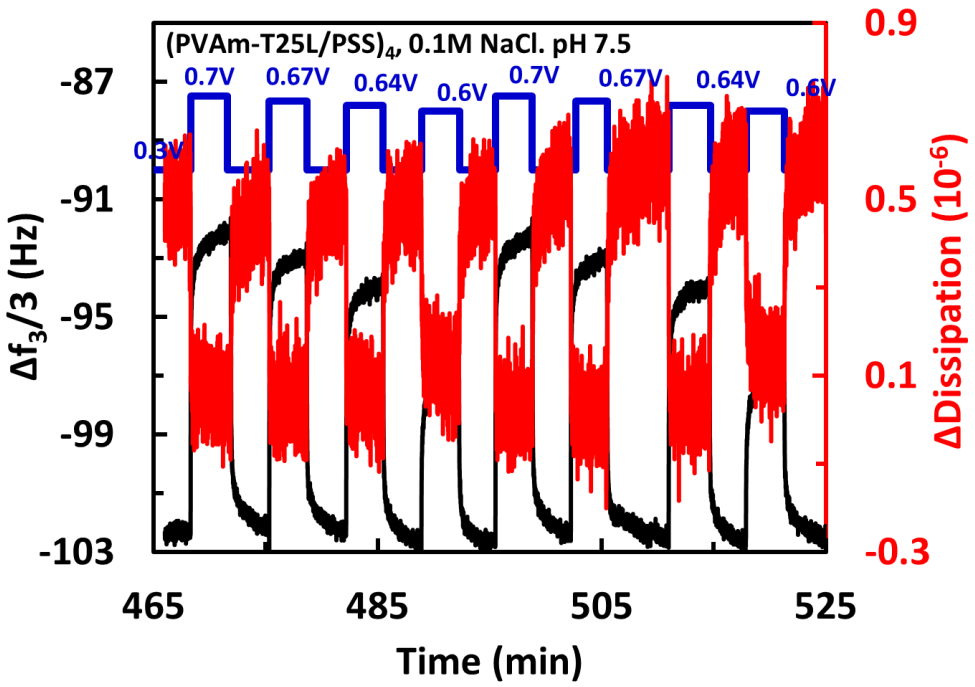

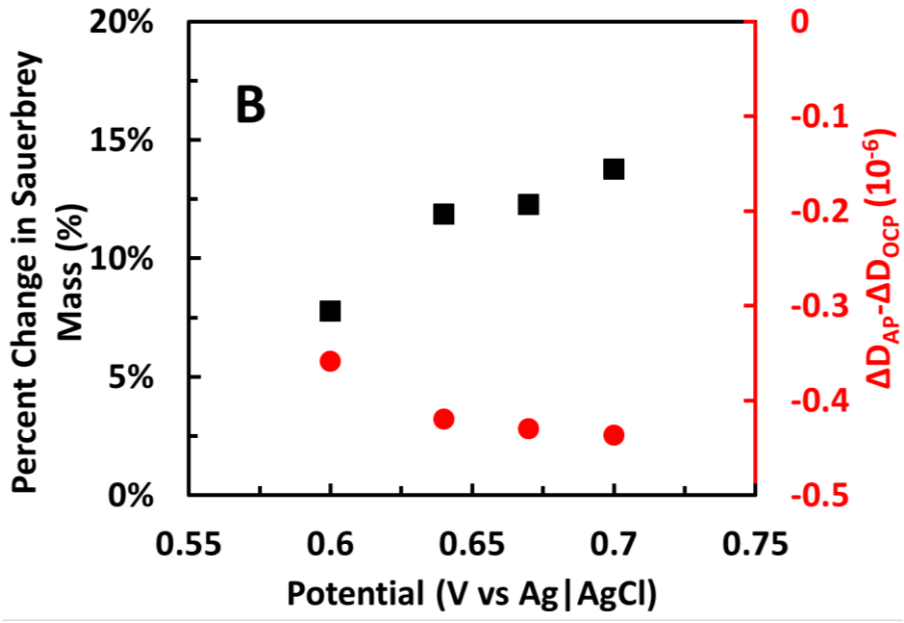

Figure S3- 7 Frequency and dissipation shifts of redox $(PVAm\text{-}T25L/PSS)_4$ multilayer film responding to the external potentials. 0.1M NaCl, pH 7.5. Δf3 is the frequency shift at applied potential under 3rd overtone, and ΔDOCP is the frequency shift at open circuit potential under the same overtone.

Table S3- 1 Summary of EQCM and ellipsometric characterization $(PVAm\text{-}T25L/PSS)_n$ multilayer films.

Bilayer Number	$\Delta f_3/3$ (-Hz)	Sauerbrey Coverage (mg/m^2)	Ellipsometric Coverage (mg/m^2)	Water Content (wt%)	Oxidation Charge (μC)	Redox-Active T ($\mu mol/m^2$)
0.5	20.6	3.65	0.4 ±0.33	89 ±9	-----	----
1	24.6	4.35	0.7 ±0.32	83 ±7	1.54 ±0.82	0.20 ±0.11
1.5	43.8	7.75	1.6 ±0.32	78 ±4	-----	----
2	49.6	8.77	2.1 ±0.40	76 ±5	3.48 ±0.87	0.46 ±0.12
2.5	69.8	12.4	3.0 ±0.19	75 ±2	----	----
3	75.5	13.4	3.4 ±0.27	74 ±2	8.1 ±1.59	1.06 ±0.21
3.5	92.3	16.3	4.3 ±0.38	73 ±2	-----	----
4	101.1	17.9	4.8 ±0.38	73 ±2	15.5 ±1.25	2.05 ±0.19

Table S3- 2 Summary of EQCM and ellipsometric characterization (PVAm-TxL/PSS)$_4$ multilayer films.

PVAm-Tx	$\Delta f_3/3$ (Hz)	Sauerbrey Coverage (mg/m^2)	Ellipsometric Coverage (mg/m^2)	Oxidation Charge (μC)	Redox-Active T Coverage ($\mu mol/m^2$)
PVAm-T4L	90.1	15.95	4.3±0.75	1.91±1.25	0.25±0.16
PVAm-T10L	96.7	17.16	4.4±0.56	5.92±1.27	0.78±0.17
PVAm-T13L	108.2	19.15	5.3±0.94	7.18±1.57	0.95±0.21
PVAm-T25L	101.1	17.89	4.8±0.38	15.5±1.25	2.05±0.19

References

(1) Chen, X. N.; Wang, Y.; Pelton, R. Ph-Dependence of the Properties of Hydrophobically Modified Polyvinylamine. *Langmuir* **2005,** *21* (25), 11673-11677.

(2) Calvo, E. Electrochemically Active Lbl Multilayer Films: From Biosensors to Nanocatalysts. *Multilayer Thin Films: Sequential Assembly of Nanocomposite Materials, Second Edition* **2012**, 1003-1038.

General expressions for PVAm compositions

Sample : PVAm-T25L

$dh := 75\%$ degree of PNVF hydrolysis

$ds := 25\%$ degree of subsititution (Tempo or any other substituent)

$MW_{nvf} := 71.08\ \mathit{Da}$ Molecular weight of NVF monomer

$MW_{vam} = 43.0682\ \mathit{Da}$ Molecular weight of vinyl amine repeat unit

$EW_{pvam}(dh) := dh \cdot MW_{vam} + (1 - dh) \cdot MW_{nvf}$ The equivalent weight of non-ionized PVAm (i.e. no counterions) based on nitrogen - it is the mass per N

$EW_{pvam}(dh) = 50.0712\ \mathit{Da}$

We now account for the affect of attaching substituents. In this case we show tempo, method can apply to any substituent.

$MW_{tempo} := 156.25 \cdot \mathit{Da}$

$MW_{sub} := MW_{vam} + MW_{tempo} + AM_C + -2 \cdot AM_H + AM_O = 225.3074\ \mathit{Da}$ Molecular weight of the substituent including the two backbone carbons. In this case it is for TEMPO

$EW_N(dh, ds, MW_{sub}) := (1 - ds) \cdot dh \cdot MW_{vam} + (1 - dh) \cdot MW_{nvf} + ds \cdot MW_{sub}$

$EW_N(dh, ds, MW_{sub}) = 98.3227\ \mathit{Da}$ $EW_N(0, 0, MW_{sub}) = 71.08\ \mathit{Da}$

$dh \cdot ds = 0.1875$ This is the number of Tempos per N

$EW_{sub}(dh, ds, MW_{sub}) := \frac{EW_N(dh, ds, MW_{sub})}{dh \cdot ds}$ This is the mass per tempo group

$EW_{sub}(dh, ds, MW_{sub}) = 524.3878\ \mathit{Da}$ $\mathit{mmol} := 0.001\ \mathit{mol}$

$\frac{1}{EW_{sub}(dh, ds, MW_{sub})} = 1.907\ \frac{\mathit{mmol}}{\mathit{gm}}$

The goal of the following calculation is to calculate average properties of PVAm derivatives

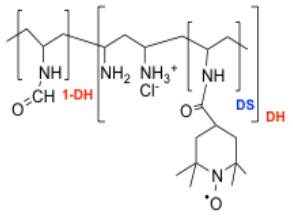

definitions of ds, dh and α

$$\alpha = \frac{y}{x+y} \qquad ds = \frac{z}{x+y+z} \qquad dh = x+y+z = 1-w$$

$$1 = w+x+y+z$$

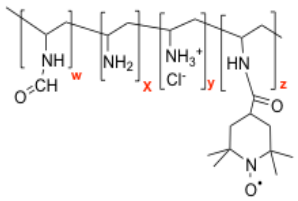

Inverse functions

$$y = \alpha \cdot (1-(1-dh)-ds \cdot dh) = \alpha \cdot (dh - ds \cdot dh) \qquad w = 1-dh$$

$$x = y \cdot \left(\frac{1}{\alpha}-1\right) = \alpha \cdot (dh - ds \cdot dh) \cdot \left(\frac{1}{\alpha}-1\right) \qquad z = ds \cdot dh$$

Parameters we can measure

Conductometric titation gives an accurate measure of the total amine content

DH - degree of hydrolysis, given by manufacturer, can measure by NMR, elemental analysis, Not by titration

DS - degree of substitution measured by changes in conductometric titration before and after substitution reactions

α difficult to measure - high performance potentiometric titration, can estimate fairly accurately from Katchalski's model - see appendix

Calculation of the equivalent weight of a substituent (TEMPO) as functions of DH, DS, pH, I

the counter ion of charged amine groups was assumed to be chloridion

$dh := 75\%$ degree of PNVF hydrolysis

$ds := 25\%$ mole fraction of amine groups bearing Tempo (or any other substituent)

$pH := 7.5$ pH during Layer-by-Layer self-assemble

$I := 0.1\ \frac{mole}{L}$ Ionic strength during Layer-by-Layer self-assemble

$\alpha_{pvam}(pH, I) = 0.4632$ degree of amine ionization - see appendix for details

$MW_{nvf} := 71.08\ Da$ Molecular weight of NVF moiety, w

$MW_{vam} = 43.0682\ Da$ Molecular weight of vinyl amine repeat unit, x

$MW_{pvamhcl} = 79.5291\ Da$ Molecular weight of vinyl amine HCl salt, y

$MW_{tempo} := 156.25 \cdot Da$

$MW_{sub} := MW_{vam} + MW_{tempo} + AM_C + -2 \cdot AM_H + AM_O = 225.3074\ Da$

Molecular weight of the substituent including the two backbone carbons. In this case it is for TEMPO, z

Equivalent weight of based on TEMPO

$$EW_{pvamt} = \frac{w \cdot MW_{nvf} + x \cdot MW_{vam} + y \cdot MW_{pvamhcl} + z \cdot MW_{sub}}{z}$$

$$EW_{pvamt}(dh, ds, I, pH) := \frac{(1-dh) \cdot MW_{nvf} + (dh - ds \cdot dh) \cdot (1 - \alpha_{pvam}(pH, I)) \cdot MW_{vam} + \alpha_{pvam}(pH, I) \cdot (dh - ds \cdot dh) \cdot MW_{pvamhcl} + ds \cdot dh \cdot MW_{sub}}{ds \cdot dh}$$

$EW_{pvamt}\left(0.750, 0.25, 0.1\ \frac{mole}{L}, 7\right) = 504.6931\ Da$

$\frac{1}{EW_{pvamt}\left(0.75, 0.25, 0.1\ \frac{mole}{L}, 7\right)} = 1.9814\ \frac{mol}{kg}$

$\alpha_{pvam}(pH, I) = 0.4632$

Equivalent weight of based on total amine

$$EW_{pvam}(dh, ds, I, pH) := \frac{(1-dh) \cdot MW_{nvf} + (dh - ds \cdot dh) \cdot (1 - \alpha_{pvam}(pH, I)) \cdot MW_{vam} + \alpha_{pvam}(pH, I) \cdot (dh - ds \cdot dh) \cdot MW_{pvamhcl} + ds \cdot dh \cdot MW_{sub}}{(dh - ds \cdot dh)}$$

For PVAm-T25L , DS=25%

$EW_{pvam}\left(0.75, 0.25, 0.1\ \frac{mole}{L}, 7.5\right) = 166.6521\ Da$

PVAm ionization versus pH

$\alpha_k \equiv 0.9$ Degree of ionization of PVAm, a variable

$I_k \equiv \frac{mole}{L}$ Ionic strength of 1:1 electrolyte

$$pK_{pvam}(I_k) \equiv 8.4 + \frac{3.5 \cdot \frac{I_k}{\frac{mol}{L}}}{0.8 + 2 \cdot \frac{I_k}{\frac{mol}{L}}}$$

The intrinsic equilibrium constant as a function of ionic strength. We derived this empirically by fitting Katchalsky's experimental data - only valid for 1:1 salt from 0 to 1 M

$A_k \equiv 47$ Nearest neighbor interaction energy which is not sensitive to ionic strength

$$x(\alpha_k) \equiv \frac{A_k \cdot (2 \cdot \alpha_k - 1) - 2 \cdot \alpha_k + \left(A_k^2 \cdot (2 \cdot \alpha_k - 1)^2 + 4 \cdot A_k \cdot \alpha_k \cdot (1 - \alpha_k)\right)^{0.5}}{2 \cdot (A_k - 1)}$$

Fraction of doublets

$$pH_{pvam}(\alpha_k, I_k) \equiv pK_{pvam}(I_k) + \log\left(\frac{\alpha_k}{1 - \alpha_k} \cdot \frac{(1 - 2 \cdot \alpha_k + x(\alpha_k))^2}{(\alpha_k - x(\alpha_k))^2}\right)$$

pH as function of α

$$\alpha_{pvam}\left(7.5, 0.1 \frac{mole}{L}\right) = 0.4632$$

$\alpha_{pvam}(pH, I_k) \equiv \mathbf{root}(pH_{pvam}(\alpha_k, I_k) - pH, \alpha_k)$ α as a function of pH

$$\alpha_{pvam}\left(7.5, 0.001 \frac{mole}{L}\right) = 0.4276$$

1. Calculating adsorbed TEMPO content based on ellipsometry

the thickness of the multilayer films was measured with ellipsometry

$$\begin{bmatrix} 1\ bilayer \\ 2\ bilayers \\ 3\ bilayers \\ 4\ bilayers \end{bmatrix} \qquad hi := \begin{bmatrix} 0.4 \\ 1.2 \\ 2.1 \\ 2.9 \end{bmatrix} \cdot nm$$

hi is the thickness of i PVAm-T4 layers with i=1,2,3, and 4.

$$\sigma_{PVAmT} := 1080 \cdot \frac{kg}{m^3}$$

σ_{PVAmT} is the density of PVAm-T, and is assumed the same density of PVAm

$$D := 10 \cdot mm$$

D is the diameter of Au substrate for multilayer films' buildup

$$A := \frac{1}{4} \cdot \pi \cdot D^2 = \left(7.854 \cdot 10^{-5}\right)\ m^2$$

A is the surface area of the Au chip which is covered by the multilayer films

$$C_i := \frac{hi \cdot A \cdot \sigma_{PVAmT}}{A} = \begin{bmatrix} 0.432 \\ 1.296 \\ 2.268 \\ 3.132 \end{bmatrix} \frac{mg}{m^2}$$

Ci is the coverage of adsorbed (PSS/PVAm-T4) multilayer films with i bilayers, i=1, 2, 3, and 4

$$n_m := 1.907 \cdot \frac{mmol}{gm}$$

TEMPO mole content in 1 g of PVAm-T4

As a result, TEMPO content of the multilayers are:

$$\begin{bmatrix} 1\ bilayer \\ 2\ bilayers \\ 3\ bilayers \\ 4\ bilayers \end{bmatrix} \qquad \Gamma_{el} := C_i \cdot n_m = \begin{bmatrix} 0.8238 \\ 2.4715 \\ 4.3251 \\ 5.9727 \end{bmatrix} \frac{\mu mol}{m^2}$$

Γel is the TEMPO content of i bilayers films with i=1,2,3, and 4.

2. Calculating redox-active TEMPO based on cyclic voltammetry

$n := 1$ number of electron tranferred in the redox center TEMPO half reaction

$F = (9.6485 \cdot 10^4)\ \frac{C}{mol}$

$A := \frac{1}{4} \cdot \pi \cdot D^2 = (7.854 \cdot 10^{-5})\ m^2$

$\begin{bmatrix} 1\ bilayer \\ 2\ bilayers \\ 3\ bilayers \\ 4\ bilayers \end{bmatrix}$ $Q := \begin{bmatrix} 1.54 \\ 3.48 \\ 8.1 \\ 15.12 \end{bmatrix} \cdot 10^{-6} \cdot C$

Q is the charge measured by Cyclic voltammetry

$\Gamma_{cv} := \frac{Q}{n \cdot F \cdot A} = \begin{bmatrix} 0.2032 \\ 0.4592 \\ 1.0689 \\ 1.9953 \end{bmatrix} \frac{\mu mol}{m^2}$

Γcv is the coverage of redox-active TEMPO on surface.

$i := 0 .. 3$

$f_i := \frac{\Gamma_{cv_i}}{\Gamma_{el_i}} \cdot 100\%$ $f = \begin{bmatrix} 0.2467 \\ 0.1858 \\ 0.2471 \\ 0.3341 \end{bmatrix}$

f is the fraction of redox-active TEMPO in (PVAm-T25L/PSS)n multilayer films.
n=1,2,3, and 4.

Chapter 4 Electrochemical Characterization of Polyvinylamine-g-TEMPO/laccase Complexes for Cellulose Wet Adhesion

I conducted most of the experiments in chapter 4. Alexander Sutherland (undergraduate student) helped with UV-vis spectroscopy, DLS, and Electrophoresis measurements. Dr. M. Monsur Ali helped with fluorescence measurement; they will be coauthors on the publication along with Professor Soleymani. I plotted the experimental data and Dr. Robert Pelton helped to analyze the data. The paper was initially written by me, and edited later by Dr. Robert Pelton.

Chapter 4 Electrochemical Characterization of Polyvinylamine-g-TEMPO/laccase Complexes for Cellulose Wet Adhesion

4.1 Introduction

Cellulose is the most abundant renewable material on earth and even though it already is a hugely important material in the form of paper and cardboard it is posed to play an increasingly large role in the renewable economy. One of the main drawbacks limiting the applications for cellulose fibers both in traditional applications and in new composite nanomaterials is its inherent hydrophilicity. Cellulose absorbs water and swells when exposed to water and vapor, which makes it difficult to make materials that are strong when they are wet. Traditionally polymeric wet strength agents are used to improve the wet strength[1]. These strengthen the fiber-fiber joints by forming a cross-linked network with themselves, the cellulose fibers or a combination of the two.

In earlier work we have established that polyvinylamine (PVAm) is a good wet strengthening agent, provided that the cellulose has first been gently oxidized to introduce reactive aldehyde groups. The improved wet strength comes from imine and aminal linkages between the primary amines on PVAm and the aldehydes on the oxidized which crosslinks the fiber-fiber joints in the fiber network.

In our early work, we used Isogai's recipe[2] to oxidize cellulose, where sodium hypochlorite (NaClO) serves as the primary oxidant, sodium bromide (NaBr) is the co-oxidant, and 2, 2, 6, 6-tetramethyl-1-piperidinoxy (TEMPO) serves as the mediator. Linear PVAm[3], PVAm nanoparticles[4-5] and PVAm coated pH- and temperature-responsive microgels[6-7] have all been studied to optimize the wet strengthening properties of PVAm. However, the practical application of the TEMPO/NaClO/NaBr oxidation method in the paper industry is limited by mainly two difficulties. First, TEMPO is expensive and may also cause environmental issues due to its toxicity; and processing large volumes of TEMPO solutions is challenge. Second, the oxidation is conducted in pH 10-11, which is too high to be used in papermaking industry.

In 2011 we immobilized TEMPO onto cationic PVAm, forming PVAm-g-TEMPO (PVAm-T)[8]. The PVAm-T adsorbs onto, oxidizes, and activates cellulose surfaces in a single step in the presence of NaClO/NaBr. Significantly less TEMPO is required since the PVAm bound TEMPO is concentrated near the cellulose surface when the cationic PVAm-T is physically adsorbed onto the cellulose[9]. PVAm-T was further explored in combination with the enzyme laccase which can oxidize cellulose at pH 5, conditions more compatible with papermaking techniques. The results demonstrated that PVAm-T/laccase oxidizes cellulose, and high wet adhesion was achieved with 10 mol% or higher TEMPO substitution[10]. TEMPO has also been grafted to anionic polyacrylic acid to create poly(acrylic acid-g-TEMPO) (PAA-T), which was employed as mediator for cellulose oxidation in the presence of laccase[11]. Also for PAA-T a ~10 mol% or higher TEMPO substitution was required to achieve high wet adhesion.

The present mechanistic view of TEMPO-mediated oxidation in the presence of laccase is that the free mediator TEMPO acts as an electron shuttle between the enzymatic pocket on laccase and the surface of the substrate where a primary alcohol is oxidized to an andehyde.[12] However, in the TEMPO-grafted polymers PVAm-T and PAA-T the TEMPO-moieties have drastically lower mobility than free TEMPO and therefore their electron shuttling ability should be strongly inhibited. Our hypothesis is instead that the polymer grafted TEMPO serves as mediator by facilitating electron hopping between neighboring TEMPO moieties. In chapter 3 we studied the redox properties of multilayer

films composed of PVAm-T and sodium poly(styrene sulfonate) (PSS). We showed that electron transport takes place not only at the interface between the electrode and the redox multilayer films, but also between TEMPO moieties. The redox properties of these PVAm-T/PSS multilayer films strengthen our electron hopping hypothesis.

In much of our work previous work the aldehyde density of TEMPO oxidized cellulose has been discussed qualitatively based on the wet adhesion achieved with PVAm. However, a quantitative method to determine the aldehyde density on cellulose surfaces has been a longstanding challenge in our group. Both X-ray photoelectron spectroscopy (XPS) and ATR-FTIR have been used to characterize the functional groups on dry cellulose membranes[3]. However, only carboxyl groups could be detected since the aldehyde groups were so active that they reacted with nearby alcohol groups, forming hemiacetal groups when the samples were dried. This led to the conclusion that the aldehyde groups on the cellulose can only be detected in wet, never dried samples. Liu *et al.*[10] used a fluorescein-5-thiosemicarbazide dye to label aldehydes in oxidized cellulose membranes. The highest intensity of fluorescent dye was detected on the exterior surfaces of the cellulose membrane, suggesting that oxidation using PVAm-T is surface specific. Xing *et al.*[13] evaluated the influence of carboxyl groups on the detection of aldehyde groups on a glass surface, using a fluorescence-labeling method with the dye Bodipy FL hydrazide and its derivatives. The study showed that the carboxyl groups have only a limited effect on the determination of aldehyde groups.

This chapter describes the efforts to correlate aldehyde density of PVAm-t/laccase oxidized cellulose with the TEMPO degree of substitution dependent adsorption and redox activity of PVAm-T/laccase complexes. The adsorption and redox properties were investigated by electrochemical quartz crystal microbalance with dissipation (EQCM-D) and aldehyde density was quantitatively determined using fluorescent labeling.

4.2 Experimental section

Materials. Polyvinylamine (PVAm) (Lupamin 5095, Mw 45 kDa, hydrolysis degree 75%), obtained from BASF Canada, was dialyzed against deionized H_2O and freeze-dried before use. N-hydroxysulfosuccinimide sodium salt (sulfo-NHS), sodium 3-mercapto-1-propanesulfonate (MPS), 4-carboxy-TEMPO, 1-ethyl-3-(3-dimethylaminopropyl) carbodiimide (EDC), Laccase from Trametes versicolor (catalog no. 51639), and solid sodium hydroxide were all purchased from Sigma-Aldrich. Acetic acid were purchased from Caledon Laboratories. Fluorescent dye Bodipy FL hydrazide (catalog no. D2371), was purchased from Life Technologies. All solutions were made with deionized H_2O

(18.2 MΩ cm^{-1}, Barnstead Nanopure Diamond system). Regenerated cellulose dialysis tubing (12-14 kDa molecular weight cut-off, MWCO) was obtained from Spectrum Laboratories. The tubing was washed thoroughly with deionized H_2O in order to remove preservatives before use.

PVAm-T Synthesis and Characterization. PVAm-T was synthesized through EDC coupling reaction[10]. PVAm-T compositions are given in Table 4- 1. In a typical experiment, 55 mg 4-carboxy-TEMPO was dissolved in 100 mL deionized water and 157 mg EDC and 170 mg Sulfo-NHS were added. The solution was stirred for 20 min at pH 5.5 at room temperature. PVAm solution (100 mg PVAm in 40 mL deionized water) was gradually added into the above solution, and the solution pH was maintained at 7.0 for 4 h with 0.1 M HCl and 0.1 M NaOH. The product was dialyzed (MWCO 3 kDa) against deionized H_2O for two weeks. The purified and dried products were obtained through lyophilization and stored in a desiccator. The amine content of PVAm-T was determined by potentiometric and conductometric titrations. The degree of TEMPO substitution was calculated from the change of the amine content.

Table 4-1 Properties of PVAm-T (67 mg/L) complexes with laccase (133 mg/L) that were adsorbed onto sulfonated gold QCMD sensors. DS is degree of TEMPO substitution on PVAm-T, $\Delta f_5/5$ and D are the QCM-D frequency changes and dissipation for adsorbed PVAm-T/complex, Γ_{el} is the mass coverage of the dried complex films estimated from ellipsometry, Q is the charge required to oxidize the TEMPO and T_{RA} is the molar coverage of redox-active TEMPO moieties.

	DS (mol%)	$\Delta f_5/5$ (-Hz)	D (10^{-6})	Γ_{el} (mg/m^2)	Q (μC)	T_{RA} (mM/m^2)
PVAm-T0	0	24.0	1.1	0.232	0	0
PVAm-T1	1	24.2	1.1	0.464	0.08±0.08	2.5
PVAm-T4	4	25.2	1.7	0.464	0.22 ± 0.16	6.7
PVAm-T6	6	41.5	2.4	0.58	0.55 ± 0.20	10.1
PVAm-T10	10	41.6	2.6	0.812	1.20 ± 0.15	21.9
PVAm-T13	13	42.5	3.5	0.928	3.13 ± 0.18	56.1
PVAm-T15	15	46.9	2.8	1.044	4.03 ± 0.30	65.4
PVAm-T17	17	75.0	5.5	1.624	6.42 ± 0.45	65.1
PVAm-T20	20	259	42	7.888	30.2 ± 1.93	88.7
PVAm-T25	25	158	20.7	4.872	20.29 ±1 .13	97.9

PVAm-T/laccase Complex Preparation. PVAm-T and laccase were separately dissolved in 50 mM acetate buffer at pH 5, making solutions with concentration 1 g/L. The PVAm-T and laccase solutions were filtered through 0.45 μm filters before use. In this study, all PVAm-T/laccase complexes were prepared by adding laccase into PVAm-T solutions. The PVAm-T solution was first diluted into the desired concentration, and then the laccase solution was added into the diluted PVAm-T solution, drop by drop under magnetic stirring. Solutions were bubbled by O_2 or N_2 before and after the mixing process. In a typical experiment, 2.5 mL of 1 g/L PVAm-T solution was first diluted into 30 mL in acetate buffer and stirred for 30 min. 5 mL of 1 g/L laccase solution was then slowly added drop wise (~2 min/mL) into dilute PVAm-T solution under magnetic stirring.

Phase Behavior Measurements. The phase behavior of the PVAm-T/laccase complexes was obtained by measuring the optical density at 500 nm with a Beckman DU800 UV-vis spectrophotometer. In a typical experiment, 3 mL PVAm-T/laccase complex solution was aged for 1h, and then added to a 10 mm silica cuvette, the optical density at 500 nm was measured immediately.

Dynamic Light Scattering (DLS). The hydrodynamic radiuses of PVAm-T/laccase complexes were measured by DLS (BI-APD Brookhaven Instrument Corp.) at a scattering angle 90^o. The Melles Griot He-Ne laser with a wavelength of 633 nm served as the laser source, and the data were analyzed with the CONTIN method using Brookhaven software 9kdlsw32, version 3.34.

Electrophoresis measurements. The electrophoretic mobility values of PVAm-T/laccase complexes were measured by a ZetaPlus (Brookhaven Instruments Corp.). The data analysis software is PALS (phase analysis light scattering) Version 2.5. Each samples were measured multi-times, and the reported mobility values were the average of 10 cycles with each consisting of 10 scans.

Gold-sulfonate EQCM-D Sensors. Q-Sense E4 QCM QSX 301 gold sensors were cleaned by piranha solution at 75 ℃ for 5 minutes and then thoroughly rinsed with deionized water. Note piranha is dangerous and appropriate precautions must be taken when working with it. The cleaned Au chip was immersed into 3 mM sodium 3-mercapto-1-propanesulfonate ethanol solution for 24 hours, followed by rinsing with ethanol and then by deionized water[14].

Adsorption of PVAm-T/laccase Complexes on Gold-sulfonate Sensor Surfaces. The adsorption of PVAm-T/laccase complexes was monitored by quartz crystal microbalance with dissipation (QCM-D). All solutions were made with 50 mM acetate buffer at pH 5. In a typical experiment, 1g/L laccase and 76.9 mg/L PVAm-T solutions were purged with nitrogen for 30 min, 5 mL laccase solution was then slowly dropped (~2 min/mL) into 32.5 mL PVAm-T13 solution with magnetic stirring and nitrogen bubbling during the mixing process. After aging the mixture for a given time with nitrogen at room temperature, the PVAm-T/laccase dispersion was pumped in the QCM at a flow rate of 0.100 mL/min for a fixed time (usually one hour) followed by rinsing with buffer. All measurements were performed at 23 ºC.

Electrochemical Quartz Crystal Microbalance with Dissipation (EQCM-D). The EQCM-D measurements were carried out with an electrochemical QCM-D cell (E401 electrochemical model from Q-Sense, Sweden). A QSX301 gold chip served as the working electrode, a platinum thin slice in the E401 electrochemical model served as the counter electrode and a low leakage "Dri-Ref 2SH" Ag|AgCl electrode (World Precision Instruments, USA) served as the reference electrode. Electrochemical measurements were performed with a Palmsens potentiostat (PalmSens, Amsterdam, Netherlands) in a conventional three-electrode system. After absorbing PVAm-T/laccase complexes, the pump was stopped before running electrochemical experiments. 50 mM sodium acetate buffer with pH 5 served as the solvent for both polymer and laccase solutions and also as the rinsing buffer. All measurements were performed at 23ºC.

Cellulose oxidation. Circular disks with diameters of 10 mm were punched from cleaned regenerated cellulose membranes. In a typical oxidation experiment, PVAm-T17 and laccase were premixed. The final concentration of PVAm-T17 is 67 mg/L and the concentration of laccase is 133 mg/L. 4 cellulose disks were immersed in the above solution. The mixed solution was oxygen bubbled and stirred for 1h. Both the PVAm-T17 and laccase solutions were filtered by syringe filter (0.45 μm) before mixing. The resulting oxidized cellulose disks were washed thoroughly with deionized water.

Aldehyde determination. The oxidized cellulose disks were immersed in 10 μM of the fluorescent Bodipy FL hydrazide methanol/water solutions (methanol: H_2O = 5:1) at room temperature for 8 h. The disks were then washed thoroughly with methanol and then by acetone.[13] Fluorescence measurements were performed on a ChemiDoc MP system (Model Universal Hood Ⅲ, Bio-Rad Laboratories, Inc.). Calibration curves were made using drop and dry method. 5 μL drops of Bodipy FL hydrazide methanol solution (0-10 μM) were placed on the non-oxidized cellulose disks (a calibration curve is

available in the supporting information Figure S4- 1). All the labeled cellulose disks were dried at room temperature before measurement.

4.3 Results

PVAm-T/laccase complex phase behavior. Polyelectrolyte complexes were prepared by mixing PVAm-T with the enzyme laccase. PVAm-T is positively charged, and laccase is negatively charged (-1.3 meq/g) under the experimental conditions (pH 5 in 50 mM acetate buffer).[11] Figure 4- 1 shows the phase boundaries of PVAm-T13/laccase complexes. PVAm-T13 was chosen for this detailed analysis because it is one of the most promising wet cellulose adhesives when used with laccase.[10] The phase behavior of PVAm-T13/laccase complex was assessed based on the criteria developed by Feng *et al.* [15]: "Soluble Complex" refers to solution with absorbance values less than 0.02 at 500 nm, and "Stable Colloid" has absorbance >0.02 but no instantly formed visible precipitates. Finally, the colloidal phases that have visible precipitates after 24 h are defined as "Unstable Colloid". The phase boundaries in Figure 4- 1 were based on a large data set – see Figure S4- 2 in the supporting information.

The mixture of laccase and PVAm-T was stable when either PVAm-T or laccase was in excess, whereas, at near charge balance unstable colloids were obtained. Some data points were also shown in Figure 4- 1 with a pair of numbers. The first value is the electrophoretic mobility of the complex, and the second value is the average hydrodynamic radius (nm). The hydrodynamic radius of the aged, colloidally stable complexes is in the range of 150-250 nm. Finally, many of our experiments, described below, were conducted using mixtures of 67 mg/L PVAm-T + 133 mg/L laccase; this composition is plotted as a large blue square in Figure 4- 1, centered in the "Unstable Colloid" domain. Note that for Figure 4- 1, all measurements were made after 24 hours. We will now show that it took 14 hours for the 67/133 composition to form visible precipitates for PVAm-T13.

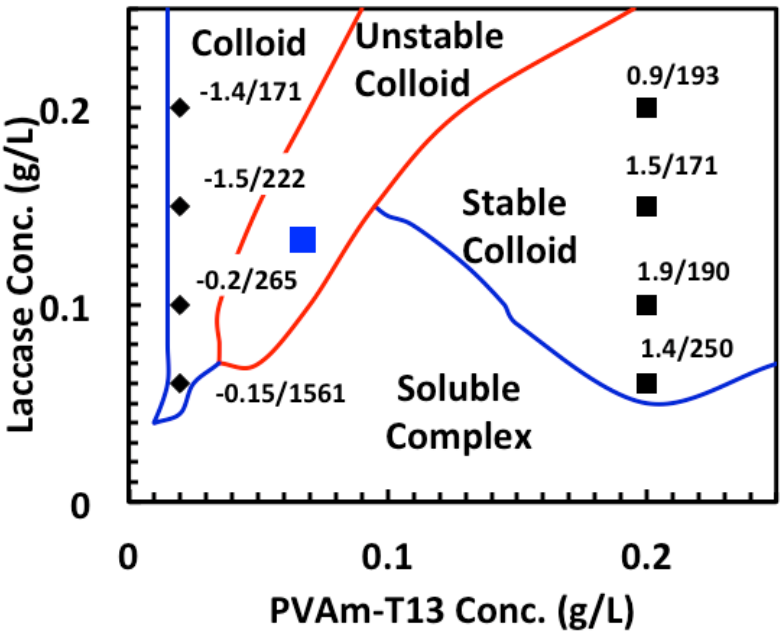

Figure 4- 1 Phase diagram for mixtures of PVAm-T13 and laccase at pH 5, in 50 mM acetate buffer. Laccase solutions were slowly dropped into PVAm-T13 solution and the mixtures were aged 24 h before characterization. The numbers next to the data points are "electrophoretic mobility/mean diameter". The single square indicates the composition used for many of the experiments described below. The data used to define the phase boundaries are shown in Figure S4- 2.

The influence of TEMPO content on phase behavior was probed by measuring the time dependent phase behavior for the PVAm-T series for PVAm-Tx (67mg/L)/laccase (133 mg/L). The evolving phase boundaries as a function of time are shown in Figure 4- 2 and these are based on a large data set shown in Figure S4- 3. With increasing TEMPO substitution, the net amine contents and net cationic charge densities are decreasing – see Figure S4- 4. For the PVAm-T13 67/133 complexes, Figure 4- 2 shows that about twelve hours of aging is required for precipitation to take place. The impact of TEMPO DS on the electrophoretic mobility values of PVAm-Tx/laccase complexes were measured (data plotted in Figure S4- 4) and the results showed that the mobility decreased with increasing substitution of amines with TEMPO-amide.

The results in Figure 4- 2 show that most of the compositions were present as slowly aggregating colloids – the higher the TEMPO DS, the lower the useful working time. In the extreme, complexes with TEMPO DS>18% precipitated quickly, limiting their ulitity as reactive adhesive primers. In summary, the solution behavior of PVAm-T + laccase mixtures displays the classic features of polyelectrolyte complexes formed between two oppositely charged polyelectrolytes. The electrochemical results below suggest that even the colloidally stable complexes slowly contract with time.

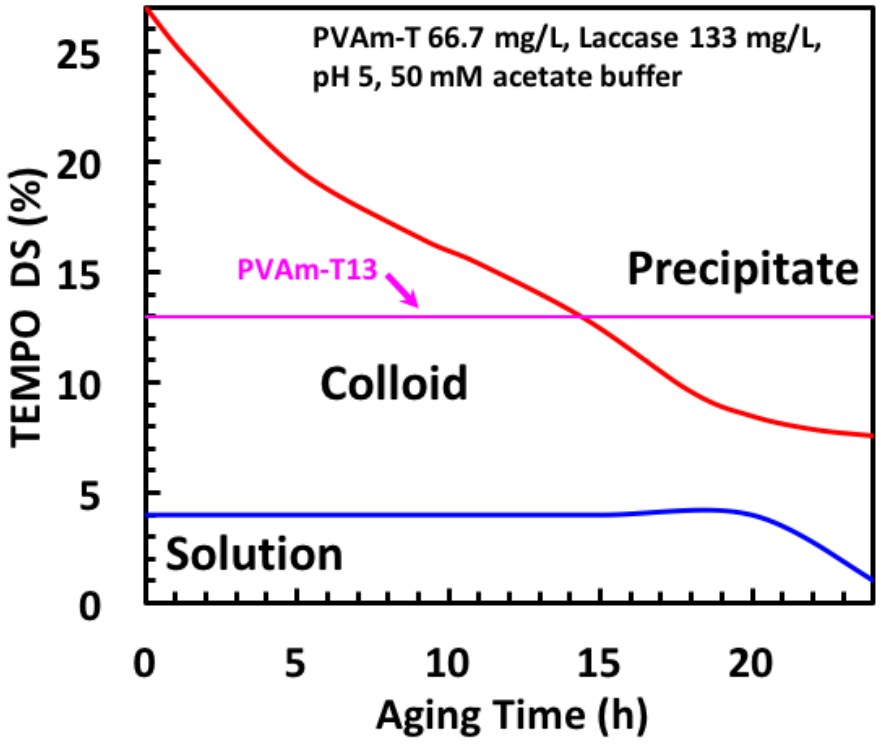

Figure 4- 2 The influence of TEMPO DS and aging time on the PVAm-T phase. The blue line is the boundary of solution and colloid states, the red line is the boundary of colloid and precipitate states. The purple line is the sample of PVAm-T13/laccase aged with different hours. The data points used to construct the boundaries are shown in Figure S4- 3.

PVAm-T/laccase adsorption on gold-sulfonate. A goal of this work was to use cyclic voltammetry to characterize the redox properties of PVAm-T/laccase complexes adsorbed on gold electrode surfaces, treated with sodium 3-mercapto-1-propanesulfonate to give negatively charged surface - gold-sulfonate. The adsorption of the cationic

PVAm-T/laccase complexes onto the gold-sulfonate surfaces was monitored by an electrochemical quartz crystal microbalance with dissipation (EQCM-D) and some results are shown in Figure 4- 3. For PVAm-T/laccase soluble complexes with TEMPO DS <6%, the adsorption reached a steady-state within 30 minutes. Furthermore, the dissipation shift was less than 10% in magnitude of frequency shift and the set of overtone curves showed good agreement (see supporting information Figure S4- 5), suggesting PVAm-T (DS<6%) / laccase complexes were not highly hydrated. By contrast, PVAm-T/laccase complexes with TEMPO DS>6%, showed a slow continual frequency drop after one hour exposure to flowing complex dispersion (see information Figure S4- 5), indicating significant hydration. To summarize both the solution and adsorption properties of PVAm-T/laccase complexes show significant time dependent behaviors making most measurements history dependent.

For some of our analysis we required an accurate mass for the adsorbed complex on the gold-sulfonate surfaces. In these cases, we dried the sensor and used ellipsometry to characterize the adsorbed layer. Figure S4- 6 shows the types of measurements are linearly related with the wet film coverage values about five times greater than the ellipsometric values.

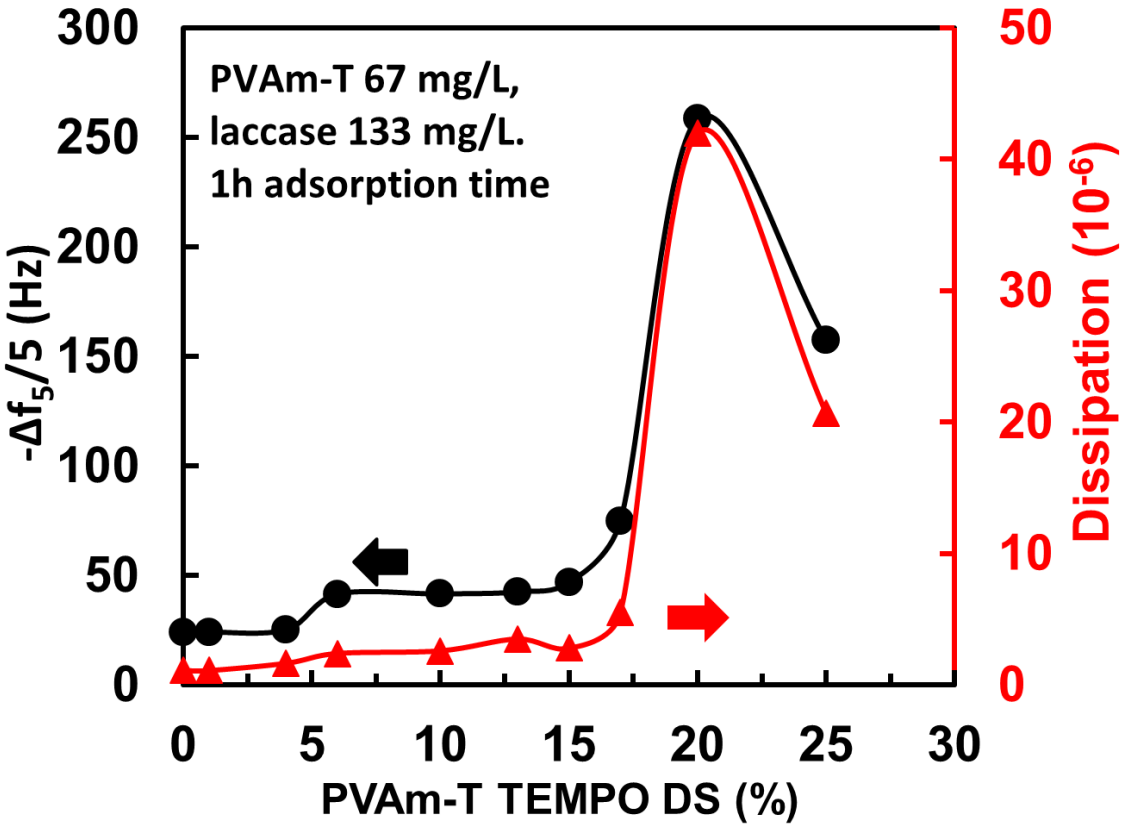

Figure 4- 3 The influence of TEMPO DS on the adsorption of PVAm-Tx/laccase complexes on gold-sulfonate EQCM-D sensors. PVAm-T (67 mg/L) was mixed with laccase (133 mg/L) under a nitrogen blanket. The reported values were obtained after the mixtures were pumped through the EQCM-D sensor for 1 h followed by a buffer rinse. The black data are the frequency shifts, and the red data are the dissipation shifts.

Redox Properties of PVAm-T/laccase Complexes. Cyclic voltammetry experiments were performed to characterize the redox behaviors of adsorbed PVAm-T/laccase complexes on gold-sulfonate EQCM-D sensors. Figure 4- 4 shows the current generated by an individual voltage sweep. As indicated in the Figure, the observed current flow is due to the reversible conversion of TEMPO moieties to the corresponding oxoammonium ion[16]. Solutions were kept under a nitrogen blanket and under these conditions laccase is not redox-active. Integration of the cyclic voltammetry curves yields the total electron flow, Q, and the Q values are for the range of PVAm-Tx/laccase complexes are given in

Table 4- 1. The Q values for the two or three lowest DS were small, approaching the sensitivity of our instrument.

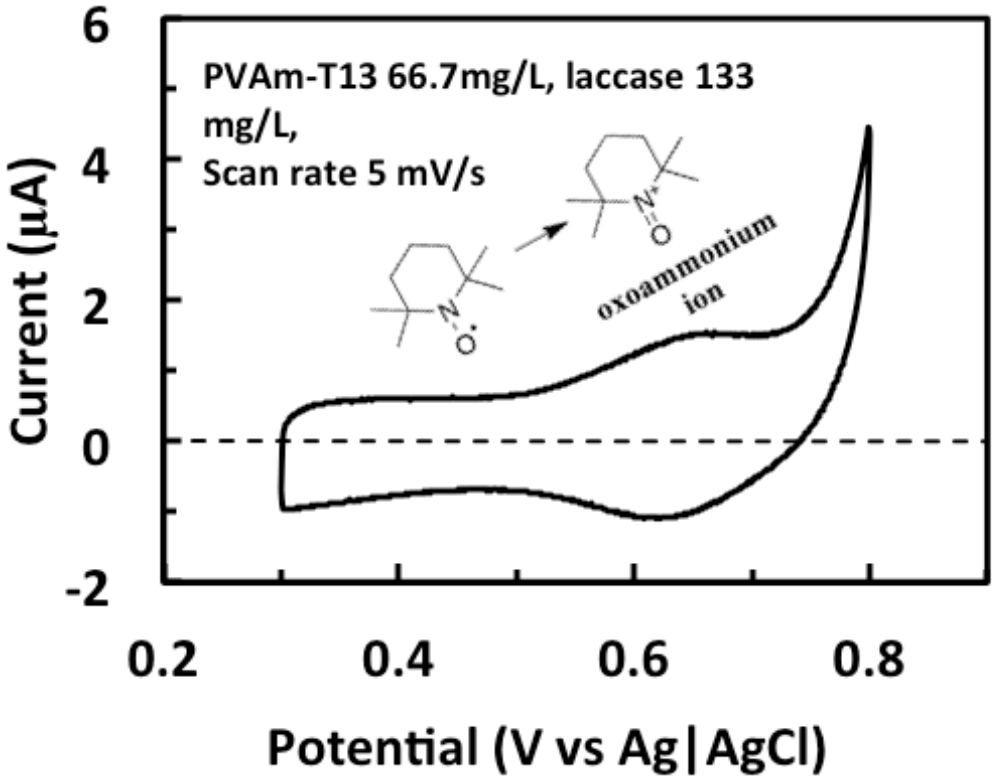

Figure 4- 4 A single cyclic voltammetry sweep for PVAm-T13/laccase complex. PVAm-T (67 mg/L) and laccase (133 mg/L) buffer solutions were mixed, and immediately added into the EQCM-D at a flow rate of 0.1 mL/min at 23 ºC. The adsorption time was 1 hour, followed by rinsing with acetate buffer. All solutions were under a nitrogen blanket. The sweep direction 0.3 V to 0.8 V, then to 0.3V.

The densities of redox-active TEMPO moieties adsorbed on the gold-sulfonate surface were directly calculated from Q and the results are shown in Figure 4- 5 as a function of the PVAm-T TEMPO content. As expected, the redox-active TEMPO density increased with the density of TEMPO moieties on the PVAm-T chains. The coverage of adsorbed

complexes on the gold sensors was estimated from ellipsometric measurements of the dried complex films. The resulting values, Γ_{el}, are summarized in Table 4-1. The experimental section summarizes the assumptions that were made to obtain theses values and an example calculation is given in the supporting information. Our Γ_{el} values should be considered rough estimates. Based on the estimated Γ_{el} values and the TEMPO contents of the polymers, we estimated the total density of TEMPO moieties on the gold-sulfonate surfaces. The fractions of the adsorbed TEMPO moieties in the PVAm-T complexes that were redox-active were estimated as the ratio redox-active to the total and the ratios are also shown in Figure 4- 5. Almost all TEMPOs were redox-active when DS>12%, however, only about 50% TEMPO was redox-active when DS<10%. In other words, our estimates suggest that the PVAm-T/laccase complexes displayed efficient TEMPO-to-TEMPO electron transport since the adsorbed layers were too thick for all TEMPO moieties to be in direct contact with the gold electrode.

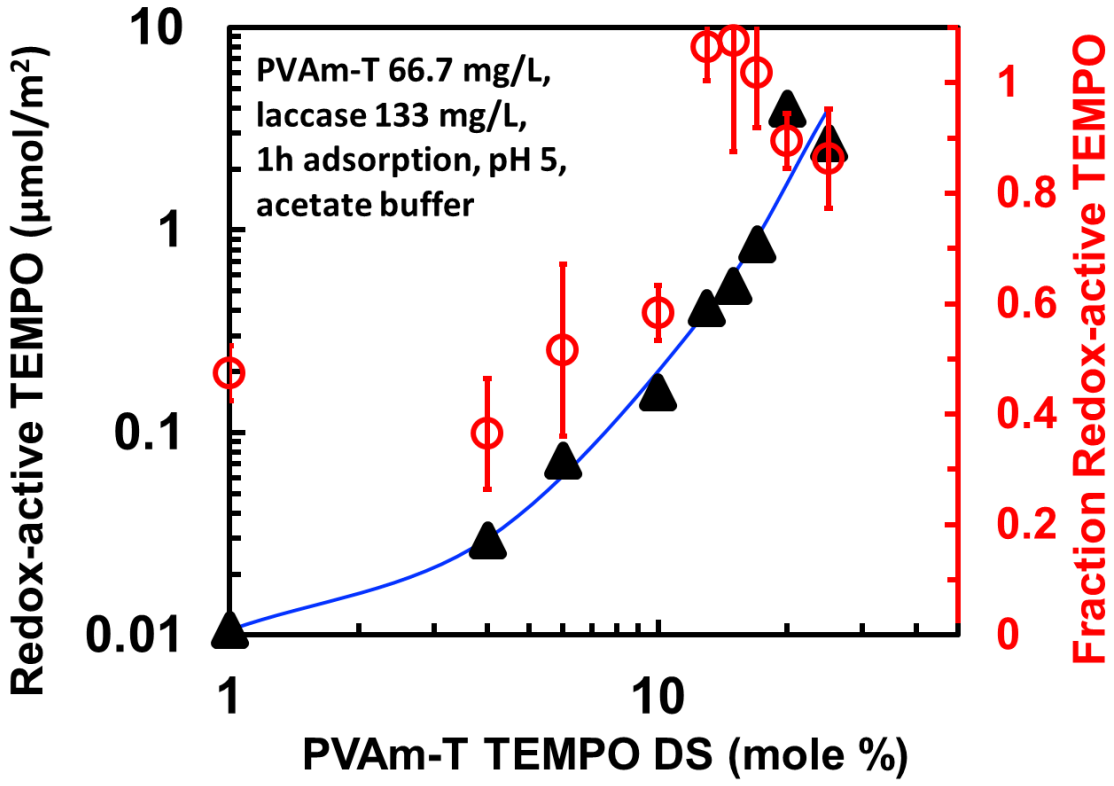

Figure 4- 5 The coverage of redox-active TEMPO in PVAm-T/laccase complexes on gold sensors, determined by cyclic voltammetry. The fraction of redox-active groups was calculated as the ratio of the redox-active TEMPO coverage to the total TEMPO coverage, estimated from the ellipsometric

characterization of the dried complex films. PVAm-T (67 mg/L) and laccase (133 mg/L) buffer solutions were mixed, and immediately added into the EQCM-D at a flow rate of 0.1 mL/min at 23 ºC. The adsorption time was 1 hour, followed by rinsing with acetate buffer. All solutions were under a nitrogen blanket.

The above solution phase studies and the adsorption characteristics showed that PVAm-T/laccase complexes changed with time. Figure 4- 6 shows the effect of aging time on both the adsorption and the redox properties of adsorbed PVAm-T17/laccase complexes. With aging, the adsorbed complex had a lower mass and dissipation suggesting the slow expulsion of water as the complex aged. The density of redox-active TEMPO moieties continuously decreased with aging time. After four hours aging the adsorbed mass was constant whereas the redox-active TEMPO content continued to decrease. We propose that changes in the adsorbed mass were due to the expulsion of water from the complex with aging whereas the decrease in redox-active TEMPO reflected decreasing TEMPO mobility, which in turn inhibited TEMPO-to-TEMPO electron transport.

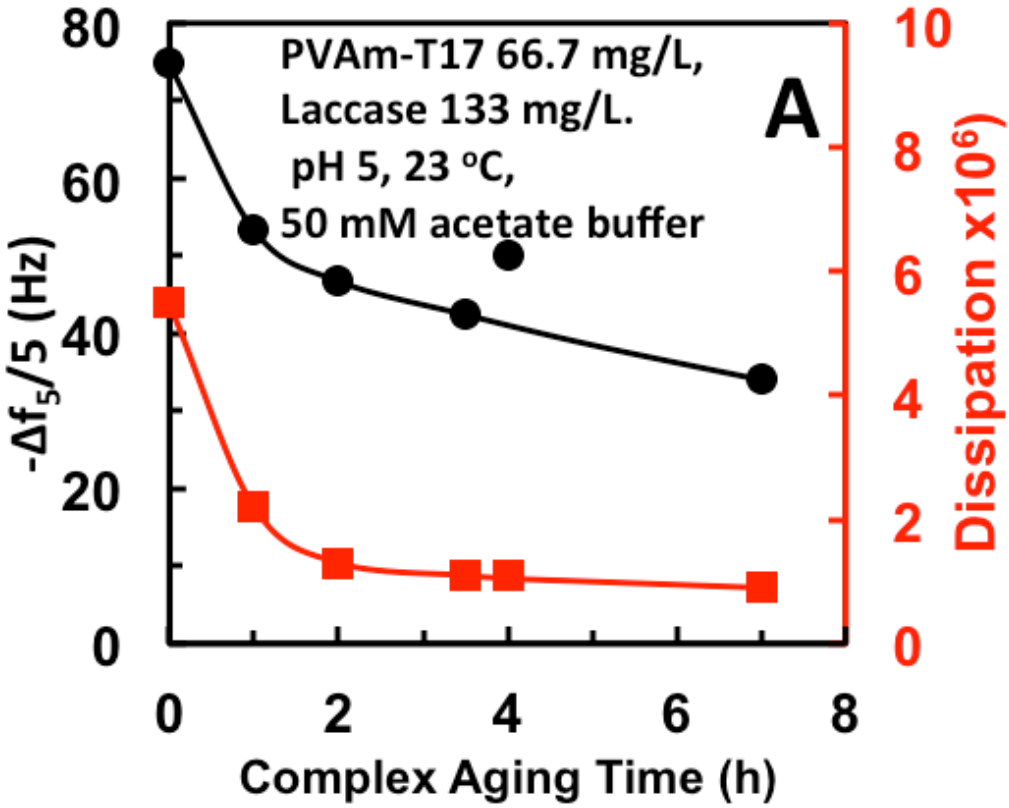

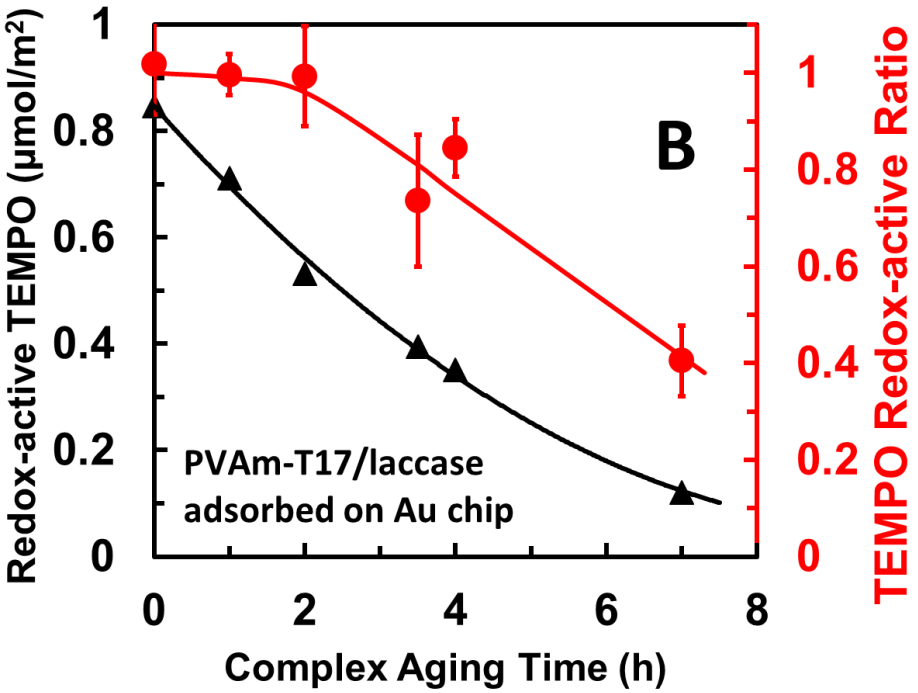
B
Redox-active TEMPO (µmol/m²)
TEMPO Redox-active Ratio
PVAm-T17/laccase
adsorbed on Au chip
Complex Aging Time (h)
0
0.2
0.4
0.6
0.8
1
0
2
4
6
8

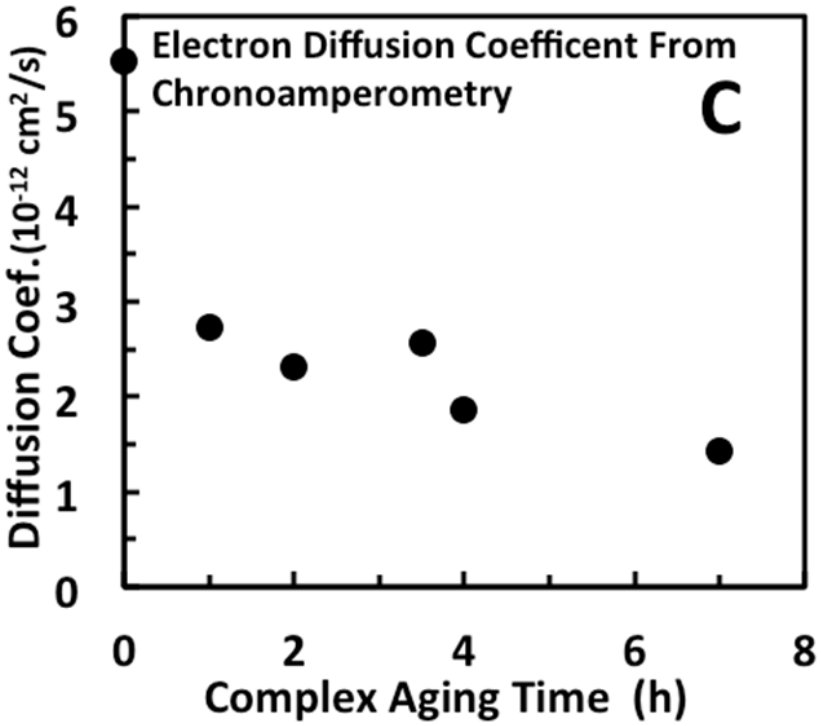
C
Electron Diffusion Coefficent From
Chronoamperometry
Diffusion Coef.(10⁻¹² cm²/s)
Complex Aging Time (h)
0
1
2
3
4
5
6
0
2
4
6
8

Figure 4- 6 Effect of pre-deposition, complex aging time on: A) adsorption density; B) redox-active TEMPO density; and, C) the apparent electron diffusion coefficient. PVAm-T (67 mg/L) and laccase (133 mg/L) buffer solutions were mixed, and aged a certain time before adding into the EQCM-D at a flow rate of 0.1 mL/min at 23 ºC.

We also employed chronoamperometry to characterize the electrochemical properties of adsorbed PVAm-T17/laccase complexes. In this technique, the current flow in response to a step change in voltage is measured as a function of time. The effective diffusion coefficient of charge transport through the complex was estimated by the Cottrell equation (see Figure S4- 7) and the results are summarized in Figure 4- 6C. The largest decrease in electron mobility is in the first hour, mirroring the change in adsorbed density in Figure 4- 6A. Taken as a whole the results summarized in Figure 4- 6 show that the ability of PVAm-T17/laccase complex to oxidize cellulose is likely to decrease by about ½ in the first hour, decreasing more slowly over the next few hours.

PVAm-T/laccase complexes oxidizing cellulose membranes. PVAm-T polymers were designed to adsorb onto cellulose, promote the oxidation of primary alcohols to aldehyde groups, and then with drying, form covalent imine and aminal bonds between cellulose and PVAm-T amine groups. As long as the cellulose is not dried, the concentration of intermediate aldehyde groups can be measured by fluorescent labeling with Bodipy FL hydrazide dye. The reactive dye forms covalent hydrazone bonds with aldehydes. Regenerated cellulose films were oxidized with our series of PVAm-Tx/laccase complexes and the density of aldehydre groups generated are shown as functions of the TEMPO DS in Figure 4- 7. There was a linear relationship between aldehyde density and PVAm-T DS.

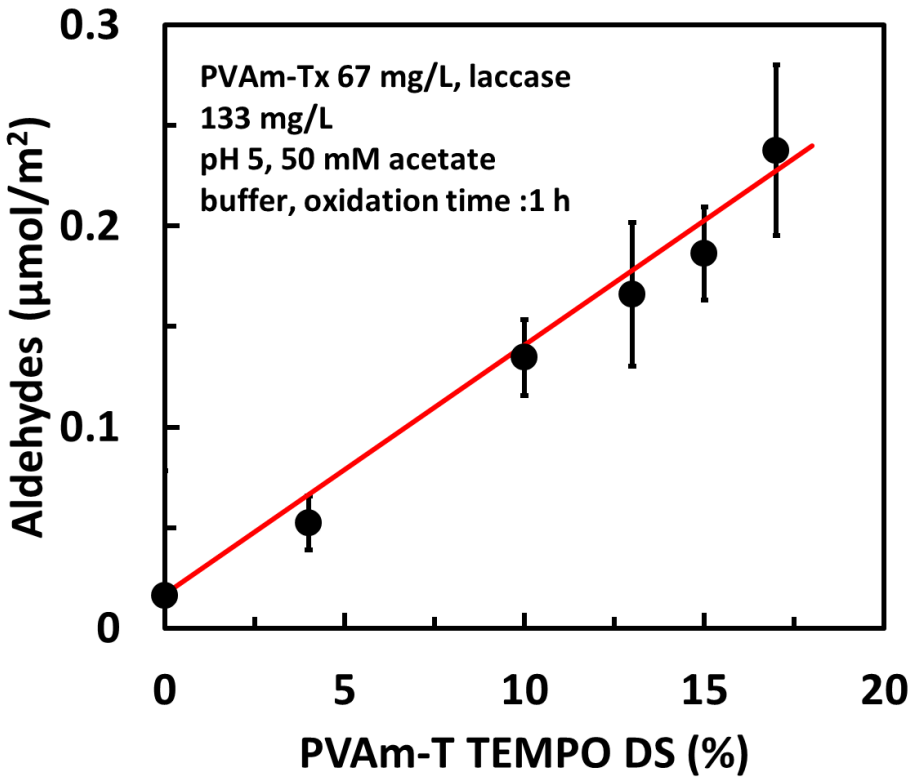

Figure 4- 7 The influence of PVAm-T DS on the density of aldehyde groups on cellulose produced by adsorbed PVAm-T/laccase complexes. Oxidation experiments were performed over 1hour in 50 mM acetate buffer solutions containing 67 mg/L PVAm-T, 133mg/L laccase, in pH 5 buffer.

Finally, it is of interest to try to relate the properties of PVAm-T/laccase complexes on gold-sulfonate to the properties on cellulose. We now make two severe assumptions: 1) the structure and the mass density of adsorbed complex are the same of both surfaces, and, 2) the redox-active TEMPO content, measured by electron transport from gold is the same as the redox-active TEMPO content, where the electron transfer is from laccase. Based on these assumptions, we can correlate the results in Figure 4- 5, with the results in Figure 4- 7 to obtain the relationship between the density of redox active TEMPO moieties and the corresponding density of aldehydes produced by the oxidation of cellulose. The result is shown in Figure 4- 8. We have fit the results to a power law suggesting that the aldehyde density is proportional close to the square root of the redox-active TEMPO density.

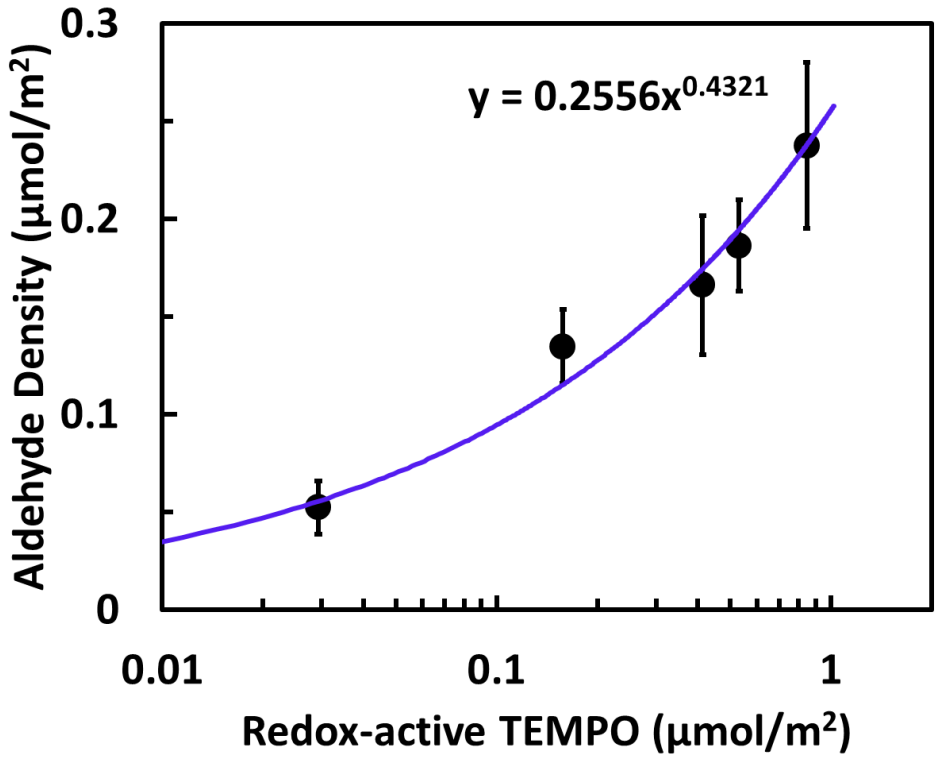

Figure 4- 8 The relationship between the redox-active TEMPO density in PVAm-T/laccase on gold and the aldehyde density produced by PVAm-T/laccase adsorbed on cellulose.

4.4 Discussion

The incentive for the present work was to develop an understanding of the process of PVAm-T/laccase complexes absorbing onto, oxidizing, and providing wet adhesion of cellulose. As mentioned in the introduction, the PVAm-T cannot shuttle back and forth between laccase active sites and primary alcohols on cellulose as small molecular TEMPO can. The hypothesis we propose is that PVAm-T serves as the oxidation mediator through electron hopping between neighboring TEMPO moieties. Figure 4- 9 shows a proposed schematic for oxidization of cellulose by PVAm-T/laccase complexes. The cationic PVAm-T forms a complex with anionic laccase, and the net positively charged PVAm-T/laccase complex adsorbs onto the cellulose surface. A TEMPO moiety close to the laccase active site is oxidized to a TEMPO oxoammonium cation

(TEMPO+). When in close enough contact to a nearby TEMPO, electron hopping occurs between the TEMPO+ and the TEMPO. The electron hopping takes place sequentially until the TEMPO+ comes in contact with a primary alcohol on cellulose. The primary alcohol is then oxidized to an aldehyde, which in turn can be further oxidized to carboxyl group following the same procedure.

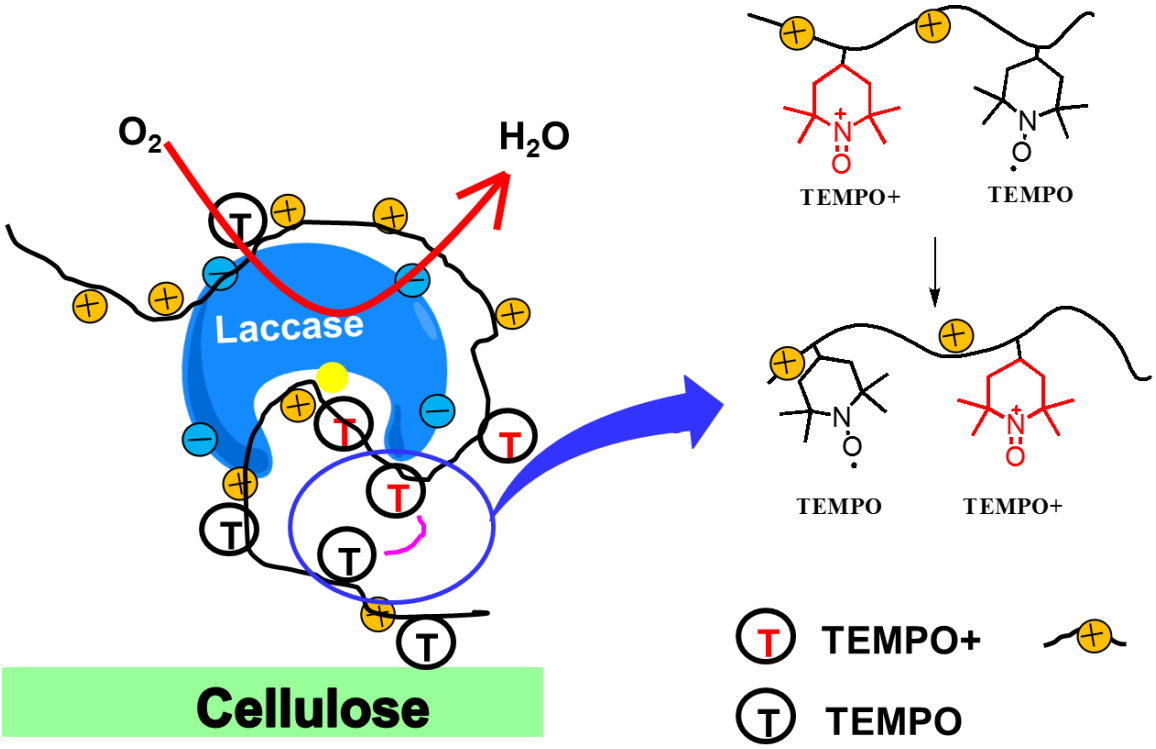

Figure 4- 9 Schematic of the proposed mechanism for cellulose oxidation by PVAm-T/laccase.

Electrochemical quartz crystal microbalance with dissipation (EQCM-D) is a combination of QCM-D and potentiostat. The QCM-D provides information about the adsorbed mass and the viscoelastic properties of an adsorbed material. The electrochemical technique monitors the electrochemical properties of the adsorbed materials *in situ*. The electrochemical results for PVAm-T/laccase demonstrated that not only the TEMPO moieties contacting the electrode surface, but also those on the outer boundary of the absorbed films were redox-active. The PVAm-T/laccase complexes films are too thick for the TEMPO moieties on the outer boundary to have direct electron

communication with the electrode. Simultaneously, these TEMPO moieties cannot diffuse to the electrode surface since they are covalently bound to PVAm chains. Therefore, the most reasonable explanation for the electron transport is electron hopping between TEMPO moieties. This explanation is also applicable to the process of cellulose oxidation by poly(acrylic acid-g-TEMPO) in the presence of laccase. In that case PVAm is pre-adsorbed onto the cellulose membranes resulting in membranes with a positive surface charge. The negatively charged poly(acrylic acid-g-TEMPO) is then adsorbed onto these surfaces. TEMPO moieties close to laccase active sites, at the surface solution interface, are oxidized to oxoammonium cations. Electron hopping between adjacent TEMPO groups then facilitates the electron transport to the cellulose primary alcohols on the underlying membrane, which are oxidized to aldehydes. A 10% TEMPO degree of substitution is required in order to have efficient TEMPO-to-TEMPO electron transfer. At lower DS, the TEMPO moieties are likely too far apart to have efficient electron hopping.

In chapter 3 it was shown that only 20-30% of the TEMPO moieties were redox-active in (PVAm-T/PSS) Layer-by-Layer films, in which the TEMPO DS was 25 mol%. Contrarily, almost all of the TEMPO moieties in PVAm-T/laccase complexes, adsorbed on the electrodes, were redox-active at the same TEMPO DS (see Figure 4- 5). Therefore, TEMPO-to-TEMPO electron transport in PVAm-T/laccase complexes films seems more efficient than in (PVAm-T/PSS) multilayer films. Although the mobility of grafted TEMPO in these films was not directly measured, the mobility of the grafted TEMPO is of large importance for the TEMPO redox-activity and the electron hopping between TEMPO moieties. This was reflected in the influence of aging time on the fraction of redox-active TEMPO in the adsorbed PVAm-T/laccase complexes. As shown in Figure 4- 6, the fraction of redox-active TEMPO decreased with aging time. A plausible explanation is that the TEMPO mobility decreases due to the expulsion of water from the complex, which in turn inhibits TEMPO-to-TEMPO electron transport, and as a result also limits the redox-activity.

In the present work, we used the dye Bodipy FL hydrazide to determine aldehyde density on oxidized cellulose surfaces. The hydrazide group of the dye reacts with the aldehyde groups on oxidized cellulose in water (see Figure 4- 10). It is worth noting that hydrazones form in water whereas imines (reaction between aldehyde and amine) do not. The aldehyde density on cellulose surfaces can be simply controlled by PVAm-T TEMPO DS and redox-active TEMPO moieties. As a result, the aldehyde density on cellulose surfaces can be simply controlled by the PVAm-T TEMPO DS and redox-active

TEMPO. The fluorescence-labeling method was believed can determine aldehyde groups not only on cellulose, but also on other substrates, such as plastics.

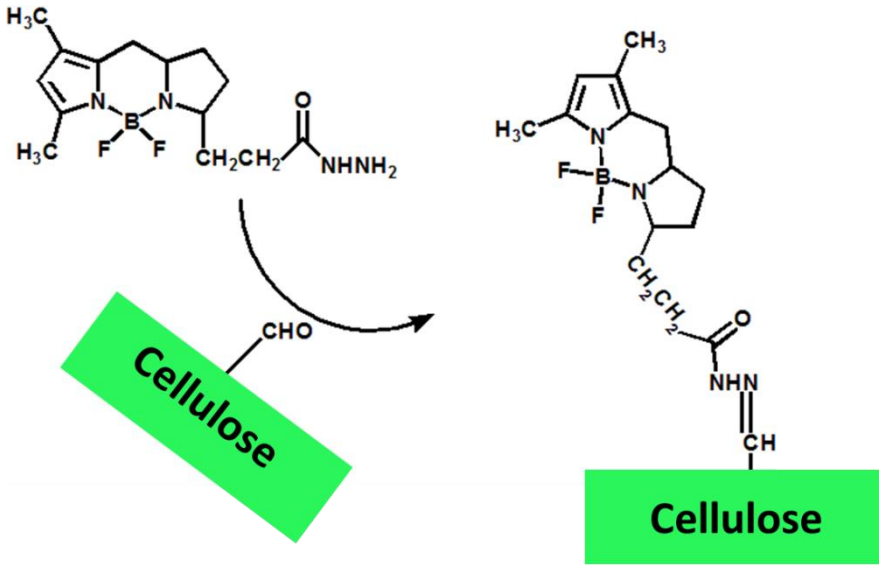

Figure 4- 10 Fluorescence-labeling of aldehyde groups on oxidized cellulose. The hydrazine group on the dye Bodipy FL forms a hydrazone with the aldehyde on oxidized cellulose.

In summary, the PVAm-T mediated laccase oxidation offers several advantages compared to the conventional TMEPO-mediated oxidation. First, the oxidation occurred at neutral pH and mild conditions which is compatible to modern papermaking technologies. Second, the TEMPO total requirement is much less than the small molecular TEMPO. According Aracri et al.'s work who oxidized cellulose with laccase and TEMPO, TEMPO dose is 2-8wt% of dry cellulose, whereas in the present work TEMPO dose was 0.5-1 wt% of dry cellulose. The polymer grafted TEMPO should be less toxic than the small molecular TEMPO. Third, the PVAm-T/laccase complexes were too large to penetrate into cellulose, as a result, only the exterior of cellulose was oxidized, which avoided weakening cellulose mechanical properties. The PVAm-T

mediated laccase oxidation also provides a new approach to functionalize cellulose surface.

4.5 Conclusions

1. TEMPO-to-TEMPO electron transport in PVAm-T/laccase complexes facilities cellulose oxidation.

2. The density of aldehyde groups generated by adsorbed PVAm-T/laccase complex scales with the square root of the surface density of redox-active TEMPO moieties measured on sulfonated gold electrode surfaces.

3. The density of aldehydes generated by adsorbed PVAm-T/laccase complex is a linear function of the TEMPO content of the PVAm-T copolymer, providing a simple route to controlling aldehyde density.

4. The PVAm-T/laccase complexes of most interest for cellulose oxidation, loose about ½ their oxidative capacity over the first two hours of aging at pH 5. The complexes would need to be continuously prepared for a commercial application.

5. The fraction of redox-active TEMPO content in adsorbed PVAm-T/laccase complexes is significantly higher (3 times) compared to PVAm-T/polystyrene sulfonate layer-by-layer assemblies.

References

(1) Espy, H. H. The Mechanism of Wet-Strength Development in Paper - a Review. *Tappi Journal* **1995,** *78* (4), 90-99.

(2) Saito, T.; Isogai, A. TEMPO-Mediated Oxidation of Native Cellulose. The Effect of Oxidation Conditions on Chemical and Crystal Structures of the Water-Insoluble Fractions. *Biomacromolecules* **2004,** *5* (5), 1983-1989.

(3) DiFlavio, J.-L.; Pelton, R.; Leduc, M.; Champ, S.; Essig, M.; Frechen, T. The Role of Mild TEMPO-Nabr-Naclo Oxidation on the Wet Adhesion of Regenerated Cellulose Membranes with Polyvinylamine. *Cellulose* **2007,** *14* (3), 257-268.

(4) Miao, C.; Pelton, R.; Chen, X.; Leduc, M. Microgels Versus Linear Polymers for Paper Wet Strenght - Size Does Matter. *Appita Journal* **2007,** *60* (6), 465-468.

(5) Miao, C.; Chen, X.; Pelton, R. Adhesion of Poly(Vinylamine) Microgels to Wet Cellulose. *Industrial & Engineering Chemistry Research* **2007,** *46* (20), 6486-6493.

(6) Wen, Q.; Pelton, R. Design Rules for Microgel-Supported Adhesives. *Industrial & Engineering Chemistry Research* **2012,** *51* (28), 9564-9570.

(7) Wen, Q.; Pelton, R. Microgel Adhesives for Wet Cellulose: Measurements and Modeling. *Langmuir* **2012,** *28* (12), 5450-5457.

(8) Pelton, R.; Ren, P.; Liu, J.; Mijoloyic, D. Polyvinylamine-Graft-TEMPO Adsorbs onto, Oxidizes, and Covalently Bonds to Wet Cellulose. *Biomacromolecules* **2011,** *12* (4), 942-948.

(9) liu, j. Mechanisms for Cellulose Reactive Polyvinylamine Graft TEMPO Adhesive. *master thesis* **2012**.

(10) Liu, J.; Pelton, R.; Obermeyer, J. M.; Esser, A. Laccase Complex with Polyvinylamine Bearing Grafted TEMPO Is a Cellulose Adhesion Primer. *Biomacromolecules* **2013,** *14* (8), 2953-60.

(11) Shi, S.; Pelton, R.; Fu, Q.; Yang, S. Comparing Polymer-Supported TEMPO Mediators for Cellulose Oxidation and Subsequent Polyvinylamine Grafting. *Industrial & Engineering Chemistry Research* **2014,** *53* (12), 4748-4754.

(12) Galli, C.; Gentili, P. Chemical Messengers: Mediated Oxidations with the Enzyme Laccase. *Journal of Physical Organic Chemistry* **2004,** *17* (11), 973-977.

(13) Xing, Y. J.; Borguet, E. Specificity and Sensitivity of Fluorescence Labeling of Surface Species. *Langmuir* **2007,** *23* (2), 684-688.

(14) Hodak, J.; Etchenique, R.; Calvo, E. J.; Singhal, K.; Bartlett, P. N. Layer-by-Layer Self-Assembly of Glucose Oxidase with a Poly(Allylamine)Ferrocene Redox Mediator. *Langmuir* **1997,** *13* (10), 2708-2716.

(15) Feng, X.; Pelton, R.; Leduc, M.; Champ, S. Colloidal Complexes from Poly(Vinyl Amine) and Carboxymethyl Cellulose Mixtures. *Langmuir* **2007,** *23* (6), 2970-2976.

(16) Isogai, T.; Saito, T.; Isogai, A. TEMPO Electromediated Oxidation of Some Polysaccharides Including Regenerated Cellulose Fiber. *Biomacromolecules* **2010,** *11* (6), 1593-1599.

Appendix: Supporting Information for Chapter 4

Chapter 4 Electrochemical Characterization of Polyvinylamine-g-TEMPO/laccase Complexes for Cellulose Wet Adhesion

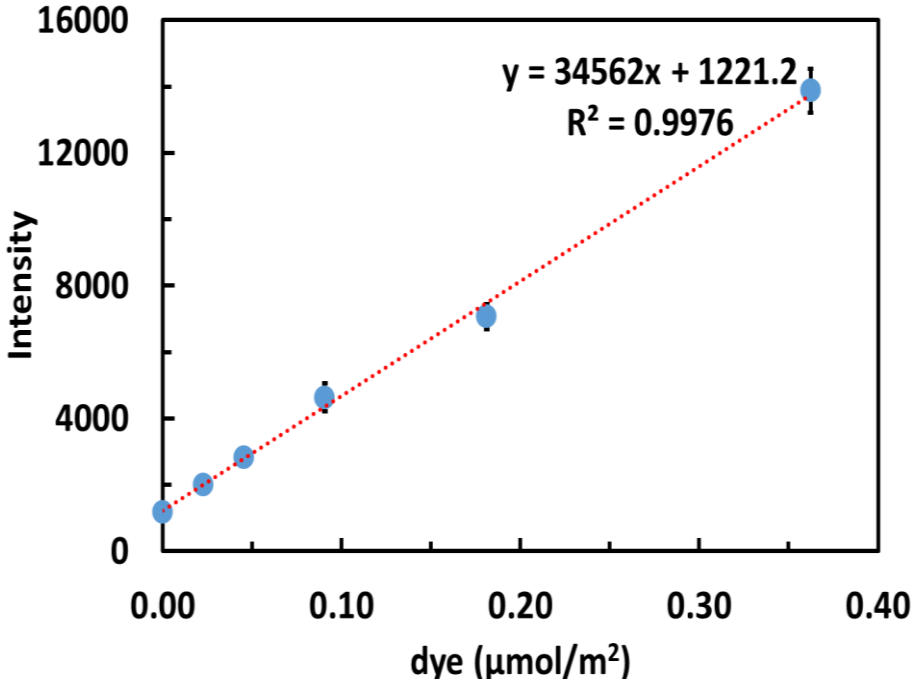

Figure S4- 1 Calibration curve for fluorescence dye Bodipy FL hydrazide on cellulose membrane.

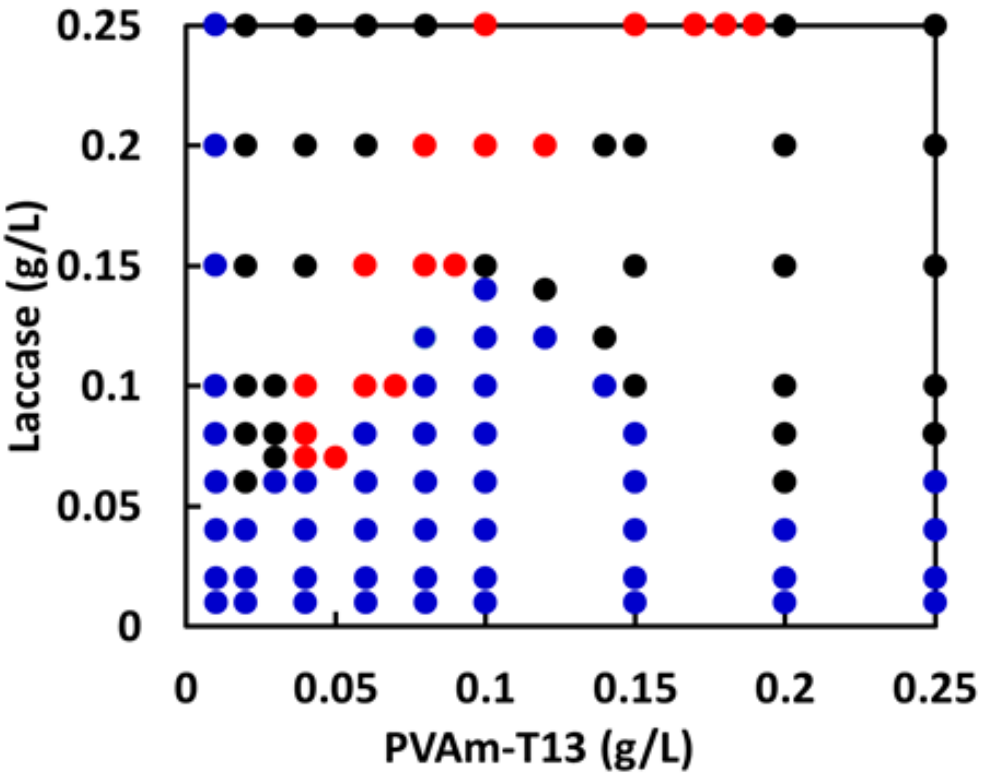

Figure S4- 2 Phase diagram for mixtures of PVAm-T13 and laccase at pH 5, in 50 mM acetate buffer. Laccase solutions were slowly dropped into PVAm-T13 solution and the mixtures were aged 24 h before characterization.

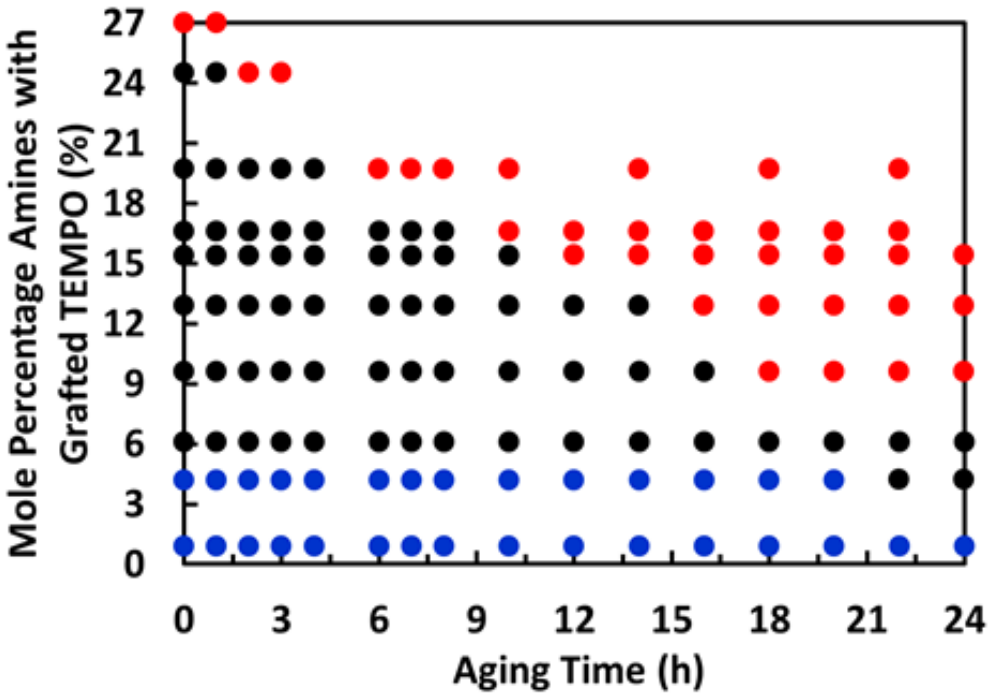

Figure S4- 3 The influence of TEMPO DS and aging time on the PVAm-T phase.

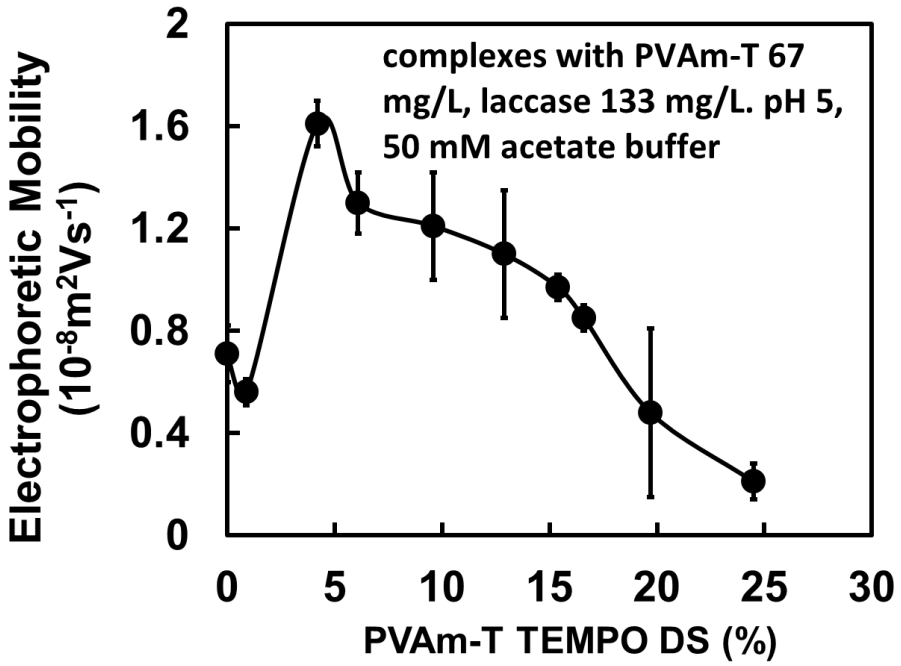

Figure S4- 4 Electrophoretic mobilities as a function of TEMPO DS. Laccase solutions were slowly dropped into PVAm-T solutions, giving a final concentration of PVAm-T is 67mg/L and laccase 133 mg/L in 50 mM sodium acetate buffer with pH 5. The measurement was carried out immediately after droping laccase into PVAm-T solution.

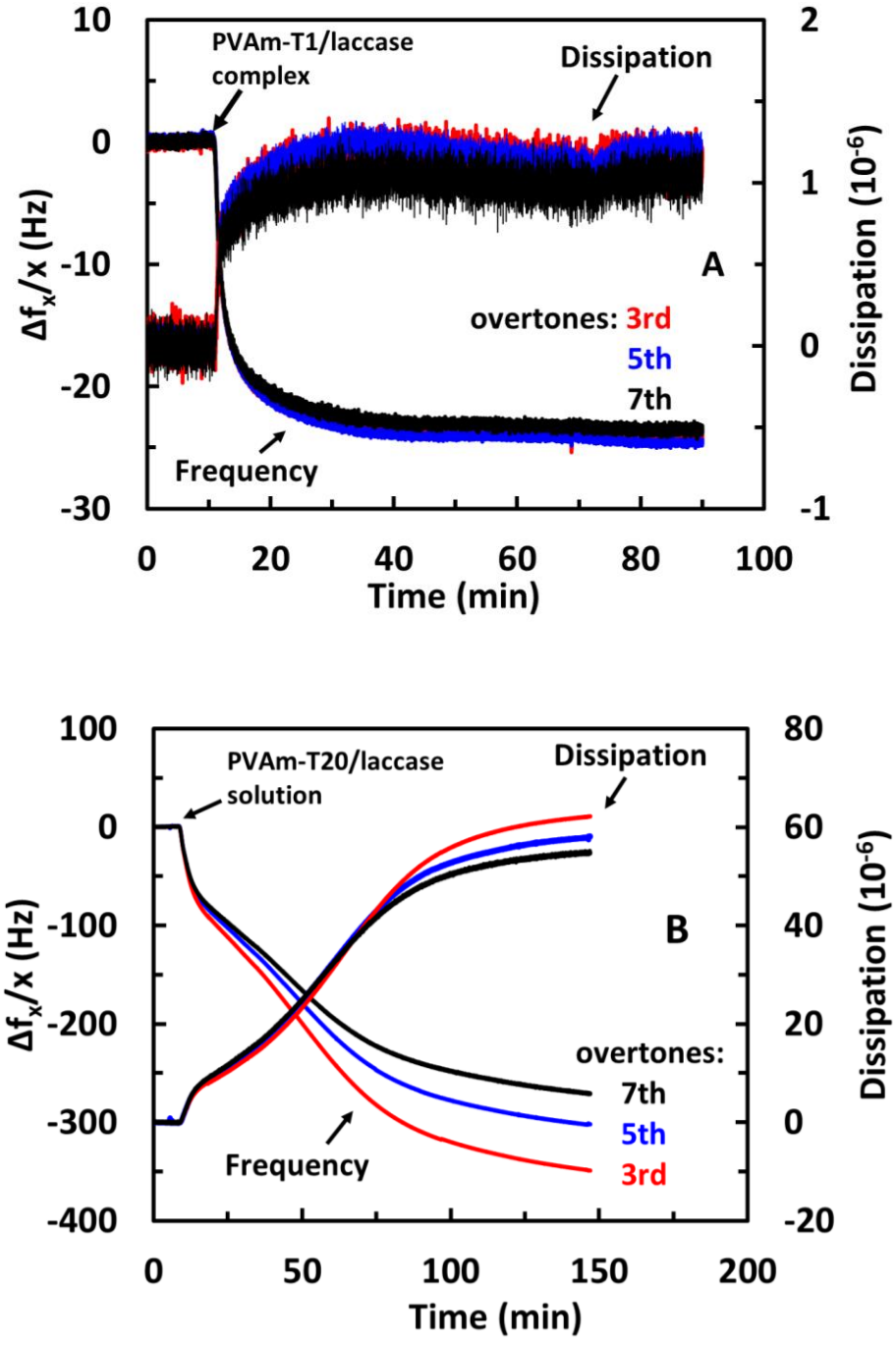

Figure S4- 5 Adsorption of (A) PVAm-T1/laccase and (B) PVAm-T20/laccase complexes on EQCM-D gold-sulfonate sensors.

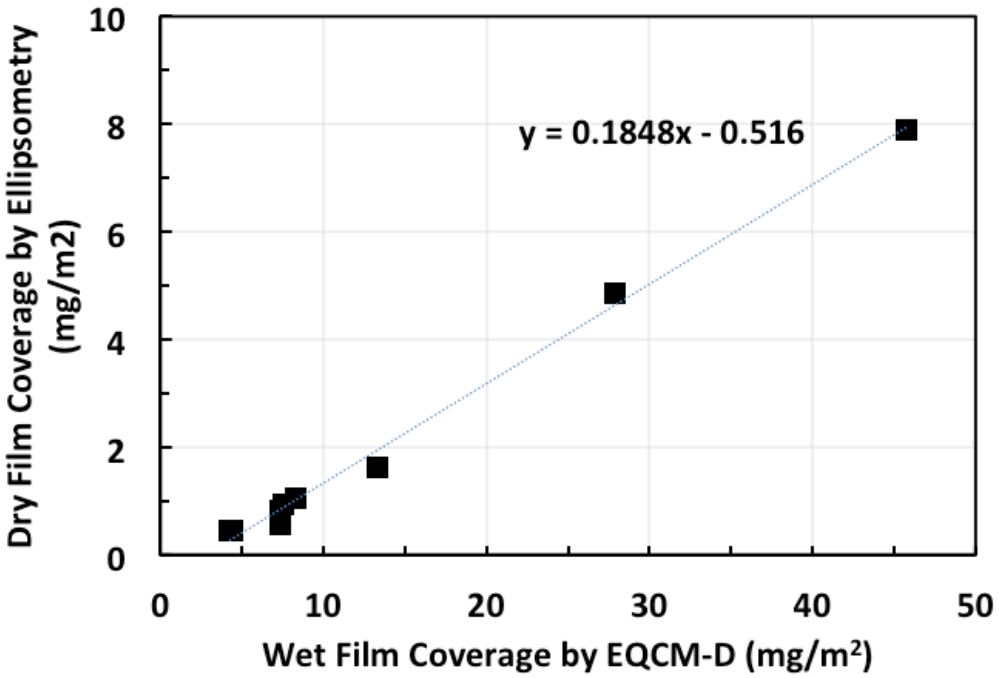

Figure S4-6 The comparison of mass coverage values measured by EQCM-D to those measured by ellipsometry of dry films.

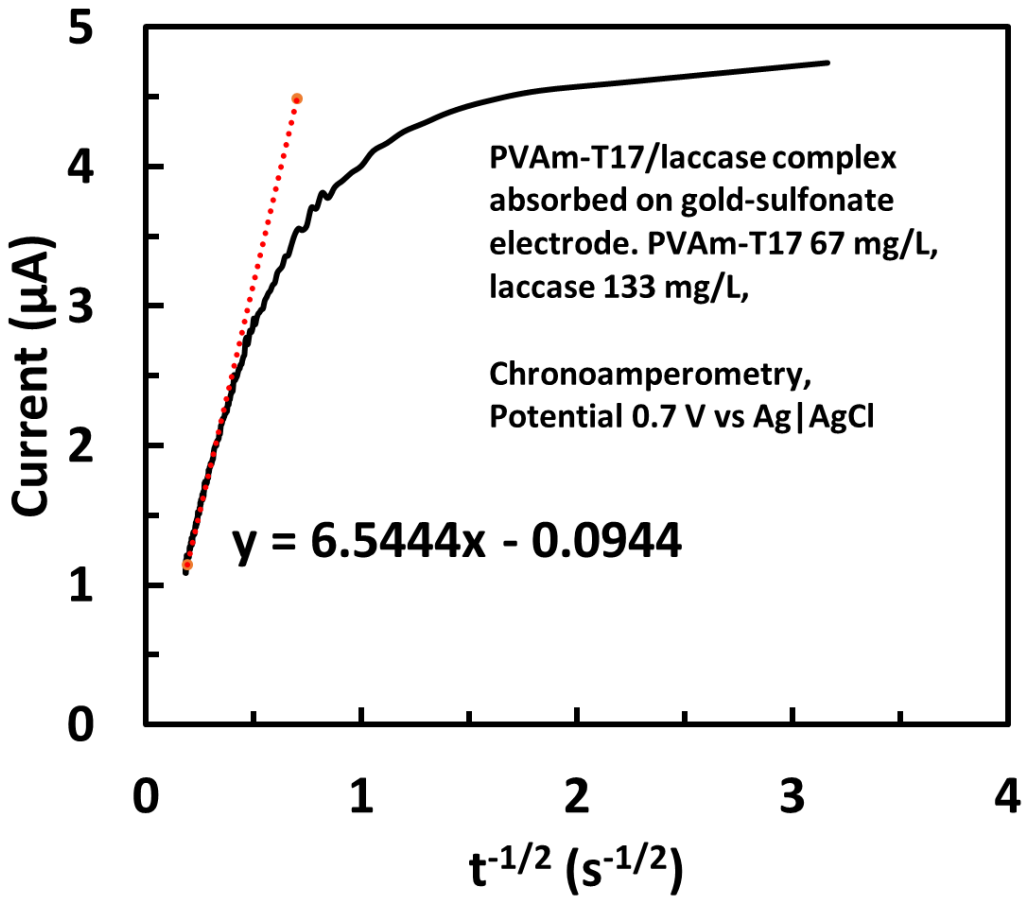

Figure S4- 7 Cottrell's plot for potential step chronoamperometry of PVAm-T17/laccase complexes absorbed on Au electrode in 50 mM acetate buffer, pH 5 with N_2 saturated. 0 hr aging time of PVAm-T17/laccase complex.

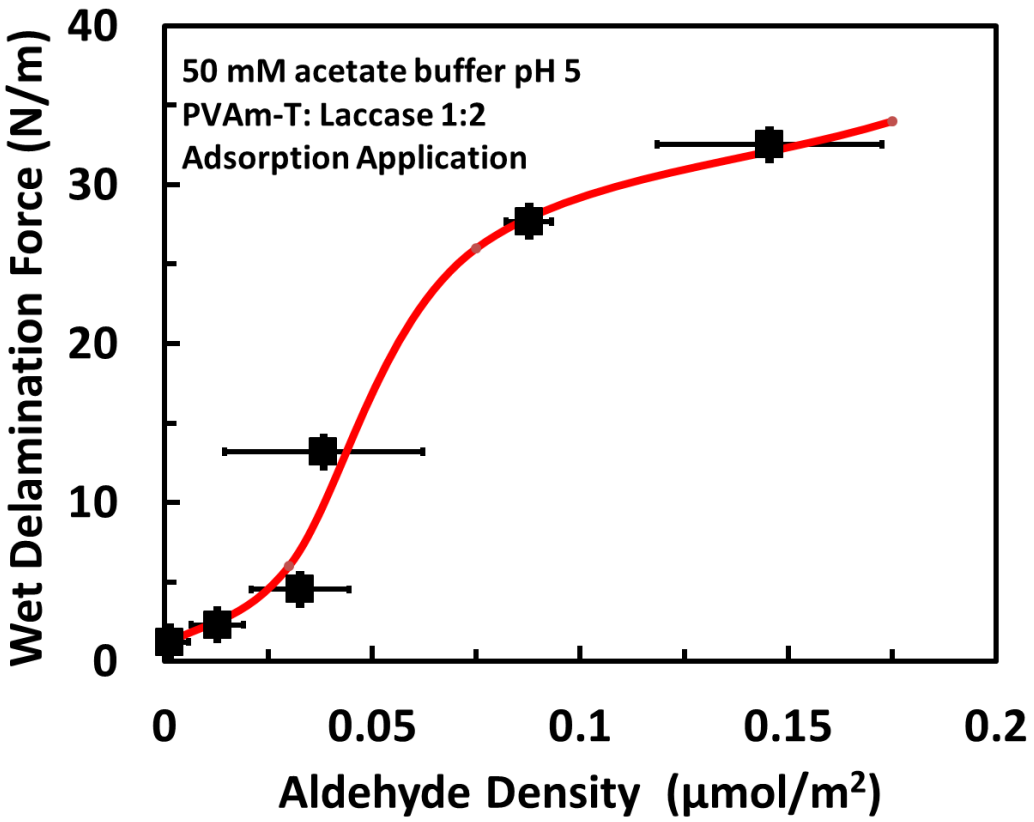

Figure S4- 8 Relationship between aldehyde density and wet Delamination Force. The wet delamination force was from Liu et al.[1]

Reference:

(1) Liu, J.; Pelton, R.; Obermeyer, J. M.; Esser, A. Laccase Complex with Polyvinylamine Bearing Grafted Tempo Is a Cellulose Adhesion Primer. *Biomacromolecules* **2013,** *14* (8), 2953-60.

1. Calculating adsorbed TEMPO content based on ellipsometry

the thickness of the adsorbed PVAm-T/laccase complex was measured with ellipsometry

$$DS := \begin{bmatrix} 0 \\ 1 \\ 4 \\ 6 \\ 10 \\ 13 \\ 15 \\ 17 \\ 20 \\ 25 \end{bmatrix} \%$$

$$h := \begin{bmatrix} 0.2 \\ 0.4 \\ 0.4 \\ 0.5 \\ 0.7 \\ 0.8 \\ 0.9 \\ 1.4 \\ 6.8 \\ 4.2 \end{bmatrix} \cdot nm$$

DS is TEMPO degree of substitution in PVAm-T/ laccase complexes

h is the thickness of PVAm-T/ laccase adsorbed on surface

$$\sigma_{PVAmT} := 1080 \cdot \frac{kg}{m^3}$$

σ_{PVAmT} is the density of PVAm-T, and is assumed the same density of PVAm

$$\sigma_{lac} := 1200 \ \frac{kg}{m^3}$$

σ_{lac} is the density of laccase

$$D := 10 \cdot mm$$

D is the diameter of Au substrate for complex adsorption

$$A := \frac{1}{4} \cdot \pi \cdot D^2 = \left(7.854 \cdot 10^{-5}\right) \ m^2$$

A is the surface area of the Au chip which is covered by complexes

$$m := \frac{h \cdot A \cdot \left(\frac{1}{3} \cdot \sigma_{PVAmT} + \frac{2}{3} \cdot \sigma_{lac}\right)}{A} = \begin{bmatrix} 0.232 \\ 0.464 \\ 0.464 \\ 0.58 \\ 0.812 \\ 0.928 \\ 1.044 \\ 1.624 \\ 7.888 \\ 4.872 \end{bmatrix} \frac{mg}{m^2}$$

m is the mass of adsorbed PVAm-T/laccase complex

$$n := \begin{bmatrix} 0 \\ 0.1442 \\ 0.5198 \\ 0.7306 \\ 1.001 \\ 1.2562 \\ 1.4212 \\ 1.5383 \\ 1.6916 \\ 1.911 \end{bmatrix} \cdot \frac{mmol}{gm}$$

n is TEMPO mole content in PVAm-T

As a result, TEMPO content in adsorbed PVAm-T/laccase complex

$$i := 0..9$$

$$\Gamma_{el_i} := \left(\frac{1}{3} \cdot m_i\right) \cdot n_i \cdot 100\%$$

Assuming 1/3 of the adsorbed mass is PVAm-T

$$DS = \begin{bmatrix} 0 \\ 0.01 \\ 0.04 \\ 0.06 \\ 0.1 \\ 0.13 \\ 0.15 \\ 0.17 \\ 0.2 \\ 0.25 \end{bmatrix} \qquad \Gamma_{el} = \begin{bmatrix} 0 \\ 0.0223 \\ 0.0804 \\ 0.1412 \\ 0.2709 \\ 0.3886 \\ 0.4946 \\ 0.8327 \\ 4.4478 \\ 3.1035 \end{bmatrix} \frac{\mu mol}{m^2}$$

Γel is the TEMPO content in adsorbed PVAm-T/laccase complexes

$n := 1$ number of electron tranferred between TEMPO and oxoammonium cation $F = (9.6485 \cdot 10^4)\ \frac{C}{mol}$

$A := \frac{1}{4} \cdot \pi \cdot D^2 = (7.854 \cdot 10^{-5})\ m^2$

$$DS = \begin{bmatrix} 0 \\ 0.01 \\ 0.04 \\ 0.06 \\ 0.1 \\ 0.13 \\ 0.15 \\ 0.17 \\ 0.2 \\ 0.25 \end{bmatrix} \qquad Q := \begin{bmatrix} 0 \\ 0.0802 \\ 0.222 \\ 0.552 \\ 1.197 \\ 3.133 \\ 4.03 \\ 6.4225 \\ 30.146 \\ 20.286 \end{bmatrix} \cdot \mu C$$

Q is the charge measured by Cyclic voltammetry

$$\Gamma_{cv} := \frac{Q}{n \cdot F \cdot A} = \begin{bmatrix} 0 \\ 0.0106 \\ 0.0293 \\ 0.0728 \\ 0.158 \\ 0.4134 \\ 0.5318 \\ 0.8475 \\ 3.9781 \\ 2.677 \end{bmatrix} \frac{\mu mol}{m^2}$$

Γcv is the coverage of redox-active TEMPO on surface.

The TEMPO redox-active ratio of adsorbed PVAm-T/laccase complexes is

$i := 1 .. 9$

$$f_i := \frac{\Gamma_{cv_i}}{\Gamma_{el_i}} \cdot 100\% \qquad f = \begin{bmatrix} 0 \\ 0.4745 \\ 0.3644 \\ 0.5157 \\ 0.583 \\ 1.064 \\ 1.0753 \\ 1.0178 \\ 0.8944 \\ 0.8626 \end{bmatrix}$$

Adsorption of PVAm-T17/laccase complexes with different aging time from QCM

$$t_{aging} := \begin{bmatrix} 0 \\ 1 \\ 2 \\ 3.5 \\ 4 \\ 7 \end{bmatrix} \cdot hr \qquad \Delta Hz := \begin{bmatrix} -75 \\ -53.3 \\ -46.7 \\ -42.4 \\ -50.2 \\ -34 \end{bmatrix} \cdot Hz$$

taging is the aging time

ΔHz is frequency shifts under 5th overtone of QCM

$$\Gamma_{sauerbrey}(\Delta Hz) = \begin{bmatrix} 13.275 \\ 9.4341 \\ 8.2659 \\ 7.5048 \\ 8.8854 \\ 6.018 \end{bmatrix} \frac{mg}{m^2}$$

Sauerbrey equation is used to calculated the adsorbed mass of PVAm-T/laccase complex though curves under different overtones were not overlapped well in QCM

$$\sigma_{cA} := 1020 \frac{kg}{m^3}$$

σ_{cA} is the assumed density of hydrated PVAm-T/ laccase complexes. The value is density of 50 mM acetate buffer

$$:= \frac{\Gamma_{sauerbrey}(\Delta Hz)}{\sigma_{cA}}$$

h is the thickness of adsorbed PVAm-T/ laccase complexes

$$h = \begin{bmatrix} 13.0147 \\ 9.2491 \\ 8.1038 \\ 7.3576 \\ 8.7112 \\ 5.9 \end{bmatrix} \ nm$$

$$\Gamma_{cv} := \begin{bmatrix} 0.8475 \\ 0.7109 \\ 0.5314 \\ 0.3939 \\ 0.3515 \\ 0.1203 \end{bmatrix} \cdot \frac{10^{-6} \cdot mol}{m^2}$$

Γ_{cv} is the coverage of redox-active TEMPO on surface from cyclic voltammetry experiment

$$C_{RAT} := \frac{\Gamma_{cv}}{h}$$

CRAT is the concentration of redox-active TEMPO in the hydrated PVAm-T/laccase complexes adsorbed on the surface.

$$C_{RAT} = \begin{bmatrix} 0.0651 \\ 0.0769 \\ 0.0656 \\ 0.0535 \\ 0.0404 \\ 0.0204 \end{bmatrix} \frac{mol}{L}$$

The diffusion coefficient of charge propogated in the adsorbed PVAm-T17/laccase complex is calculated by Cottrell equation

Cottrell equation

$$i = \frac{nFA\sqrt{d_T}C_{RAT}}{\sqrt{\pi}\sqrt{t}}$$

i is current, t is time

$$D := 10 \ mm$$

D is the diameter of the Au surface for complex adsorption

$$A := \frac{1}{4} \cdot \pi \cdot D^2$$

$$A = \left(7.854 \cdot 10^{-5}\right)\ m^2$$

A is the surface area for complex adsorption

$$\phi := \begin{bmatrix} 6.543 \\ 5.432 \\ 4.267 \\ 3.662 \\ 2.356 \\ 1.043 \end{bmatrix} \cdot \mu A \cdot \sqrt{s}$$

ϕ is the slope of i vs $\sqrt{t}$ obtained from chronoamperometry

$$n := 1$$

n is the number of elctrons transfered between TEMPO and oxoammonium cation

$$F = \left(9.6485 \cdot 10^4\right)\ \frac{C}{mol}$$

F is Faraday constant

$$i := 0 .. 5$$

$$d_{T_i} := \left(\frac{\phi_i \cdot \sqrt{\pi}}{n \cdot F \cdot A \cdot C_{RAT_i}} \right)^2$$

dT is the diffusion coefficient of charge propagating the adsorbed PVAm-T/ laccase complexes

$$d_T = \begin{bmatrix} 5.5232 \cdot 10^{-12} \\ 2.7324 \cdot 10^{-12} \\ 2.3165 \cdot 10^{-12} \\ 2.5597 \cdot 10^{-12} \\ 1.8651 \cdot 10^{-12} \\ 1.4315 \cdot 10^{-12} \end{bmatrix} \frac{cm^2}{s}$$

Chapter 5 Concluding Remarks

Polyvinylamine (PVAm) is a relatively new, commercially available, polyelectrolyte which has the highest primary amine density of all polymers. Due to the versatility of amine groups and the wide range of polymer molecular weight and degree of hydrolysis available, the potential applications of PVAm cover almost every aspect where water-soluble polymers can be used. Our interests involve using PVAm as a paper wet strength additive. Over the past 15 years, a number of approaches to using PVAm for improving wet strength been investigated, including the use of linear PVAm with different molecular weights and hydrolysis degrees, PVAm nanoparticles, PVAm coated responsive microgels, PVAm boronate and PVAm polyelectrolyte complexes. The actual wet strengthening mechanism of PVAm is the formation of covalent bond between amine groups of PVAm and aldehyde groups on the cellulose surface. Native cellulose does not contain aldehydes; therefore mild TEMPO-mediated oxidation was used to introduce aldehyde groups in all the above mentioned cases.

TEMPO-mediated oxidation of cellulose was first reported over 20 years ago. Advantages such as high product yield, high selectivity, and only slight degradation of cellulose attracted attention from both academia and industry. However, the environmental impact and cost efficiency have limited its practical applications. Several patents and scientific publications approach this problem by suggesting the recovery and reuse of TEMPO for the oxidation of small organic substrates. Methods include distillation and extraction of waste as well as immobilization of TEMPO on solid carriers. The recovery and recycling has so far almost exclusively been done on a laboratory scale; TEMPO recycling from large volumes of solutions in the production of paper offers big engineering challenges.

Recent work from the Pelton lab have provided an alternative approach to reduce the cost and environmental impact of TEMPO-mediated oxidation by grafting TEMPO onto PVAm or poly(acrylic acid). This way TEMPO can be concentrated near the cellulose surface, since the polyelectrolyte grafted TEMPO adsorb onto cellulose (or modified cellulose). As a result, less TEMPO is required for the oxidation and the environmental impact is lowered since the immobilized TEMPO is less toxic than the small molecular TEMPO.

This thesis work describes new insights into the role of polymer grafted TEMPO as mediator for cellulose oxidation. The results provide a better understanding of the process of polymer grafted TEMPO adsorbing to, oxidizing, and promoting wet adhesion of cellulose. The main contributions of this work are given as follows:

1. Polymer grafted TEMPO adsorbs onto cellulose membranes (or pre-treated cellulose membranes) in the presence of laccase. A TEMPO moiety close to the laccase active site is oxidized to an oxoammonium cation, which then is transferred to the cellulose membrane surface through electron hopping between TEMPO moieties on the polymer chain. When an oxoammonium cation is in close enough proximity to a primary alcohol on the cellulose surfaces, the alcohol is oxidized to an aldehyde.

2. For the first time, the redox-activity of polyvinylamine-g-TEMPO (PVAm-T)/laccase complexes were directly measured, using electrochemical quartz crystal microbalance with dissipation (EQCM-D), a combination of QCM-D and a potentiostat. The redox-activity of PVAm-T/laccase complexes was influenced by the degree of TEMPO substitution (DS). When DS<10%, only 50% of the grafted TEMPO moieties were redox-active, whereas when DS>12% almost all the grafted TEMPO were redox-active. These results showed that around 10% TEMPO substitution was required in order to have efficient TEMPO-to-TEMPO electron transfer. At lower DS, the TEMPO moieties are likely too far apart to facilitate efficient electron hopping.

3. For the first time, the aldehyde density on cellulose membrane surfaces oxidized by PVAm-T/laccase complexes was determined through the use of the fluorescent dye Bodipy FL. Wet never dried samples were analyzed to avoid hemiacetal crosslinking between the highly reactive aldehyde groups and alcohols in drying samples. Two severe assumptions were made based on the EQCM-D measurements, which were performed on modified gold (1) the structure and the mass density of the adsorbed complex is the same on both surfaces, and (2) the redox-active TEMPO content, measured by electron transport from gold is the same as the redox-active TEMPO content, where the electron transfer is from laccase. The relationship between aldehyde density on oxidized cellulose and the amount of redox-active TEMPO was built, as well as the relationship between aldehyde density on oxidized cellulose and the TEMPO degree of substitution in the PVAm-T/laccase complex. The aldehyde density on oxidized cellulose scaled with the square root of the density of redox-active TEMPO, and was a linear

function of TEMPO degree of substitution in the PVAm-T/laccase complexes. As a result, the aldehyde density on cellulose surfaces is controllable by varying the TEMPO degree of substitution and redox-active TEMPO in PVAm-T/laccase complexes.

4. Multilayer films composed of PVAm-T and poly(styrene sulfonate) are stable and redox-active, whereas, multilayer films composed of PAA-T and poly(ethyleneimine) decompose under the same external potential. Beside the polymer type, the redox-activity of covalently bound TEMPO in redox films is influenced by TEMPO degree of substitution, film structure (Layer-by-Layer or complex), and the hydration of films. These provide various tools to design desired TEMPO redox films.
5. The net charge of poly(acrylic acid-g-TEMPO) turns from negative to positive due to the protonation of carboxyl groups and disproportionation of TEMPO moieties with decreasing pH. It shows potential for applications in surface modification.
6. The polymer grafted TEMPO/laccase system provides a new platform to functionalize cellulose surfaces, and this approach can also be used to introduce aldehyde and carboxyl groups to other polysaccharide surfaces containing primary alcohols.